

TECHNISCHE UNIVERSITÄT MÜNCHEN

Ingenieurfacultät Bau Geo Umwelt

Lehrstuhl für Kartographie

# Conflation of Road Networks from Digital Maps

Andreas Philipp Hackelöer

Vollständiger Abdruck der von der Ingenieurfacultät Bau Geo Umwelt der Technischen Universität München zur Erlangung des akademischen Grades eines Doktor-Ingenieurs (Dr.-Ing.) genehmigten Dissertation.

Vorsitzender: Prof. Dr. Peter Rutschmann

Prüfer der Dissertation:

1. Prof. Dr.-Ing. Liqiu Meng
2. Prof. Dr.-Ing. habil. Volker Schwieger
3. Prof. Dr. Jukka M. Krisp

Die Dissertation wurde am 20.6.2016 bei der Technischen Universität München eingereicht und durch die Ingenieurfacultät Bau Geo Umwelt am 11.11.2016 angenommen.



Meinem Vater



## Danksagung

Mein besonderer Dank gilt Prof. Dr.-Ing. Liqiu Meng für die Betreuung meiner Promotion und die Unterstützung, die ich am Lehrstuhl erfahren habe.

Weiterhin ausdrücklich danken möchte ich Prof. Dr. Jukka Krisp und Dr.-Ing. Klaas Klasing für ihre Betreuung und Unterstützung, ebenso Prof. Dr.-Ing. habil. Volker Schwieger, der sich als Zweitprüfer zur Verfügung gestellt hat.

Ferner danke ich Mathias Jahnke, Holger Kumke, Stefan Peters, Christian Murphy, Jian Yang, Nina Polous, Linfang Ding, Luise Fleißner und allen anderen Mitgliedern des Lehrstuhls.

Schließlich gilt mein Dank auch meinen Brüdern Felix und Martin, meiner Mutter und meiner Familie.



## Abstract

Digital maps are virtual images of geographical real-world entities such as roads, buildings, or rivers, which are used in various applications relying on digital cartographic data, such as automotive navigation systems or smartphone-provided location based services. In the automotive context, the modelling of road networks within digital maps is of particular interest, since the road network is employed for positioning the car on the map as well as for several other functions of a navigation system, such as route calculation and guidance. In addition, an increasing number of driving assistance systems beyond navigation requires information about the road network, e.g. in order to adapt the driving behavior to certain road conditions.

A representation of a real-world road network within a digital map is always subject to a certain modelling. Thereby, a model is chosen to incorporate all relevant information for the targeted applications, while, at the same time, omitting any aspects of reality deemed irrelevant for that purpose in order to reduce complexity and costs. Since there are many different ways of modelling a road network, digital maps from different vendors representing the same area may differ greatly in the way the network is modelled. For example, a road with two physically divided carriageways for each driving direction may be modelled as being a single road with the additional semantic information of having a physical divider, or it may be modelled as consisting of two independent roads. Apart from deliberate vendor-specific decisions regarding the road model and the way roads are described within the model, several other aspects such as the method used for map creation and its accuracy as well as the time the data was recorded lead to variations between digital maps of the same area. For example, if the road network was derived from aerial photography, its geometry will very likely differ from a road network created from GPS traces, and if a change has occurred to the topology such as the replacement of a crossing with a roundabout, a digital map incorporating this change will exhibit differences to an older version even from the very same vendor.

This doctoral thesis is concerned with referencing, conflation, analysis, and comparison of road networks of digital maps. The term “referencing” is used here to describe techniques which allow for the unique identification of geographical entities across different digital maps. Road Network Conflation is concerned with finding accurate mappings between geographical structures of road networks, ranging from elementary structures such as crossings to aggregated high-level entities such as sequences of topological edges. Conflation therefore employs various methods in order to analyze and compare different road networks so as to identify commonalities as well as differences.

After an introduction explaining the motivation as well as the structure of this thesis, the state of the art in the domain of Georeferencing is described. The subdomain of Road Network Conflation is established within a taxonomy of georeferencing methods. Then, common Road Network Conflation approaches are classified, introduced and compared. With this groundwork, the problem domain of Road Network Conflation is then explored in great detail. A formal definition of the problem is proposed, and the problem of ambiguity on multiple levels of abstraction is discussed thoroughly.

As a novel approach towards the Road Network Conflation problem, the Iterative Hierarchical Conflation (IHC) framework is introduced. It consists of two phases – Bottom-Up phase and Top-Down phase – and five stages, which are arranged in a so-called Matching Pipeline. The phases along with the stages visited over each phase are described in detail.

The IHC is evaluated using several samples from digital maps of different vendors. At first the evaluation methodology, which is proposed as a standard for further research in the field, is disclosed, then, the results of the evaluation are described. Finally, conclusions are drawn and an outlook is given on further developments in the domain.

As primary research findings, it can be concluded that IHC offers high reliability in terms of both correctness and completeness in the rural sample regions and provides a high correctness while maintaining a considerable, but not perfect completeness in the urban sample regions. Thereby, the IHC framework avoids a large number of heuristics and only requires very few parameters to deliver acceptable results. Results are generated at high speeds, which enables on-the-fly matching in automotive applications. The IHC follows a systematic approach for the resolution of ambiguities using topological alteration in virtual network layers. The generic design of the IHC allows for the conflation of road networks which only provide very basic map information limited to elementary topology along with road segment and node geometry, so that it can be used with very heterogeneous data sources.

## Zusammenfassung

Digitale Karten sind virtuelle Abbilder realer geographischer Objekte wie Straßen, Gebäude oder Flüsse. Sie werden in zahlreichen Anwendungen eingesetzt, in denen digitale kartographische Daten benötigt werden, wie etwa Fahrzeug-Navigationssysteme oder via Smartphone verfügbare ortsbasierte Dienste. Im Automobilbau ist die Modellierung von Straßennetzen innerhalb digitaler Karten von besonderem Interesse, da das Straßennetz sowohl für die Positionierung des Fahrzeugs auf der Karte als auch für verschiedene weitere Funktionen eines Navigationssystems benötigt wird, wie etwa die Routenberechnung und die Zielführung. Zudem benötigt eine zunehmende Zahl von Fahrassistenzsystemen abseits der Navigation Informationen über das Straßennetz, etwa um das Fahrwerk an wechselnde Eigenschaften der Straße anzupassen.

Die Repräsentation eines Straßennetzes der realen Welt in einer digitalen Karte ist immer konkreten Modellierungsentscheidungen unterworfen. Dabei wird ein Modell bevorzugt, das einerseits möglichst alle relevanten Informationen für die vorgesehenen Anwendungen enthält, andererseits jene Aspekte der Realität ignoriert, die für diese Anwendungen als irrelevant betrachtet werden, um Komplexität und Kosten zu reduzieren. Da es viele verschiedene Möglichkeiten gibt, ein Straßennetz zu modellieren, können digitale Karten der gleichen geographischen Region verschiedener Hersteller sich in ihrer Modellierung erheblich unterscheiden. So kann zum Beispiel eine Straße mit baulich getrennten Fahrspuren für jede Fahrtrichtung entweder als einzelne Straße mit der zusätzlichen Semantik einer baulichen Trennung modelliert werden oder auch in Form von zwei unabhängigen Straßen mit separaten Geometrien repräsentiert sein. Abgesehen von beabsichtigten herstellerspezifischen Entscheidungen bezüglich des Straßenmodells und der Art, wie Straßen darin beschrieben sind, können zudem einige weitere Aspekte zu Unterschieden zwischen digitalen Karten des gleichen Gebiets führen, wie etwa die zur Kartenerstellung verwendeten Verfahren und deren Genauigkeit oder auch die Aktualität der Kartendaten. So ist es wahrscheinlich, dass die Geometrie eines aus Luftbildern extrahierten Straßennetzes erheblich von der Geometrie eines aus GPS-Positionsaufzeichnungen abgeleiteten Straßennetzes abweicht, und Änderungen der Topologie wie der Austausch einer Kreuzung durch einen Kreisverkehr führen zu erheblichen Unterschieden zwischen Karten verschiedener Versionsstände, selbst wenn diese Karten vom gleichen Hersteller stammen.

Diese Dissertation beschäftigt sich mit Referenzierung, Verschneidung (Conflation), Analyse und Vergleich von Straßennetzen in digitalen Karten. Der Begriff "Referenzierung" wird hier verwendet, um Verfahren zu beschreiben, welche die eindeutige Identifikation geographischer Objekte über verschiedene digitale Karten hinweg ermöglichen. Die Verschneidung von Straßennetzen ("Road Network Conflation") befasst sich mit der Erkennung möglichst genauer Zuordnungen zwischen geographischen Strukturen von Straßennetzen, von elementaren Strukturen wie Kreuzungen bis hin zu aggregierten komplexen Objekten wie etwa Folgen topologischer Kanten (Verbindungen im Straßengraphen). Dabei werden verschiedene Verfahren eingesetzt, um verschiedene Straßennetze zu analysieren und zu vergleichen mit dem Ziel, Gemeinsamkeiten und Unterschiede zu identifizieren.

Nach einer Einführung, welche die Motivation und Struktur der vorliegenden Arbeit erläutert, wird die Domäne der Georeferenzierung beschrieben. Road Network Conflation wird als Teilgebiet dieser Domäne innerhalb einer Taxonomie von Georeferenzierungsmethoden eingeordnet. Im Anschluss werden übliche Ansätze für Road Network Conflation klassifiziert, vorgestellt und verglichen. Auf dieser Grundlage folgt eine detaillierte Untersuchung des Problemgebiets. Eine formale Definition des

Road-Network-Conflation-Problems wird vorgeschlagen, und das Problem der Mehrdeutigkeit auf verschiedenen Abstraktionsniveaus wird ausführlich diskutiert.

Als neuartiger Ansatz für Road Network Conflation wird das Iterative Hierarchical Conflation (IHC)-Framework vorgestellt. Das IHC besteht aus zwei Phasen - Bottom-Up und Top-Down - und fünf Stufen, die in der so genannten Matching-Pipeline durchlaufen werden. Die Phasen und die Stufen, die im Verlauf jeder Phase besucht werden, werden im Detail beschrieben.

Der IHC wird mittels mehrerer Stichproben von digitalen Karten verschiedener Hersteller evaluiert. Zunächst wird dabei die verwendete Methodologie, die als Standard für weitere Forschungen in der Domäne vorgeschlagen wird, offengelegt. Anschließend werden die Ergebnisse der Evaluation beschrieben. Den Abschluss bilden eine Schlussfolgerung und ein Ausblick auf zukünftige Entwicklungen in dem Gebiet.

Zu den wichtigsten Forschungsergebnissen gehört die Feststellung, dass der IHC hohe Zuverlässigkeit bezüglich sowohl Korrektheit als auch Vollständigkeit in den ländlichen Beispielregionen liefert und hohe Vollständigkeit bei solider, aber nicht perfekter Vollständigkeit in den städtischen Testdatensätzen bietet. Dabei vermeidet das IHC-Framework eine große Zahl von Heuristiken und benötigt nur vergleichsweise wenige Parameter, um gute Ergebnisse zu erzielen. Die Ergebnisse werden mit hoher Geschwindigkeit erzeugt, was On-the-Fly-Matching in automobilen Anwendungen ermöglicht. Der IHC folgt einem systematischen Ansatz für die Auflösung von Mehrdeutigkeiten mit Hilfe von topologischen Änderungen in virtuellen Schichten des Straßennetzes ("Virtual Network Layers"). Der generische Entwurf des IHC erlaubt die Verschneidung von Straßennetzen, zu denen nur wenige Informationen vorliegen; ausreichend ist elementare Topologie zusammen mit der Geometrie von Straßensegmenten und Knoten. Auf diese Weise kann der IHC mit sehr heterogenen Datenquellen eingesetzt werden.

## Contents

Abstract .....	7
Zusammenfassung.....	9
Contents .....	11
1 Introduction .....	15
1.1 Motivation.....	15
1.2 Example scenarios for automotive applications of conflation.....	17
1.2.1 Information Transfer .....	17
1.2.2 Map Fusion.....	18
1.2.3 Onboard conflation / Multiple Maps on Vehicle .....	18
1.3 Structure of the Thesis .....	18
2 State of the Art.....	21
2.1 Basics of Georeferencing.....	21
2.2 Tasks and Methods in the Georeferencing Domain.....	22
2.2.1 Georeferencing of Raster Images.....	22
2.2.2 Georeferencing of Vector Data .....	23
2.3 Taxonomy of Georeferencing Methods .....	24
2.3.1 Classification by type.....	24
2.3.1.1 Vector referencing.....	24
2.3.1.2 Raster referencing.....	24
2.3.2 Classification by identification category .....	25
2.3.2.1 Topological Properties.....	25
2.3.2.2 Geometrical Properties .....	25
2.3.2.3 Shared geometrical / topological properties .....	26
2.3.2.4 Semantic properties .....	26
2.3.3 Classification by application scenario .....	26
2.3.3.1 Map Manipulation.....	27
2.3.3.2 Map Creation.....	27
2.3.3.3 Map Validation .....	27
2.3.3.4 Map Matching .....	27
2.3.3.5 Georeferencing of media .....	27
2.4 Road Network Conflation.....	27
2.5 Road Network Conflation Methods .....	30
2.5.1 Point-based approaches.....	30
2.5.1.1 Definitions and prerequisites .....	30

2.5.1.2	Geometrical point matching techniques .....	32
2.5.1.3	Topological point matching techniques .....	33
2.5.1.4	Combined geometrical / topological point matching techniques.....	34
2.5.2	Line-based and structural approaches .....	36
2.5.2.1	Buffer Growing .....	37
2.5.2.2	Multi-Stage Matching .....	37
2.5.2.3	Delimited Stroke Oriented Matching .....	38
2.5.3	Comparison of Road Network Conflation Methods .....	39
3	Exploration of the Research Domain.....	42
3.1	Formal Definition of Road Network Conflation.....	42
3.2	The Problem of Ambiguity.....	43
3.2.1	Ambiguity on the Level of Point Objects .....	44
3.2.2	Ambiguity on the Level of Line Objects .....	45
4	The Iterative Hierarchical Conflation (IHC) Framework .....	48
4.1	Overview of the Matching Pipeline .....	48
4.2	The Bottom-Up Phase.....	49
4.2.1	Preprocessing .....	49
4.2.2	Node Matching .....	49
4.2.3	Elementary Matching .....	52
4.2.4	Combined Matching .....	52
4.2.5	Structural Matching.....	54
4.3	The Top-Down Phase.....	54
4.3.1	Combined Matching .....	54
4.3.2	Elementary Matching and Point Matching.....	56
4.4	Detection of Structural Anomaly at Roundabouts .....	56
5	Implementation and Evaluation.....	60
5.1	Implementation.....	60
5.2	Evaluation Methodology .....	63
5.3	Environment .....	64
5.4	Datasets .....	64
5.5	Results .....	65
5.5.1	Results for urban samples .....	65
5.5.2	Results for rural samples .....	67
6	Conclusions and Outlook.....	70
6.1	Conclusions.....	70

---

6.2	Outlook.....	71
7	References.....	74
8	Appendix: Ground Truth Definitions for Evaluation .....	82
8.1	Boston Sample.....	82
8.2	Munich Sample.....	87
8.3	Eutin Sample.....	91
8.4	Sullivan Sample .....	95
8.5	Moosach Sample .....	97



## 1 Introduction

### 1.1 Motivation

The following motivation is partly based on the introduction section of the paper “Road Network Conflation: An Iterative Hierarchical Approach” [1].

A road network can be described as the structure given by the topology and geometry of roads, streets and transport links within a certain area. Maps depicting road networks have a long history, dating back to a time as early as Ancient Egypt, where maps such as the Turin Papyrus Map showed pedestrian routes along dry river beds [2]. Around the year 1500, the Nurembergian cartographer Erhard Etzlaub published his “Rom-Weg” map designed to help pilgrims find their way to Rome, which introduced the representation of a route by a sequence of points interconnected with lines, where each line between two neighboring points had a fixed distance of one German mile (7,4 km) [3]. This development finally led to the modern road maps, which offer an accurate depiction of cross-city as well as inner city routes for automobiles enriched with semantic information such as gas stations or speed restrictions. While Etzlaub had to rely on the testimony of travelling merchants, nowadays advanced methods of georeferencing are employed in order to accurately assign the geographical objects used in a road map to geographical locations. Maps are increasingly authored and maintained in digital form, which may either be raster or vector based.

In recent times, digital vector maps have gained importance in the field of automotive navigation. These maps organize georeferenced information in several layers. The topological layer consists of a representation of the road network given by its induced graph, where crossings and intersections correspond to nodes in the graph, and the routes interconnecting these crossings correspond to edges. By defining several classes of roads, ranging all the way from international highways down to small city streets, and assigning these classes to the edges of the graph, a routing such as the shortest or the fastest way between two point locations on the map can efficiently be computed using shortest-path algorithms such as the Dijkstra algorithm [4]. In contrast, the geometrical layer of a digital map contains a description of the geometrical shape of the objects stored in the map. Often, the road geometry is approximated via a sequence of shape points, where each shape point is given by its coordinates and the road geometry is defined as the polyline constituted by the shape points. While a road is usually represented as a one-dimensional entity, more detailed maps, e.g. those required for driver assistance systems, may store additional information such as the width of a road or the boundaries of different lanes. In addition, digital road maps may contain polygonal two-dimensional objects such as footprints of buildings or special areas like parking zones.

All geographical entities found in a digital road map are georeferenced using a geodetic reference frame such as WGS-84 [5]. This way, a person is able to derive his or her position within the map by matching the position (often gained from GPS satellites) with the geographical references found in the map, so that e.g. a car whose GPS coordinates point to a location some meters away from a road is identified as being located exactly on that road. This process is called Map Matching. Digital road maps usually enforce internal consistency, i.e. there is only one unique representation of a single geographical object. However, multiple maps of the same region may vary greatly, to the extent that a geographical object present in one map may be entirely missing in the other, or may be assigned to a different georeference. Also, it may (partly) correspond to multiple objects in the other map, e.g. if

a road with lanes separated by a physical divider is modeled as a single road in one map and as two one-way roads in the other.

The problem of identifying geographical entities across different maps is called conflation [6]. The outcome of a conflation process between two maps is a projection from one map to the other, which defines how the geographical entities found in the two maps are related (the similarities), thereby also identifying the objects which are unrelated (the differences). Within the domain of conflation, Road Network Conflation is concerned with conflating road networks.

Several applications have contributed to the increasing relevance of Road Network Conflation, especially in the domain of automotive navigation and driver assistance systems. One important application is the so-called "Learning Map". For example, if a car has sensed a certain environmental condition not present in the map but important to automotive subsystems, which often is the case if this condition has a limited validity period, such as a hole in the road, it can be beneficial to record this condition along with a geospatial reference indicating the according road segment on the map. However, the recorded ("learned") information is lost once the underlying map is exchanged with another map which either does not have the according road segment or is using a different internal ID for it. The map may be exchanged with another map of a different vendor because this vendor offers better coverage, but the most common reason is an update to a more recent version, since digital maps age quickly, especially in emerging countries such as China with high building activities. For the learned information to survive, a conflation between the old and the new road network must be found which provides a mapping for the relevant geographical objects, such as road segments. Then, this information can be transferred from the old to the new map employing the mapping.

Road Network Conflation is also very useful for the incremental updating of maps. Even today, being a shared medium, modern cellular networks have limited capacity. Thus, uploading an entire map via a mobile network is both expensive as well as time-consuming. In order to keep an automotive on-board map updated, an increment may be transferred instead which represents the difference between the old and the new map. There are several methods to find differences between arbitrary binary data, but the smallest increment can be determined by the output of an ideal conflation algorithm.

In addition, being able to identify geographical objects across different maps may be used for quality evaluation of maps. Given a reference map e.g. issued by local authorities, the map to be evaluated may be conflated with the reference map in order to quantitatively as well as qualitatively describe the proximity to the reference map in terms of geometry and topology to evaluate properties such as coverage and accuracy.

A quite obvious use case is map fusion. Conflation may be employed in order to author a new, more comprehensive map based on less detailed maps. It therefore provides a means of identifying how geographical objects in the source maps relate, so that attributes as well as geographical features may be exchanged and combined accordingly.

Finally, conflation represents a way to georeference geographical objects relatively, though not absolutely, independent of a certain map. The reference is relative to a map in the sense that any map where it shall be transferred to must offer sufficient similarity to the original map so that a mapping can be found by the conflation algorithm. Thus, from this point of view, conflation can also be seen as

an aspect of a geographical reference system, in the sense that map-dependent georeferences can be extended to map-agnostic georeferences if used in combination with a powerful conflation algorithm.

Current approaches to the conflation of road networks originate from the domain of geographical information systems and focus on concepts which aim to derive line-to-line assignments from dedicated regions so that the results can manually be investigated and corrected. From the perspective of the automotive industry, there is a growing demand for a flexible framework targeting the conflation of road networks as found in automotive maps. This framework should, on the one hand, extend existing conflation methods in such a way that problems typical to the domain, such as the identification of similarities between complex structures found in modern traffic such as roundabouts, are dealt with accordingly. On the other hand, it should offer sufficient modularity and performance as well as matching correctness and completeness so that it can be embedded into a partly or fully automated tool chain which employs road network conflation tailored to the needs of driving assistance and car navigation systems. In detail, the following research questions arise in this context:

- How can a generic approach be achieved which aims to avoid a large number of heuristics?
- How can the choice of algorithms contribute to the required performance level for automotive applications?
- How can structural similarities be identified and propagated down to the level of elementary objects such as links and nodes?
- Is there a systematic way of dealing with ambiguities so that potential problems can be identified over the course of the conflation process, and maps based on conflated information can reach the required quality and reliability level for automotive applications?
- What is the most generic and reduced type of road network data actually required for performing road network conflation? If less information is required, more heterogeneous data sources of different standards can be employed.

This thesis introduces a novel concept called the Iterative Hierarchical Conflation, which aims to represent a step forward in answering these research questions.

## **1.2 Example scenarios for automotive applications of conflation**

Recently, several scenarios have become reality or are being investigated by the automotive industry which make use of conflation algorithms. Three scenarios, Information Transfer, Map Fusion, and Multiple Maps on Vehicle, will be demonstrated here.

### **1.2.1 Information Transfer**

Several environmental conditions cannot be recorded in a map due to their temporally limited validity. This is especially relevant with respect to local danger situations such as heavy rain or obstacles on the road. In this scenario, when a car observes a local danger situation such as an obstacle behind a curve which can be detected by using onboard sensors such as a camera or ultrasound, it records the exact position of the obstacle. The position is recorded relative to the onboard map of the vehicle, i.e. by referring to the current street segment along with an offset. The reference is sent to a cloud backend via a mobile network along with information about the map (vendor and version) used onboard the car. In order to transfer this information to a fleet of vehicles which employ different map versions from different vendors, the backend may first conflate the source map with every destination map the reference shall be transferred to. Then, using the conflation result, the corresponding georeferences which refer to the destination maps can be deployed to the fleet. Finally, all receiving vehicles use the

transferred information to issue a warning about the obstacle if the driver is approaching it. In the same fashion, the information can later be sensed and broadcasted to the fleet that the obstacle has been removed and no longer poses a threat.

### 1.2.2 Map Fusion

Modern automotive navigation systems are expected to offer a large database of Points of Interest (POI). This raises the question of how POI databases from different sources, such as OpenStreetMap, can be merged into a single database. Of course, an obvious solution would be to simply transfer the POI locations, as given by the WGS-84 coordinates. However, in this case, there would be no referencing between the POIs and the road segments they relate to, leading to errors such as the displacement of gateways. As long as a POI is recorded along with a reference to a road segment in the source database, it is possible to conflate the source and destination map, then transfer the POI reference to the destination map. This way, the resulting POI database refers to road segments of the map onboard the vehicle.

### 1.2.3 Onboard conflation / Multiple Maps on Vehicle

There are situations when a vehicle may carry two different maps onboard. For example, there may be a low-resolution map (Standard Definition map, SD) used for classical infotainment functions and another high-resolution map (High Definition map, HD) with more accurate geometry which is required by advanced driving assistance functionality. These two maps need not necessarily originate from the same vendor. In order to correlate both maps, the vehicle may perform an onboard conflation. Thus, it can be ensured that functions depending on both maps share a similar view of the position of the car and its surrounding road network, even if the maps deviate to a certain extent.

## 1.3 Structure of the Thesis

This thesis consists of six chapters.

In Chapter 1, the concept of Road Network Conflation is introduced along with several applications which have recently gained importance in the market, especially concerning the automotive industry. Thereafter, the structure of the thesis is described in detail.

Chapter 2 portrays the State of the Art in the field. It starts with an introduction to basic aspects of georeferencing, which represents the foundation of Road Network Conflation. Problems and methods in this domain are explained and investigated. Methods of georeferencing are then classified through the use of a taxonomy. From there, the subdomain of Road Network Conflation is delved into. Current approaches to Road Network Conflation are elicited. This chapter is based, in part, on results of the papers “Georeferencing: A Review of Methods and Applications” [7] and “Road Network Conflation: An Iterative Hierarchical Approach” [1].

Chapter 3 is dedicated to the problem domain. Therefore, at first, a formal mathematical definition of the Road Network Conflation problem is proposed. Based on this groundwork, the problem of ambiguity, which necessarily arises when conflating non-trivial road networks, is discussed. Ambiguity may appear on every possible layer of abstraction from elemental point objects to aggregated high-level structures, which are dealt with in separate sub-chapters. This chapter, as well as the following two, include results of the paper “Road Network Conflation: An Iterative Hierarchical Approach” [1].

Chapter 4 is concerned with the core of this Thesis, the Iterative Hierarchical Conflation (IHC) framework. This framework represents an advanced approach towards the Road Network Conflation

problem by means of a so-called Matching Pipeline, which consists of two phases (Bottom-Up and Top-Down) and multiple stages which are visited over the course of each phase in order to iteratively find and refine associations between objects on different levels of abstraction. After an overview of the Matching Pipeline concept, both phases and the stages visited therein are described in detail.

Chapter 5 explains the implementation and evaluation of the IHC framework approach. The methodology employed for the evaluation is disclosed, followed by a description of the environment which was used to conduct the experiments. The datasets involved in the evaluation are introduced. Finally, the evaluation results are described and discussed. The IHC has been tested with maps from different vendors and regions of different characteristics. Results were compared to ground truth definitions in order to derive statistical quality measures.

Finally, Chapter 6 draws conclusions out of the results obtained and provides an outlook to upcoming developments and challenges in the field of Road Network Conflation.



## 2 State of the Art

### 2.1 Basics of Georeferencing

Georeferencing can be seen as an umbrella term for techniques which are concerned with the unique localization of geographical objects. The term “geographical object” in a broader view refers to any kind of object or structure which can reasonably be related to a geographical location, such as points of interest (POIs), roads, places, bridges, buildings, or agricultural areas. A geographical location is an entity which represents a spatial reference. Geographical locations can be defined in multiple spatial dimensions: 0-dimensional (points), 1-dimensional (lines), 2-dimensional (areas), and, rarely, 3-dimensional (bodies). For example, POIs can be referenced to 0-dimensional point locations, while road segments can be referenced to line locations. Buildings, even if they are represented as 3D models, are usually referenced to 2-dimensional area locations, since they are assumed to stand on the ground level.

Hill [8] distinguishes between *informal* and *formal* means of referring to locations. Informal georeferencing describes colloquial references to geographical objects such as place names, while formal georeferencing covers the domain of exact location referencing in science and technology e.g. using spatial reference systems. Over the course of the following, we will focus on investigating formal georeferencing techniques.

There are various definitions for the term “Georeferencing”. E.g., Sommer and Wade define georeferencing as „aligning geographic data to a known coordinate system so it can be viewed, queried, and analysed with other geographic data” [9]. Coarser views include the domain of georeferencing multimedia [10] and the exploration of means for the identification of geographical objects in general.

Generally, three distinct types of information can be used to refer to geographical objects.

- (1) Geometrical information that describes geometric properties of an object, such as the layout and shape of a road segment.
- (2) Topological information that deals with properties which are preserved under continuous deformations of objects; in the context of georeferencing, the graph structure induced by networks of certain geographical objects, such as roads or rivers, is of primary concern for topological investigations.
- (3) Semantic information that includes various kinds of semantic properties related to a geographical location, such as the name of a place or road. Common methods of georeferencing consider at least one type, but often a combination of these types of information in order to uniquely identify a geographical object.

The process of identifying geographical objects and assigning them to geographical locations is essentially a matching process, which may also be referred to as the identification of homologous objects. When a map is authored from scratch, the author defines geographical objects, locations as well as assignments between them. Georeferencing usually takes place using a geodetic reference system such as WGS-84 [11], which comprises a standard coordinate frame for the Earth, a reference ellipsoid and a geoid which defines a nominal sea level. Other reference systems may also be adopted depending on specific application fields. To some extent, navigation devices can be used for data

collection within a map-making process. GPS trackers deliver coordinates within the WGS-84 geodetic reference system which can be related to a certain geographical reference on a map. However, often the process of assigning objects to locations is nontrivial. The different types of geographical objects to be matched on a map range from raster images such as aerial or satellite imagery to entities on pre-authored digital vector maps. Depending on the type of matching required, various kinds of methods and algorithms have evolved. Section 2.3 gives a classification of matching types and introduces appropriate methods for dealing with these matching problems.

The outcome of a matching process is an assignment between geographical objects and geographical locations. Often the object to be referenced on a certain map originates from another map with its own geographic reference system. In this case, a matching delivers correspondences between these two maps which express commonalities as well as differences, i.e. the information which objects could and which could not (or only partially) be identified on both maps.

The combination of map data from several sources in order to create a new map is called conflation. Longley et al. [12] define conflation in the context of geographic information systems as “the process of combining geographic information from overlapping sources so as to retain accurate data, minimize redundancy, and reconcile data conflicts”. Conflation is performed by using matching strategies for different structures (often nodes, segments and edges) to identify correspondences between maps in order to correlate and combine the data into a new map. According to a classification approach proposed by Yuan and Tao [13], conflation can be divided into *horizontal* (combining neighboring areas) and *vertical* conflation (combining different maps of the same area). While horizontal conflation is usually done between vector maps, vertical conflation may also be performed between raster-vector or vector-raster pairings of maps [14].

## 2.2 Tasks and Methods in the Georeferencing Domain

### 2.2.1 Georeferencing of Raster Images

A common task of the georeferencing domain involves assigning certain objects contained in raster images to location references. This is performed by employing methods and techniques from several fields, ranging from Remote Sensing and Photogrammetry to Computer Vision, Image Processing and Pattern Recognition.

Raster imagery depicting a geographical area is often obtained via satellite or aerial photography. Raw images are pre-processed and orthorectified (geometrically corrected) in order to eliminate distortions e.g. caused by camera tilt, topographic relief or optical properties of the lens. The processed images are then partitioned into multiple segments according to segmentation algorithms, such as Edge Detection [15], Region Growing [16], or Split-and-Merge [17]. The segments are further processed via Feature Extraction, which applies a dimensionality reduction in order to facilitate a classification of objects being shown in the image [18]. This way, subsets of pixels can be classified according to categories such as “road” or “farmland” using an appropriate classifier (classification algorithm) for the given features.

In order to georeference raster images, they are connected to digital maps via so-called Ground Control Points (GCPs) [19]. GCPs are landmarks located at salient positions which are chosen so that they can easily be identified in satellite or aerial imagery, such as road crossings or artificial targets. Since orthorectified images are at uniform scales, it is sufficient to correlate several (at least 3) GCPs to sets of pixels within an image which have been classified accordingly. In this way, the remaining pixels and

thus, also other identified features and objects can be georeferenced to positions on a map. GCPs may be pre- or postmarked; premarking involves marking control points with targets before flight, while in the process of postmarking, GCPs are selected after the flight based on natural image features which are deemed most suitable for this purpose [20]. Depending on whether a GCP is used for horizontal or vertical referencing, differently shaped artificial targets or natural features may be appropriate. Premarking provides an expansive means to identify locations in relatively featureless terrain, while postmarking has the advantage that a GCP can be chosen in a convenient location. However, natural features are not as well defined as artificial targets.

### 2.2.2 Georeferencing of Vector Data

Georeferencing vector data involves finding an assignment between a vector and a corresponding element within a digital map. In the simplest form, a coordinate pair must be assigned to a certain map. This problem is known as *Map matching*. Often the given coordinates are subject to a varying level of inaccuracy, e.g. when they are obtained from consumer-grade GPS devices. Thus, certain filtering, rectification and validation must be conducted in order to match coordinates on a map. For example, a map matcher working on a navigation device used for street navigation must obey the constraint that a valid position may only be located on a road segment.

The process of georeferencing complex vector data which may also possess a spatial extent, such as a line, an area or a road network, to a vector map is called Location Referencing. For example, the term *point location* refers to Points of Interest (POIs) such as a bus stop, while the term *line location* describes a sequence of (road) segments which comprise a route, e.g. from one city to another.

Location Referencing can be done statically or dynamically [21]. Static location referencing approaches such as the European Traffic Message Channel standard (TMC) [22] or the Japanese Vehicle Information and Communication System standard (VICS) [23] use predefined location codes or lookup tables in order to uniquely identify locations on a map. In contrast, dynamic location referencing techniques such as ISO 17572-3 / AGORA-C [24], the improved AGORA-C variant proposed by Xi [25], OpenLR [26], TPEG-LOC [27], MEI-LIN [28] or TPEG-LOC2 / ULR [29] aim to provide a location referencing scheme which describes a location in a “map-agnostic” way, i.e. without employing hard-coded references to segments or nodes of a certain map. Thus, locations encoded using dynamic location referencing approaches can be decoded and referenced on any map which offers sufficient topological and geometrical similarity to the map used in the encoding process.

For the problem of georeferencing an entire road network (rather than e.g. a line location) to another vector map of the same area, the term *Road Network Matching* has been coined [30]. Road Network Matching investigates the similarities between the road networks of the maps to be matched (usually two), thereby suggesting a mapping from the set of road segments in the first (source) map to the set of road segments in the second (destination) map. The mapping between segments may be of *1:1* type in the simplest form, but also *1:n*, *n:1* and *m:n* type mappings may be needed to accurately describe correspondences between road segments of the maps.

In order to deal with the complexity involved with *m:n* type mappings, approaches have been proposed which aim to find correspondences on higher levels of abstraction. E.g., Qian et al. [31] suggest a reduction of the road network to so-called *strokes* which are derived from the road network. Mappings can then be investigated on the stroke level, rather than on the level of individual segments or nodes. The *Intelligent Hierarchical Conflation* (IHC) framework introduced in this thesis represents a novel

approach for systematically dealing with complex matching cases, including  $m:n$  type mappings, on multiple levels of aggregation.

## 2.3 Taxonomy of Georeferencing Methods

Georeferencing can be seen from different perspectives. It may be classified by type (vector or raster referencing), by identification category (semantic, topological or geometrical), and by application scenario. Georeferencing by type approaches the domain from a structural perspective which focuses on the organizational methods employed for recording and referencing geographic data. In contrast, georeferencing by identification category addresses the domain with respect to mathematical categories of properties used for the unique identification of geographical entities. While these two classes maintain a technical perspective, georeferencing by application scenario provides a means of organizing the georeferencing domain from a holistic, application-oriented point of view.

### 2.3.1 Classification by type

Georeferencing can be divided into two types: vector and raster referencing. Figure 2-1 shows a classification approach of the types of georeferencing.

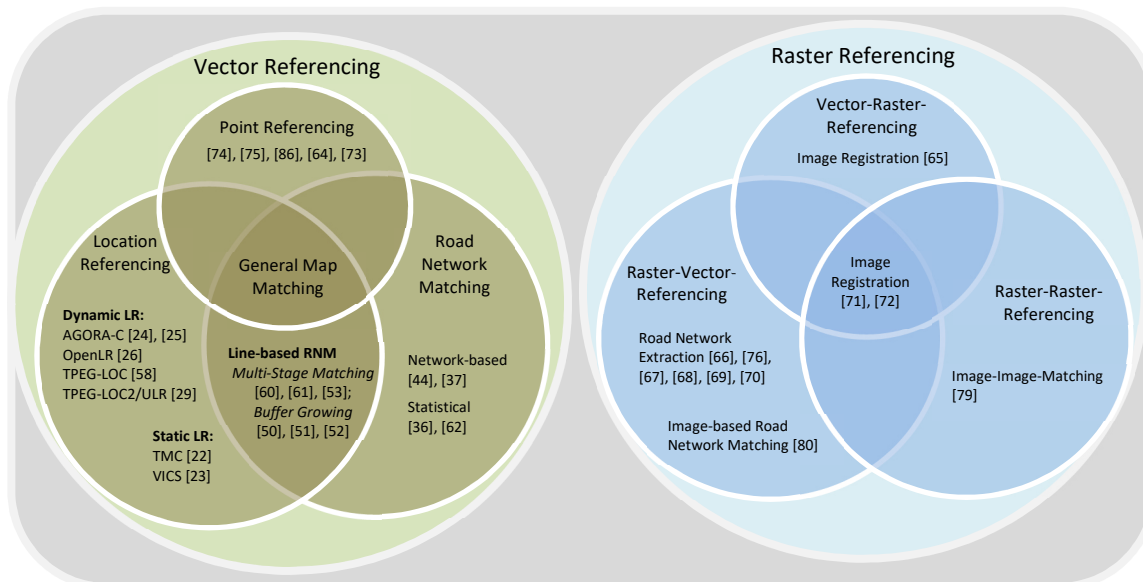


Figure 2-1: Types of Georeferencing.

#### 2.3.1.1 Vector referencing

Vector referencing deals with identifying locations which can be described by means of vectors. It can further be divided into Point Referencing, Location Referencing and Road Network Matching. Point referencing is the unique identification of a geographical point location, e.g. given by its WGS-84 coordinates, in a reference frame. In order to identify a position on a digital map, a projection from the input space (such as GPS sensor raw data or an object in a raster image given by a set of pixels) into the reference system of the digital map must take place. While the term Location Referencing usually refers to the identification of routes consisting of sequences of vectors (e.g. road fragments) or polygons defining areas, Road Network Matching is concerned with finding correspondences between graphs induced by the road networks of different maps (see 2.2.2).

#### 2.3.1.2 Raster referencing

Raster referencing is concerned with the problem of correlating pixels contained in raster images with geospatial references. In detail, it involves a projection of features between two geospatial reference

frames, where at least one feature space is comprised of sets of pixels from raster image data (see 2.2.1). Depending on the desired direction and pairing type (Vector-to-Raster, Raster-to-Vector or Raster-to-Raster), different methods must be employed to find suitable correlations. The domain of image registration is concerned with finding appropriate transformations between images, enabling mappings between different coordinate systems.

### 2.3.2 Classification by identification category

There are three categories for properties which may be used to uniquely identify geographical entities: topological, geometrical, and semantical. Figure 2-2 shows a classification of these identification categories.

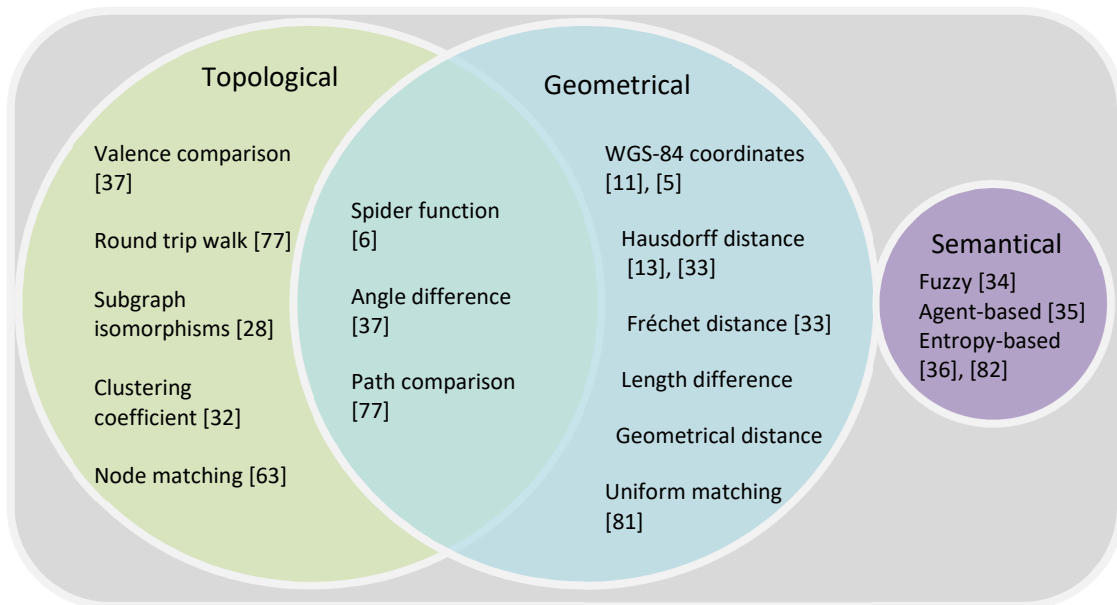


Figure 2-2: Identification categories.

#### 2.3.2.1 Topological Properties

Topological properties are properties which are preserved under continuous deformations of objects. The most important objects present in digital maps with respect to topological investigations are structures which induce a graph, such as a road network. The fact that topological properties are agnostic of geometrical deviations between two maps facilitates the use of topology to identify geographical entities within different maps regardless of minor differences in shape, position or other geometrical properties. However, maps originating from different vendors may reveal major topological differences, e.g. regarding the modelling of crossings. Examples for topological properties include the number of roads joining a crossing (valence of the node of the induced graph) as well as the existence of subgraph isomorphisms [28] or the clustering coefficient [32]. Also, the adjacency of polygons may be used to characterize geographical entities.

#### 2.3.2.2 Geometrical Properties

Geometrical properties describe the geometry of an object. Various geometrical parameters can be used to identify geospatial entities. E.g., point locations are identified via their coordinates, while line locations are given by their geometrical shape. When dealing with polygons, other properties such as the covered area provide an additional means for referencing. If the georeferencing process involves the conflation of different maps containing objects which share geometrical properties, relative metrics such as the Hausdorff distance [13] [33] are criteria for proper referencing of objects. As

geographical databases exhibit a varying precision of geometrical records, geometrical properties of objects should not be used as a single means of identification.

### 2.3.2.3 Shared geometrical / topological properties

Some properties share geometrical as well as topological aspects. E.g., point objects located on a road network may be identified via the angles of incident edges, as it is done by the spider function [6], which calculates an index assigned to node based on the quantization of these angles into sectors.

### 2.3.2.4 Semantic properties

Semantic properties in general are all properties which determine the meaning of an object. In digital maps, all information not falling into the geometrical or topological category can be considered semantical. This includes data such as the names of places, streets or POIs, street numbers, speed limits posted on road segments, the importance of a segment within the road network, etc. Semantic information is often useful for identifying geographical entities, since e.g. street names found on digital maps rarely match within a small geographical area if they do not represent the same street. However, it should never be used as a single means of identification, since large differences in semantic attributes must not necessarily imply that different entities are described. For example, there are various ways to spell a street name, and also sometimes multiple street names for the same street. The extent to which semantic attributes are recorded as well as their quality greatly varies between different maps. Several approaches have been proposed for dealing with the fuzziness of semantic properties, notably using fuzzy logic [34], agents [35] as well as information entropy [36].

### 2.3.3 Classification by application scenario

Most applications of georeferencing techniques fall into one of the following categories: Map editing, map creation, map validation, map matching, georeferencing of media. Figure 2-3 shows a classification of the application scenarios of the georeferencing domain.

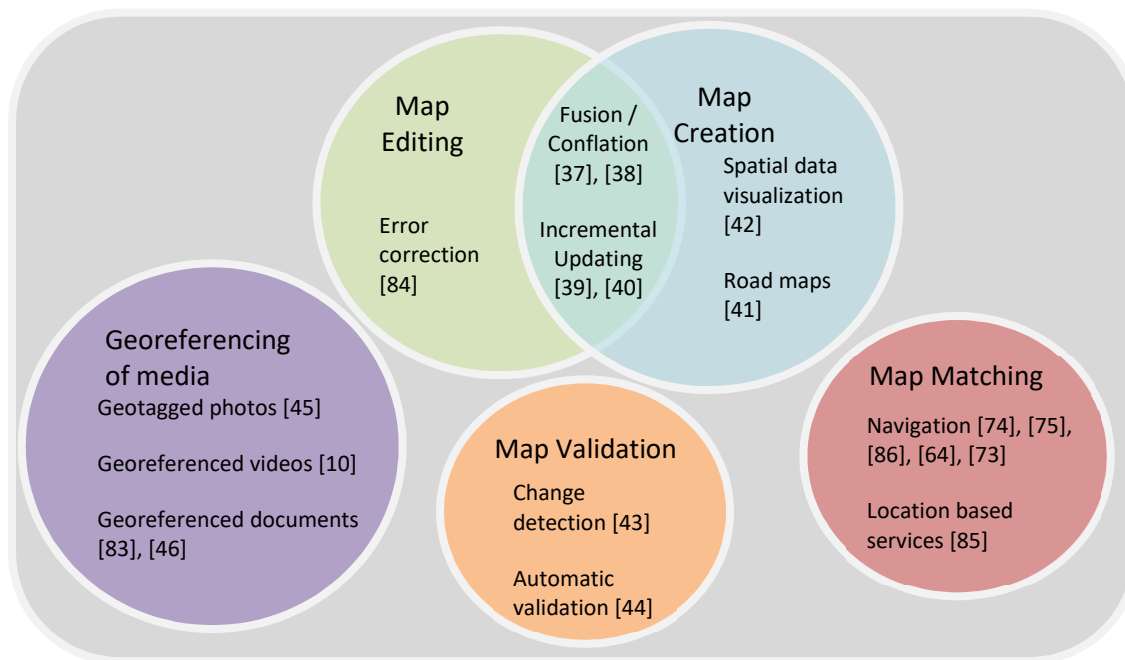


Figure 2-3: Application scenarios.

### 2.3.3.1 *Map Manipulation*

Map manipulation is the process of altering certain objects in maps. This may e.g. be required to correct errors present in a map which can be detected using map validation. As a result of a conflation process [37] [38], additional attributes such as POIs can be merged into a map. Incremental updating is used in order to only replace those parts of a map which have changed in a more recent version, which can be derived via change detection. The problem of incremental updating is of rising concern to the automotive navigation industry [39] [40].

### 2.3.3.2 *Map Creation*

Maps may be authored from scratch, for example by creating geographical entities and references based on satellite or aerial imagery (see 2.2.1) or highly accurate GPS traces [41]. Another option is to create maps by combining two or more source maps into a new map using conflation methods [37] [38]. In general, it is possible to create visualizations of any data possessing spatial references [42].

### 2.3.3.3 *Map Validation*

Map validation is concerned with evaluation of certain properties in maps, such as geometrical correctness or the presence of a normal form with respect to certain topological properties. Quality metrics used to assess a map can be derived by detecting and evaluating changes. E.g., regression errors may be identified using change detection [43]. Automatic validation [44] aims to validate a map according to such quality metrics without the need for assistance provided by a human operator.

### 2.3.3.4 *Map Matching*

Matching a point on a vector map is a requirement for navigation (e.g. for cars or pedestrians). Also, other applications needing exact positioning, such as location based services, rely on map matching in order to identify the position of the user on a map.

### 2.3.3.5 *Georeferencing of media*

Zheng et al. [10] describe various applications of enhancing media (photos, videos, and documents) with geographical references, which are often encoded as WGS-84 coordinates. E.g., photo layers for services such as Google Earth provide the user with crowd-sourced geo-tagged imagery of millions of locations around the globe. Snavely et al. [45] introduce a method for determining the exact position of images in three-dimensional space, including the angle of the camera, which enables the 3D exploration of photo collections. Also, videos and travel logs may be georeferenced in order to associate them with geographical locations where a video was shot or the author of a travel log has been. Spatial Markup Languages such as SpatialML [46] allow for embedding spatial references into natural language documents.

## 2.4 **Road Network Conflation**

As it has been elaborated before, Road Network Conflation is concerned with the unique identification of geographical entities across different road networks. These entities range from elemental structures – such as crossings represented by nodes in the network – to aggregated high-level entities such as topological edges, sequences of edges or even subgraphs of the induced graph of the road network. The road networks to be conflated are investigated with regard to topological, geometrical and semantic information in order to identify similarities and differences.

The elements of Road Network Conflation are illustrated in Figure 2-4: Point Referencing, Location Referencing, and Road Network Conflation (from left to right).

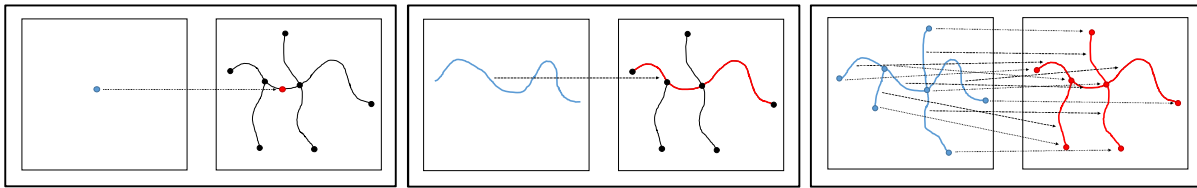


**Figure 2-4: Point Matching, Location Referencing, Road Network Conflation (from left to right).**

In this figure, the dashed arrows symbolize associations between the geographical entities. While in the case of Point Referencing, a 0-dimensional entity given by a geographical position is projected into a road network, Location Referencing implies the association of a 1-dimensional route with a sequence of road segments within a road network. Road Network Conflation, in contrast, aims to establish associations between two different road networks. In this example, a 1:1 correspondence can easily be identified between the two networks, which rarely occurs in real-world settings. Associations are shown at the level of topological nodes and road segments.

Topologically, each map consists of a graph (the road network) given by *edges* and *nodes* (vertices), where a node represents a geographical point referenced via its coordinates in a suitable reference system (e.g. WGS-84), and an edge is given by a relation which describes a connection between two nodes. For the purposes of conflation, the graph may be seen as being undirected to simplify the process. It should be noted that many map providers insert bivalent nodes (nodes which are only incident to two edges) at locations where attributes change which are recorded per edge. Occasionally, the terms *0-cells* for nodes, *1-cells* for edges, and, subsequently, *2-cells* for polygons consisting of a sequence of edges are used [47].

Geometrically, the shape of a road segment represented by an edge in the graph is often described via *shape points* (not explicitly shown in the figures), where a sequence of shape points constitutes the geometrical layout of the road segment corresponding to an edge. Like nodes, shape points are defined by their coordinates. Continuous shape geometry is created by employing linear interpolation between shape points. Alternatively, concepts such as splines may be used to model road geometry.

Figure 2-5 shows a road map of the village of Moosach, near Munich, Germany, provided by the Bavarian State Office for Survey and Geoinformation, Munich, which is called ATKIS Basis-DLM. This area is overlaid with a road map built from geographic data provided by the Volunteered Geographic Information (VGI) project OpenStreetMap (OSM).

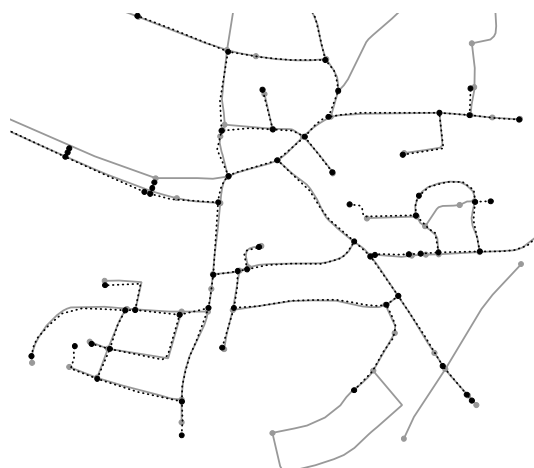


**Figure 2-5: Overlay of two maps of the same region (gray solid: ATKIS, black dashed: OpenStreetMap).**

As can be seen in Figure 2-5, several problems surface when dealing with the road network conflation problem in real-world scenarios:

1. *Topological differences:*

The two maps do not share the same topology. Rather, roads are present in one map which are missing in the other map. Also, due to a varying level of detail, even roads present in both maps may be modelled with a different number of nodes. In addition, structures such as complex intersections may be modelled differently, resulting in a different placement of nodes and edges.

2. *Geometric differences:*

Due to varying accuracy in the recorded coordinates, the geographical location of nodes representing the same topological entity may differ between the maps to a great extent. On the other hand, nodes in close proximity do not necessarily imply a topological relationship. The same applies to the geometrical layout of road segments between the maps.

3. *Semantic differences:*

Nodes and edges carry semantic information, such as the name of a road. While semantic similarity of two edges in different maps often indicate that the same road is referenced, semantic dissimilarity rarely implies the opposite, since semantic attributes as well as the extent to which they are recorded vary greatly across different map providers and sources. E.g., street names may be spelled differently, and there may also be multiple names for the same street.

Figure 2-6 depicts the same crossing (Reichenbachplatz in Munich, Germany) as modelled by two different map vendors. It can clearly be seen in this real-world example that major topological as well as geometrical differences can occur between road networks of different sources representing the same geographical entity.



**Figure 2-6: Differences in modelling of road networks between two map vendors**

Finally, Figure 2-7 shows another real-world example to illustrate the problem of finding associations between road networks of different maps of the same region.

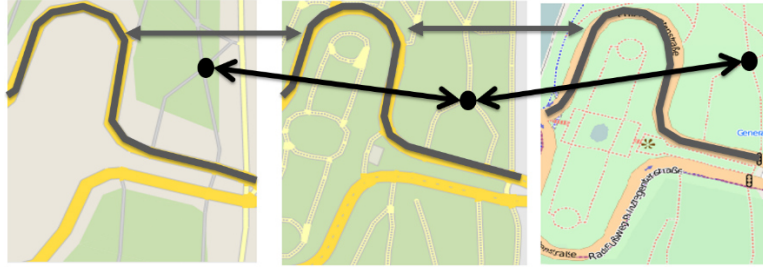


Figure 2-7: The same region of the inner city of Munich as seen by three different map vendors

Several different approaches have been proposed to tackle the Road Network Conflation problem. These are introduced in the following section, starting with point-based approaches, followed by line-based and structural methods.

## 2.5 Road Network Conflation Methods

### 2.5.1 Point-based approaches

#### 2.5.1.1 Definitions and prerequisites

In order to discuss point-based approaches, some definitions are needed. The following gives a formal definition of solutions to the point matching problem for two road networks with respect to topological nodes.

**DEFINITION 1: POINT MATCHING FOR TWO ROAD NETWORKS.**

Given are two undirected simple graphs  $G_1, G_2$  representing a road network:  $G_i = (V_i, E_i), i \in \{1,2\}$ , where  $V_i$  is the set of vertices of graph  $G_i$ , and  $E_i$  the edge relation of Graph  $G_i$ , and  $E_i \subseteq (V_i \times V_i)$ . Then, a *point matching* is a pair  $(p_1, p_2)$ , where  $p_1 \in V_1$  and  $p_2 \in V_2$ .

**DEFINITION 2: SOLUTION TO THE POINT MATCHING PROBLEM FOR TWO ROAD NETWORKS.**

A *solution* to the point matching problem for two road networks is a relation  $S \subseteq (V_1 \times V_2)$ , i.e., a set of *point matchings*.

**DEFINITION 3: LEFT-UNIQUE SOLUTION TO THE POINT MATCHING PROBLEM FOR TWO ROAD NETWORKS.**

A *left-unique solution* to the point matching problem for two road networks is an injective relation  $S_l \subseteq (V_1 \times V_2)$ .

**DEFINITION 4: RIGHT-UNIQUE SOLUTION TO THE POINT MATCHING PROBLEM FOR TWO ROAD NETWORKS.**

A *right-unique solution* to the point matching problem for two road networks is a functional relation  $S_r \subseteq (V_1 \times V_2)$ .

**DEFINITION 5: UNIQUE AND COMPLETE SOLUTIONS TO THE POINT MATCHING PROBLEM FOR TWO ROAD NETWORKS.**

A *unique solution* to the point matching problem for two road networks is a right-unique and left-unique relation  $S_u \subseteq (V_1 \times V_2)$ . Note that  $S_r \cap S_l$  is a unique solution. If  $S_u$  is also surjective and left-total, it is a *complete solution*.

Notes:

- A solution according to Def. 2 represents an  $m:n$  type mapping between nodes of  $V_1$  and  $V_2$ .
- A left-unique solution according to Def. 3 represents a  $1:n$  type mapping between nodes of  $V_1$  and  $V_2$ .
- A right-unique solution according to Def. 4 represents a  $n:1$  type mapping between nodes of  $V_1$  and  $V_2$ .
- A unique solution according to Def. 5 represents a  $1:1$  type mapping between nodes of  $V_1$  and  $V_2$ .
- A complete solution only exists if  $|V_1| = |V_2|$ .

Point matching algorithms determine and evaluate point matching candidates (i.e., a subset of all point matchings) with respect to certain metrics. In general, a metric is defined as follows:

**DEFINITION 6: METRIC DEFINITION FOR POINT MATCHING.**

A *metric* on a set  $X := V_1 \cup V_2$  is a function  $d: X \times X \rightarrow \mathbb{R}$  where  $\forall x, y, z \in X$ , these conditions must be satisfied:

- (a)  $d(x, y) = 0 \Leftrightarrow x = y$
- (b)  $d(x, y) = d(y, x)$
- (c)  $d(x, z) \leq d(x, y) + d(y, z)$

In the context of the point matching problem, a metric can be used as a distance function between two points of a point matching. The distance according to the metric can then be interpreted as the degree of dissimilarity of the two involved points. This distance may be normalized, e.g. by projecting it onto the interval  $(0; 1]$ , where 1 corresponds to the lowest possible distance (0, meaning equality) and 0 corresponds to an infinitely long distance. We call such a projection a *score*, because it is positively correlated with the expected quality of the matching from the perspective of the interpretation of the according metric. The overall score which an algorithm attributes to a point matching may be a weighted combination of multiple scores from different metrics.

In order to limit the computational effort, point matching algorithms usually only evaluate a small subset of all possible point matchings. Most point matchings are discarded beforehand due to spatial constraints, since it is assumed that the probability of two points representing the same spatial entity quickly becomes extremely low as the distance between the points increases beyond several kilometers. The fact that point matching algorithms, unlike pure graph matching approaches, may not only rely on topological but also on geometric information thus greatly simplifies the point matching problem, since it reduces the number of potential candidates.

While a complete solution as defined in Def. 5 may seem desirable, it only exists for very simple scenarios where the two maps being compared are virtually identical (e.g., very minor map updates). In real-world applications, usually both maps contain several nodes which cannot reasonably be matched to the other map.

Point matching algorithms deliver a set of point matchings, where each point matching is assumed to identify the same geographical entity across both maps. This is done by evaluating the degree of similarity between point matchings close enough to become candidates according to certain metrics,

then selecting those point matchings for the solution which are considered similar enough that they may reasonably represent the same spatial feature (e.g. by applying a global or local threshold on the score). In general, this solution is ambiguous, implying that any point on any of the two maps may be matched to more than one point in the other map. It is possible to establish unique solutions by discarding all matchings related to a node except the highest-rated point matching. However, in special cases, a geographical entity represented by one topological node in one map may be (partially) represented by multiple nodes in the other map (e.g. bivalent nodes, differing level of detail, or complex intersections), so these cases must be recognized and dealt with separately. The problem of ambiguity with regard to point matching is further discussed in 3.2.1.

With these definitions and prerequisites, we may now proceed to the introduction of point-based approaches, which may be either geometrical, or topological, or both.

### 2.5.1.2 Geometrical point matching techniques

Geometrical point matching techniques only consider geometrical information (i.e., coordinates) for evaluating a point matching. Even though the distance between point coordinates may be calculated in any p-norm, the only metric of practical relevance is the Euclidean distance metric.

#### Euclidean

Obviously, spatial proximity is a strong constraint for the selection of matching candidates. In the Euclidean plane, the distance  $\text{dist}(p, q)$  of two points  $p = (p_x, p_y)$  and  $q = (q_x, q_y)$  is given by

$$\text{dist}(p, q) = \sqrt{(p_x - q_x)^2 + (p_y - q_y)^2}.$$

While for small geographical regions, Euclidean geometry is a good approximation, a more exact measure for the distance between two points on the surface of the Earth is the great-circle distance, which describes the shortest distance between any two points on the surface of a sphere following a path on the surface. The great-circle distance can be computed using the spherical law of cosines or the numerically better-conditioned Haversine formula [48]. The approaches presented in this thesis use a Euclidean distance metric applied to a *Universal Transversal Mercator* (UTM) projection of WGS-84 coordinates for calculating distances, as it provides sufficient accuracy and can be computed efficiently.

A straightforward approach to conduct Euclidean point matching calculates the Euclidean distance  $\text{dist}(p, q)$  for each point matching pair  $(p_i, q_j) \in (V_1 \times V_2)$  which possesses all properties of a metric function as defined in Def. 6. To extract a right-unique solution  $S_r$ , each  $p_i \in V_1$  is assigned to a  $q_j \in V_2$  where  $\text{dist}(p_i, q_j)$  becomes minimal so that  $(p_i, q_j) \in S_r$  and  $(p_i, q_{k \neq j}) \notin S_r \forall q_k \in V_2$ . In order to gain a left-unique solution  $S_l$ , each  $q_j \in V_2$  may only be related to a  $p_i \in V_1$  where  $\text{dist}(p_i, q_j)$  becomes minimal so that  $(p_i, q_j) \in S_l$  and  $(p_{k \neq i}, q_j) \notin S_l \forall p_k \in V_1$ . Finally, a unique solution  $S_u = S_r \cap S_l$  can be derived.

This approach is obviously inefficient as it evaluates every possible point matching pair. However, by employing a spatial index (e.g. a kd-tree) and only evaluating neighbors within a sufficiently large radius, Euclidean matching may be performed efficiently without losing substantial accuracy.

The Euclidean distance may be projected to a score of the interval  $(0; 1]$  by using the following formula:

$$\text{score}_{\text{PE}}(p_i, q_j) = \frac{1}{1 + \left(\frac{\text{dist}(p_i, q_j)}{c \cdot r}\right)^2}$$

where  $c \in \mathbb{R}^+$  is a correction factor and  $r \in \mathbb{R}^+$  is the node search radius. Note that  $\lim_{\text{dist} \rightarrow \infty} \text{score}(p_i, q_j) = 0$  for any  $c, r$  with  $c \cdot r > 0$ . A function graph of this projection for  $c = r = 1$  can be seen in Figure 2-8.

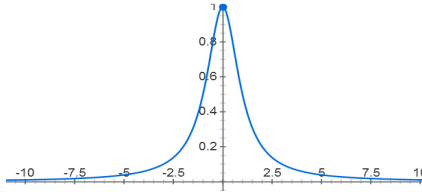


Figure 2-8: Score Projection of Euclidean Distance (for  $c=r=1$ )

### 2.5.1.3 Topological point matching techniques

Topological point matching techniques employ topological information such as the valence (number of incident edges) per node.

#### Node Valence

The valence, or *degree*, of a node in a graph is defined as the number of edges incident to the node, where loops are counted twice.

The *Node Valence* point matching approach is concerned with the differences in valence found between the two nodes of a point matching. The larger this difference grows, the lower the probability becomes that both nodes reference the same geographical entity. However, minor differences in valence are no guarantee that the nodes are a bad matching, since the two maps may differ in actuality or level of detail so that e.g. small roads may only be present in one map. Also, a valence difference of zero does not imply node equality, so that node valence on its own does not qualify as a metric, since it violates condition (a) in Def. 6.

The valence difference may be combined with the Euclidean distance to obtain an order in case of equal valence difference. Since point matchings of large geometrical distances are unlikely to represent a proper solution, the search for matching candidates regarding a node may be limited to its neighborhood within a certain radius. Only within this neighborhood, node valence needs to be evaluated. The lower the difference of valence is, the higher the assumed similarity of two nodes. If two matching candidate pairs are assigned to the same equivalence class regarding their valence difference, the pair with the lower Euclidean distance is assumed to be more similar. Depending on properties of the maps to be matched such as node density or dispersion, Node Valence may require a fine-tuning of the search radius to provide acceptable solutions.

A straightforward approach for calculating a score based on valence difference is reflected by the following formula:

$$\text{score}_{\text{NV}}(p_i, q_j) = \frac{1}{1 + |\text{val}(p_i) - \text{val}(q_j)|}$$

### 2.5.1.4 Combined geometrical / topological point matching techniques

Combined geometrical / topological point matching techniques are employed by algorithms which follow both geometrical as well as topological approaches and combine them in order to achieve better matching results.

#### Spider Index

Rosen and Saalfeld [47] describe a point matching technique called the *Spider Index*, which overlays a node with a circular 8-sector discretization of 45° angle intervals similar to a compass rose. Each sector corresponds to one bit within an 8-bit number. Figure 2-9 shows the original illustration by Saalfeld [6].

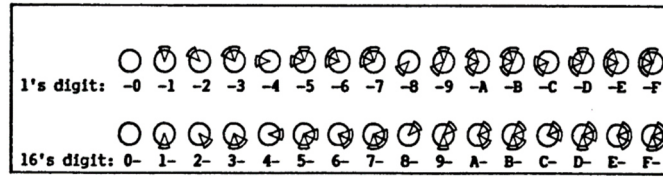


Figure 2-9: Spider Index, reproduction of original image from [6].

A bit is set to true if and only if there is an incident edge that falls into the corresponding sector. Thus, each node  $p$  can be described by an 8-bit number with bits  $p_{b_1} \cdots p_{b_8}$ . For two nodes  $p \in V_1$  and  $q \in V_2$  the score of the spider index is then calculated as

$$\text{score}_{\text{SI}} = \frac{1}{8} \sum_{i=1}^8 \vartheta(p_{b_i}, q_{b_i}),$$

where  $\vartheta(p_{b_i}, q_{b_i}) = p_{b_i} \leftrightarrow q_{b_i}$  is the binary equivalence function, i.e.  $\vartheta = 1$  if bits are equal and  $\vartheta = 0$  if they are different. Note that we have normalized the score to the interval  $[0; 1]$ .

Due to the information loss resulting from the quantization, two nodes may still be considered equal if the angles of their incident edges are different within the limits of a sector. Moreover, it may happen that two nodes are not considered equal if the angles of their incident edges are rotated by a tiny degree, but beyond the limits of a sector. Yet, compared to Node Valence, the Spider Index offers a more accurate measure for node equality, as it not only accounts for topological valence difference, but also geometrical angle difference.

As with Node Valence, the Spider Index alone does not qualify as a metric, since two matching candidate pairs whose bit difference regarding their Spider Index is zero may still be different. However, in the same way as with Node Valence, the Spider Index may be turned into a metric by combining it with the Euclidean distance, so that Euclidean distance determines an order where the Spider Index does not discriminate.

#### Exact Angular Index

The *Exact Angular Index* (EAI) is a novel similarity index first introduced by Hackeloeer et al. in [49]. Like the Spider Index, the EAI aims to find point matching solutions which consider both topological valence and geometrical angle difference of incident edges. However, the EAI does not employ quantization. Rather, the best mapping between the edges of the two nodes of a matching candidate, i.e. the mapping which minimizes the angle differences between the vectors derived from the

geometrical shapes of the edges, is determined by evaluating all possible edge mappings. Then, a score is calculated based on the sum of minimum angle differences according to the mapping relative to the largest possible sum of angle differences, where differences in valence are counted as the worst possible angle differences.

Formally, the algorithm follows these steps to iteratively assign a score to point matchings  $\{(p_i, q_j) | p_i \in V_1, q_j \in V_2\}$  for each  $p_i$  with incident edges  $E_{p_i} \subseteq E_1$ :

- For each incident edge of  $p_i$ , calculate the geographical heading, i.e. the angle between the vector given by the first linear segment of the edge and true north in clockwise direction. The result is a heading function  $h_{p_i}: E_{p_i} \rightarrow \mathbb{R}$ .

- Search for nodes  $q_1, \dots, q_n \in V_2$  in  $G_2$  within a fixed radius around the position of  $p_i$ . If no surrounding nodes can be found, no matching partner can be assigned to  $p_i$ , so the algorithm continues with the next node  $p_{i+1}$ .

- For each found node  $q_j \in V_2$  with incident edges  $E_{q_j} \subseteq E_2$ :

1. Calculate the heading function  $h_{q_j}: E_{q_j} \rightarrow \mathbb{R}$ .
2. Calculate the best-mapping function  $b_{q_j}^{p_i}: E_{p_i} \rightarrow E_{q_j}$  which determines the optimum mapping from each edge incident to  $p_i$  to an edge incident to  $q_j$  regarding their angle difference, using  $h_{p_i}$  and  $h_{q_j}$ . If  $|E_{p_i}| > |E_{q_j}|$ , there are edges  $\overline{E_{p_i}} \subseteq E_{p_i}$  which could not be mapped to edges of  $E_{q_j}$  and  $b_{q_j}^{p_i}(e) = \emptyset \forall e \in \overline{E_{p_i}}$ .
3. Calculate the sum of all angle differences  $s_{\text{all}}$  by adding up the differences between the headings of all best-mappings gained from  $b_{q_j}^{p_i}$ :

$$s_{\text{all}} = \sum_{k=1}^n \Delta \left( h_{p_i}(e_k), h_{q_j}(b_{q_j}^{p_i}(e_k)) \right)$$

where  $1 \leq k \leq n$ ,  $\{e_1, \dots, e_n\} \subseteq E_{p_i} \setminus \overline{E_{p_i}}$  and  $\Delta(\alpha, \beta)$  is the angle difference computed by  $\Delta(\alpha, \beta) = \text{mod}(|\alpha - \beta|, 360)$ .

4. If there is a difference in valence between  $p_i$  and  $q_j$ , add an angle difference of  $180^\circ$  per missing or redundant edge to get the normalized sum of all angle differences  $s_{\text{norm}}$ :

$$s_{\text{norm}} = s_{\text{all}} + 180 \cdot |\text{val}(p_i) - \text{val}(q_j)|$$

where  $\text{val}(p)$  is the valence of node  $p$ .

5. Calculate the largest possible sum of angle differences  $s_{\text{largest}}$ :

$$s_{\text{largest}} = 180 \cdot \max(\text{val}(p_i), \text{val}(q_j))$$

Then project the quotient of  $s_{\text{norm}}$  and  $s_{\text{largest}}$  onto a score in the interval of  $[0; 1]$  which expresses the degree of similarity by subtracting it from 1:

$$\text{score}_{\text{EAI}}(p_i, q_j) = 1 - \frac{S_{\text{norm}}}{S_{\text{largest}}}$$

The best-mapping function  $b_{q_j}^{p_i}$  employs a queue for edges  $Q = \{e_{p_i}^1, \dots, e_{p_i}^n\} \subseteq E_{p_i}$  which are not mapped yet, a mapping relation  $M \subseteq (E_{p_i} \times E_{q_j})$  holding established mappings, a record function  $R: E_{q_j} \rightarrow (E_{p_i}, \mathbb{R})$  storing the best angle difference found for a destination edge found so far along with its source edge, and an angle difference function  $\text{ad}_{q_j}^{p_i}: (E_{p_i}, E_{q_j}) \rightarrow \mathbb{R}, (e_1, e_2) \mapsto \Delta(h_{p_i}(e_1), h_{q_j}(e_2))$ .

Initially,  $Q = E_{p_i}$ ,  $M = \emptyset$  and  $R(e) = (\emptyset, \infty) \forall e \in E_{q_j}$ . The algorithm then repeats the following steps until  $Q = \emptyset$ :

1. Take one edge  $e_{p_i}^k$  from queue  $Q$  so that  $Q := Q \setminus \{e_{p_i}^k\}$ .
2. Create sorted list  $(d_1, \dots, d_n)$  of angle differences between  $e_{p_i}^k$  and each  $e_{q_j}$  incident to  $q_j$  using  $\text{ad}_{q_j}^{p_i}$ . Also store the assignment between  $d_i$  and  $e_{q_j}$  as function  $\text{ea}: \mathbb{N} \rightarrow E_{q_j}, i \mapsto e_{q_j}$ .
3. For each  $(d_i, \text{ea}(i))$ : Iteratively verify record  $R(\text{ea}(i)) = (e_{p_i}^{\text{old}}, \partial_{q_j}^{\text{old}})$ . If  $d_i < \partial_{q_j}^{\text{old}}$ , enqueue  $e_{p_i}^{\text{old}}$  ( $Q := Q \cup \{e_{p_i}^{\text{old}}\}$ ), update  $R(\text{ea}(i)) := (e_{p_i}^k, d_i)$ , and leave iteration (since everything that follows would be a worse assignment, as the list is sorted). Otherwise, proceed until a new difference record has been found or there are no differences left.

If  $Q = \emptyset$ , add all projections of  $R(e_{q_j}) = (e_{p_i}, x)$  to  $M$  ( $M := M \cup \{e_{p_i}, e_{q_j}\}$ ) where  $R(e) \neq (\emptyset, \infty)$ . Then,  $M$  holds the optimum mapping and the algorithm terminates.

### Exact Angular Index + Distance

It is possible to calculate a weighted score  $\text{score}_w(p_i, q_j)$  which incorporates both the Exact Angular Index as well as the Euclidean distance with the following formula:

$$\text{score}_w(p_i, q_j) = w_1 \cdot \text{score}_{\text{EAI}}(p_i, q_j) + w_2 \cdot \text{score}_{\text{PE}}(p_i, q_j)$$

where  $w_1 = |1 - w_2| \in [0; 1] \subseteq \mathbb{R}$  describes the weight given to the topological similarity of the nodes expressed by the EAI score, and  $w_2 = |1 - w_1| \in [0; 1] \subseteq \mathbb{R}$  stands for the weight given to the geometrical similarity of the nodes expressed by the Euclidean score.

### 2.5.2 Line-based and structural approaches

The following matching algorithms are line-based and structural approaches to the conflation of road networks:

- *Buffer Growing* [50], [51], [52]
- *Multi-Stage Matching* [37], [53]
- *Delimited Stroke Oriented Matching* [54], [14]

### 2.5.2.1 Buffer Growing

Walter [50] describes a geometric matching approach for line objects using the concept of Buffer Growing, which is also employed by Mantel & Lipeck [51] for the matching of geometric datasets. Zhang & Meng [55] suggest a road-matching approach based on Buffer Growing which also accounts for systematic geometric deviations by using unsymmetrical buffers.

Buffer Growing assumes a certain similarity regarding the location of the line objects to be matched, which may require preceding transformations. A line object originating from the Reference Network which we call the *reference link sequence* is encircled by a buffer, and then the Matching Network is spatially searched for all line objects which are fully covered by that very buffer, which we call *matching link sequences*. A result list holds assignments between reference link sequences and matching link sequences. In each iteration, the matching link sequence is added to the result list along with the corresponding reference link sequence as long as it cannot be derived from concatenating prior results, and then the reference link sequence along with the buffer boundary is extended by one link. The process stops when either certain pre-defined boundaries are reached, such as nodes having a valence of 1 or a valence of at least 3, or if the reference link sequence exceeds an arbitrary number of links. Figure 2-10 shows the original illustration of Walter explaining the process.

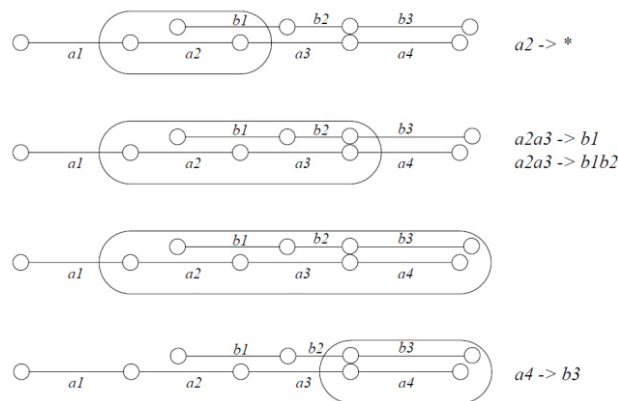


Figure 2-10: Buffer Growing. Reproduction of original image from [50], p.64.

Buffer Growing already implies a limitation on the number of link sequence pairs to be evaluated by means of the size of the buffer. In order to further limit the number of necessary comparisons, Walter suggests to employ geometrical restrictions regarding the length, the angle or the shape of the line objects to be compared, as it e.g. can be considered unlikely that line objects are correlated if they intersect at an angle of 90 degrees [50]. Still, the approach suffers from high combinatorial complexity, as no prior filtering derived from node assignments is performed.

### 2.5.2.2 Multi-Stage Matching

Xiong [37] proposes a three-stage approach for Road Network Conflation which consists of the stages node matching, segment matching, and edge matching. These stages are first processed bottom-up, i.e. from nodes via segments to edges, and then top-down, i.e. from edges via segments to nodes. In the bottom-up process, associations between nodes are established, which are then used to associate segments and edges. The edge mapping is aggregated from the segment mapping gained from associating the nodes. The top-down process propagates edge correspondences down to the level of elementary nodes in order to identify additional node associations.

For associating the nodes in the first stage, Xiong includes geometrical point distance as well as topological similarity, calculated by a metric which considers the angle difference of incident edges of a node similar to the Spider Index introduced by Saalfeld [6]. The segment mapping of the second stage incorporates several distance measures between segments. Edges are matched throughout the third stage by searching within a pre-defined maximum matching distance, while accounting for requirements such as minimum length and maximum angle difference.

Volz [53] describes an approach which relies on combined edge and node matching. First, the network is preprocessed. On the one hand, geometric deviations are reduced by applying a rubber sheeting transformation on warping vectors derived from so-called “warping nodes” considered to expose a high degree of correspondence. On the other hand, a topological splitting takes place which transfers nodes from the Reference Network to the Matching Network if no matching candidates can be found, in order to reduce ambiguities. After these preprocessing steps, seed nodes are identified in the Reference Network, which are required to have more than two incident edges. Then, for each seed node, matching candidates are selected from the Matching Network within a fixed radius. The candidates must possess the same number of incident edges as the seed node with nearly the same angle (a difference of max. 5 degrees is accepted). The process is repeated vice versa, i.e. with switched roles of the Matching and Reference Network. The nodes of a node pair are considered seed nodes if there is mutually only one counterpart.

Once the seed nodes have been associated, the respective line objects, which correspond to link sequences, are compared. Their similarity score is calculated based on a number of topological and geometrical distance metrics such as length difference, angle difference, average line distance and Vertex-Hausdorff distance. If this score exceeds a certain threshold, the line objects are identified as a matching. Finally, multiple iterations are performed in order to successively re-associate nodes by incorporating more tolerant criteria, which leads to the identification of new matching pairs. If 1:2 edge matchings are found, these are treated separately using another similarity score so as to decide if a real-world ambiguity situation has been identified.

Both approaches rely on a node matching algorithm which derives a similarity score between two nodes from the position of incident edges within discrete sectors. However, it has been shown that non-sector-oriented point matching algorithms lead to more accurate results [49].

#### 2.5.2.3 *Delimited Stroke Oriented Matching*

Delimited Stroke Oriented Matching (DSO) is a Road Network Conflation algorithm introduced by Zhang [14] which builds upon the Buffer Growing approach. After several preprocessing steps, a matching procedure is carried out which consists of five steps which are repeated at three different levels. The DSO algorithm operates on entities called *Delimited Strokes*, which are line objects corresponding to link sequences.

During preprocessing, topological ambiguity is eliminated by displacing ambiguous nodes to the node closest to the respective matching partner. Then, the Delimited Strokes are constructed, depending on the level. In level 1, a Delimited Stroke represents “a series of connected objects which have *good continuity* to each other and are delimited by *efficient terminating nodes*”. In level 2, it represents “an object chain which is delimited by crossings or dead-ends”, and in level 3, it “is equal to an object” [14]. The term “good continuity” refers to the Gestalt laws and is influenced by the sharpness of turning angles. Nodes are considered “efficient terminating nodes” if they follow several rules, such as having

a valence larger than three or a valence of one. If a node has a valence of three, additional context information such as the continuity of incident edges is considered for deciding whether a node belongs to this group.

In the matching process, first potential matching pairs are identified by investigating the area within a fixed search radius around the start and end nodes of a Delimited Stroke (step 1). Then, incorrect potential matching pairs are excluded by accounting for differences in orientation, length, average area, shape, and location (step 2). The remaining matching pairs are subject to a further investigation, which removes some ambiguity by calculating a similarity score based on topological and geometrical differences and selecting the pair with the highest score (step 3). A so-called *network-based selection* detects conjoint Delimited Strokes and arranges them into a single network, which is then used for *network-based matching* (step 4). In this sense, a network is defined as a series of oriented Delimited Strokes which are interconnected by nodes which represent a crossing or an intersection. The similarity of the matching networks is computed based on the similarity of the incorporated Delimited Strokes. If two or more promising matching pairs have been identified, multiple matching networks are derived, of which the best match is selected based on the network similarity score. Finally, the node pairs on twigs of the matched networks are used as seeds for matching-growing, which leads to the identification of new Delimited Stroke matching pairs (step 5). The growing continues as long as the new matched pairs exhibit sufficient geometrical and topological similarity. The remaining fragments are subject to a subsequent process which employs a decomposition of the Delimited Strokes in order to account for partial correspondences.

Situations such as the presence of roundabouts or dual carriageways are identified via a pattern matching approach and separated from the general matching process, so that specialized heuristics can be employed. In addition, a semantical matching process takes place which associates geographical objects based on the similarity of their semantic attributes, e.g. by calculating the Levenshtein distance.

While the DSO algorithm is capable of dealing with numerous matching cases, the large number of heuristics involved leads to a very high overall complexity of the process in terms of both computation time as well as necessary parameter adjustments.

### 2.5.3 Comparison of Road Network Conflation Methods

Table 2-1 gives an overview the methods introduced before, which have been selected as representatives for the state of the art.

Category	Name	Advantages	Disadvantages
Point-based / Geometrical	Euclidean	Simple concept, low computational complexity, fairly good results for sparse road networks	Does not account for topological similarity leading to bad results for dense road networks
Point-based / Topological	Node Valence	Simple concept, low computational complexity	Topological similarity alone is not sufficient for good results
Point-based / Combined	Spider Index	Accounts for geometrical as well as topological similarity, better results than purely geometrical approaches	Quantization of angles into sectors leads to errors at sector borders

	Exact Angular Index	Calculates the optimum solution by evaluating all possible assignments of edges, best results of all point-based matching approaches	Computational complexity increases nonlinearly with the number of incident edges
Line-based and structural	Buffer Growing	Fairly simple concept, good results for road networks of low complexity	High computational complexity, no prior filtering derived from node assignments, no structural analysis, no refinement of identified line-to-line assignments
	Multi-Stage Matching	Topological splitting reduces ambiguities, associations are derived on the level of nodes, segments and edges, dedicated treatment of 1:2 associations between edges	No structural analysis beyond the edge level, no dedicated treatment of ambiguities between nodes, node similarity is computed with a quantization-based approach similar to Spider Index
	Delimited Stroke Oriented Matching	Very thorough examination (five steps on three levels) incorporating a large number of heuristics, similarities are identified on the stroke and the network level, semantical matching	No generic approach for the identification of similarities on the structural level, large number of heuristics employed leads to very high overall computational complexity, no comprehensive concept for ambiguities

**Table 2-1: Advantages and Disadvantages of Road Network Conflation Approaches**



### 3 Exploration of the Research Domain

This chapter aims to deeply explore the research domain. It starts with a proposal of a formal mathematical definition of Road Network Conflation. The problem of ambiguity can then be discussed, which necessarily arises when conflating non-trivial road networks. Ambiguity may appear on every possible layer of abstraction from elemental point objects to aggregated high-level structures, which are dealt with in separate sections. The formal definition of the conflation is based on the work which has first been published in [1].

#### 3.1 Formal Definition of Road Network Conflation

Let  $M_1 := (N_1, E_1)$  a graph representing a road network, where  $E_1 \subseteq (N_1 \times N_1)$ , and  $M_2 := (N_2, E_2)$  another graph representing a road network of the same area, where  $E_2 \subseteq (N_2 \times N_2)$ .  $M_1$  is also called the *Reference Network*, while  $M_2$  is called the *Matching Network*. We call  $N_i := \{N_i^1, \dots, N_i^{n_i}\}$ ,  $n_i \in \mathbb{N}$  the *nodes* of road network  $M_i$  and  $E_i := \{E_i^1, \dots, E_i^{m_i}\}$ ,  $m_i \in \mathbb{N}$  the *links* of road network  $M_i$ . The nodes of both graphs are allowed to be bivalent, reflecting the fact that road networks of digital road maps often contain bivalent nodes, e.g. at places where a crossing existed in a prior version of the map or where a link-specific attribute such as a speed limit changes its value. We then call  $S_i := (E_i^j, E_i^k, \dots, E_i^x)$  a *link sequence* created from the concatenation of consecutive links of the edge relation  $E_i$ . A link sequence corresponds to a simple path from the starting node of  $E_i^j$  to the ending node of  $E_i^x$ .

We define a *node matching relation*  $P \subseteq (N_1 \times N_2)$  as a set of node pairs, where for each pair the first node is taken from the nodes of  $M_1$  and the second node is taken from the nodes of  $M_2$ . Thus, any  $p = (p_1, p_2) \in P$  assigns a node  $p_1 \in N_1$  to a node  $p_2 \in N_2$ . Note that in general, we neither require  $P$  to be functional, nor injective, i.e., one node of  $N_1$  may be assigned to multiple nodes of  $N_2$ , and vice versa. This is motivated by the fact that many-to-many relationships between nodes may and are likely to exist when conflating road networks from different sources. A node matching relation represents a solution to the road network conflation problem on the elementary level of topological nodes.

In order to refine our solution towards the level of aggregated structures such as links and link sequences, we define a *link sequence matching relation*  $L \subseteq (S_1 \times S_2)$  as a set of link sequence pairs, where for each pair the first link sequence consists entirely of consecutive links taken from  $E_1$  and the second link sequence consists entirely of consecutive links taken from  $E_2$ . A link sequence matching relation represents a solution to the road network conflation problem on the level of one-dimensional structures. Again, many-to-many relationships between link sequences of the road networks to be conflated may exist. This may e.g. be the case if the modeling of a road with a physical divider differs between the road networks.

So far, we have only defined solutions which allow for describing total correspondences, i.e. situations where a link or a sequence of links of  $M_1$  corresponds to another link or sequence of links of  $M_2$  a whole. However, often partial correspondences are present. For example, it may occur that we have two links  $e_a, e_b \in E_1$  and another link  $e_x \in E_2$ , and  $e_a$  corresponds to  $e_x$  only for the first couple of meters from the start of  $e_x$ , and the remainder of  $e_x$  corresponds to  $e_b$  in its entirety (see Figure 3-1).

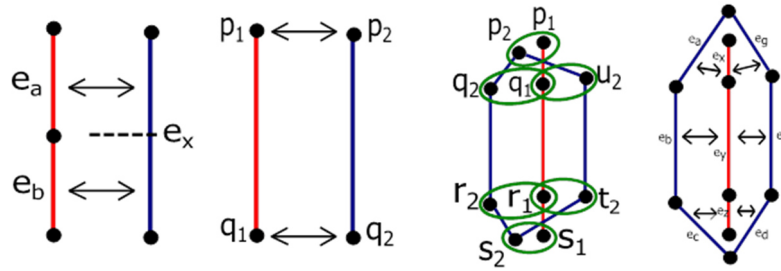


Figure 3-1: From left to right: partial correspondence, 1:1 correspondence, one-to-many node correspondences, one-to-many link correspondences.

As a simple concept for dealing with partial correspondences, we suggest to employ *virtual nodes* along with *virtual links*. If a partial correspondence is identified, the involved links are split up into separate virtual links which are interconnected via a virtual node, and the virtual nodes and links are added to the respective road network. Node and link sequence matching assignments may then refer to these virtual entities in order to describe partial correspondences. Since a road network also includes a geometrical layer, some geometric modifications are necessary to update the geometry so as to match the altered topology. E.g., if the geometry of a link is given by a sequence of shape points, and the chosen split point is not identical to one of these shape points, then a new shape point must be created at an intermediate position along the straight line between the neighboring shape points. Formally, we need a set  $N_{i_v}$  of virtual nodes to be added to  $N_i$ , a set  $E_{i_v}$  of virtual links, where at least one of the two nodes in the link is virtual, and a projection  $V_i: (E_i, N_{i_v}) \rightarrow (E_{i_v}, E_{i_v})$  which assigns a link involved in a partial correspondence to the two virtual links which are created from splitting the link at the position of the respective virtual node.

Taking these considerations into account, it is possible to express a solution to the Road Network Conflation Problem for two road networks on the level of both elementary topological nodes as well as composite line structures by the tuple  $R = (P, L, N_{1_v}, E_{1_v}, V_1, N_{2_v}, E_{2_v}, V_2)$ . The problem of Road Network Conflation can then be defined as finding the optimal  $R$ . Sometimes it is demanded that the conflation result exclusively describes one-to-one correspondences. In this case, we require both  $P$  and  $L$  to be injective as well as functional relations, and special strategies must be applied to deal with real-world ambiguities, such as replacing all nodes assigned to a node with a single merged virtual node which may e.g. be placed at their center of gravity.

### 3.2 The Problem of Ambiguity

Ambiguity can arise on different levels of aggregation, which are discussed here in detail. In general, four different types of assignments between objects are possible (see Figure 3-2). Out of these, three (1:n, n:1, and m:n) introduce the problem of ambiguity.

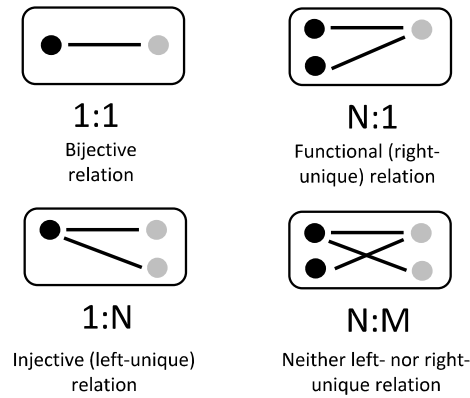


**Figure 3-2: Types of Assignments**

### 3.2.1 Ambiguity on the Level of Point Objects

Ambiguity between point objects occurs if there are topological points – the *nodes* according to the definitions of 3.1 – in the road networks to be conflated which do not relate to each other in the form of a 1:1 association. The following cases are possible:

- (a) 1:n relationship: A single node in the reference network corresponds to multiple nodes in the matching network. The third image in Figure 3-1 illustrates such a relationship. There,  $q_1$  is associated with  $q_2$  as well as  $u_2$  and  $r_1$  is associated with  $r_2$  and  $t_2$  (formally,  $\{(q_1, q_2), (q_1, u_2), (r_1, r_2), (r_1, t_2)\} \subseteq P$ , where  $P$  is the node matching relation as defined in 3.1). This type of relationship is common in situations where the reference network models a road with separate carriageways as one single topological entity with the additional semantic information of having separate carriageways, while the matching network models the very same road as two topological entities, one for each carriageway. Also, differences in the level of detail between the maps to be conflated may cause such a relationship, as can be seen in Figure 3-3: We have the single node pairs  $(a_1, b_1)$ ,  $(a_3, b_4)$  and  $(a_4, b_6)$ , while  $b_2, b_3$  as well as  $b_5$  are all associated with  $a_2$ .

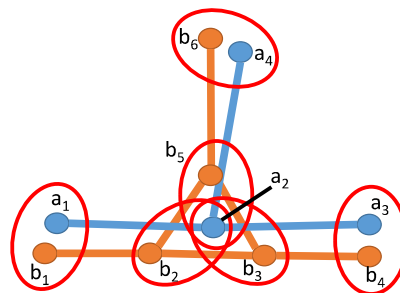


**Figure 3-3: Example for 1:n relationship caused by different level of detail. Node associations are shown as ellipses.**

- (b) n:1 relationship: Multiple nodes in the reference network correspond to a single node in the matching network. This relationship represents the same situation as (a), but with swapped roles of the road networks.
- (c) m:n relationship: A single node in the reference network corresponds to multiple nodes in the matching network, but at the same time, this node is part of a set of multiple nodes which correspond to a single node in the matching network. This often happens if the road networks differ greatly in their topologies, e.g. because one of the networks represents an updated version of the region where construction work has changed parts of the topology. Consider the example in Figure 3-4: While it seems reasonable that  $a_1$  relates to  $b_1$  in the form of a 1:1

relationship and  $a_4$  relates to  $b_4$  and  $b_6$  in the form of a 1:n relationship, the associations between the remaining nodes are unclear. In fact, there seem to be two clusters involved: One cluster consisting of nodes  $\{b_2, b_3, b_5\}$  and the other cluster consisting of nodes  $\{a_2, a_3\}$ . Arguably, one might say that these clusters are related in 1:1 fashion, which is what the Iterative Hierarchical Conflation Framework introduced later in this thesis (chapter 4) actually aims to detect. However, on the level of individual nodes, this would lead to an m:n relationship between the nodes of the two road networks. More precisely, the following set constitutes the node matching relation in this sense:  $\{(a_2, b_2), (a_2, b_3), (a_2, b_5), (a_3, b_2), (a_3, b_3), (a_3, b_5)\}$ . Often, it can be hard to decide even for human beings if, and if so, what kind of m:n relationship exists. Without further structural high-level information, such as the knowledge that a certain cluster of nodes belongs to a roundabout, transferring information based on such a node assignment becomes difficult and error-prone, since the identified relation cannot be broken down to simple composites.

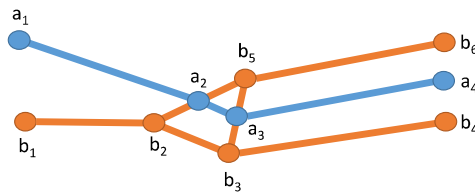


Figure 3-4: Example for unclear m:n relationships between nodes.

### 3.2.2 Ambiguity on the Level of Line Objects

Ambiguity on the level of line objects (*links* and *link sequences* according to the definitions in 3.1) can be divided into the same subtypes as for point objects (1:n, n:1, and m:n). As can be seen in the fourth image of Figure 3-1, 1:n type (and, respectively, n:1 type) relationships of links may often be derived from corresponding 1:n type node correspondences. However, this does not always apply: For example, in Figure 3-3, there is an 1:n type node assignment which effectively represents a contraction of the three nodes of the triangle to the one node in the middle belonging to the other road network. Thus, the three links which form the triangle cannot be assigned to any link. This reflects the fact that information from a map possessing a high level of detail cannot be transferred to a map possessing a lower level of detail as a whole without losing parts of this information, in this case, details on the structure of the intersection.

m:n relationships of links also occur in reality. Consider Figure 3-5: Even though we only have 1:1 relationships between nodes, from the topological point of view,  $a_1$  may as well correspond to  $b_1$  as it may correspond to  $b_3$ . At the same time,  $b_1$  corresponds to  $a_1$  but also to  $a_3$ . It should be noted that this kind of ambiguity can often be ruled out by geometrical comparisons, as does the IHC Framework, which is explained in the according section 4.

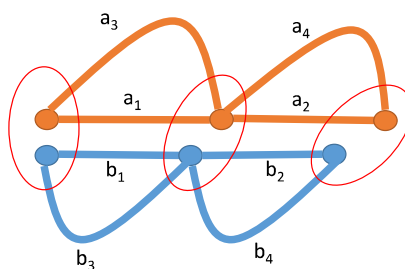
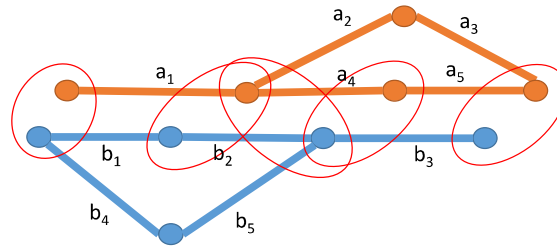


Figure 3-5: m:n relationships between links. Node assignments shown as ellipses.

If we now further look at composite line objects, the *link sequences*, things get more complicated. Consider Figure 3-6: Here we have several m:n relationships between nodes. As a result,  $a_1$  corresponds to the link  $b_1$  but also to the link sequence  $(b_1, b_2)$  and finally also to the link sequence  $(b_4, b_5)$ . On the other hand,  $b_2$  corresponds to  $a_4$  but also to the contraction of its start and end node to a single node in the other network, thus the assignment of  $b_2$  to its eradication (“null assignment”) is another option.  $b_3$  corresponds to  $a_5$  but also to the link sequence  $(a_4, a_5)$  and finally to the link sequence  $(a_2, a_3)$ .



**Figure 3-6: m:n relationships between nodes (shown as ellipses) may cause m:n relationships between links and also between links and link sequences (not shown in the image for clarity).**



## 4 The Iterative Hierarchical Conflation (IHC) Framework

The Iterative Hierarchical Conflation (IHC) framework represents the core of this thesis. It constitutes an advanced approach for the Road Network Conflation by means of a so-called Matching Pipeline consisting of two phases (Bottom-Up and Top-Down) as well as multiple stages which are visited in each phase so as to iteratively find and refine associations between objects on different levels of abstraction. First, an overview of the Matching Pipeline concept is given, followed by a detailed explanation of both phases and the stages visited therein.

The IHC Framework mainly employs three concepts in order to deal with the complexity introduced by m:n mappings: First, if the geometry suggests that only partial correspondences are present (see 3.1), *virtual nodes* are inserted, which subsequently lead to the creation of *virtual links*. By running the conflation process on virtual nodes and links, many ambiguities can be resolved. Second, nodes are clustered in order to prevent m:n node assignments, to the cost of creating *virtual geometries*. Third, *structural matching* is employed in order to identify 1:1 mappings between high-level composite structures in cases where assignments between elementary structures identified in preceding matching steps look chaotic.

### 4.1 Overview of the Matching Pipeline

Figure 4-1 depicts an overview of the Matching Pipeline.

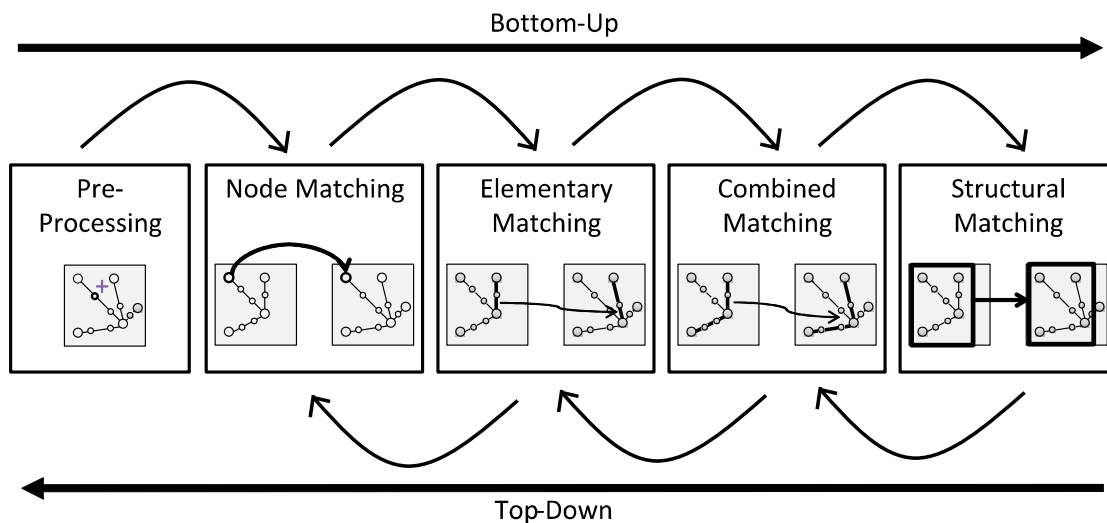


Figure 4-1: The Matching Pipeline of the IHC Framework.

The Matching Pipeline basically consists of five stages: *Preprocessing*, *Node Matching*, *Elementary Matching*, *Combined Matching*, and *Structural Matching*, where the Combined Matching may be repeated several times in order to find more assignments. The input of each stage is comprised of the output of all preceding stages, so that the matching result can be successively improved as more information regarding correspondences has been learned. Processing is divided into two phases: The *bottom-up* phase, where correspondences between elementary structures are aggregated, and the *top-down* phase, where correspondences between composite structures are decomposed (Figure 4-2).

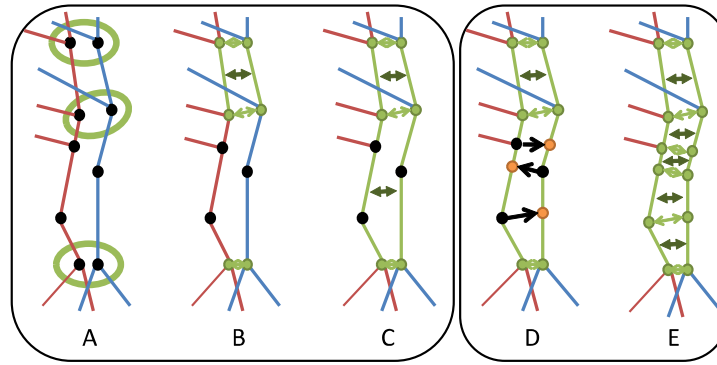


Figure 4-2: Bottom-up phase (left) and top-down phase (right). Virtual nodes shown in orange.

## 4.2 The Bottom-Up Phase

In the course of the bottom-up phase, correlations between elementary structures are identified, which are then combined in order to derive assignments between more complex structures.

### 4.2.1 Preprocessing

In order to normalize the road networks to be conflated, certain preprocessing must take place, depending on their deviance. E.g., if there is a systematic geometric shift between both networks, it is possible to manually identify the shift and remove it so that the matching network is centered on the reference network. Also, it may be beneficial to harmonize the shape point resolution in each map to facilitate spatial queries. After normalization, index structures must be created which enable efficient spatial search for nodes as well as for shape points. This may e.g. be performed with a k-d-tree or a quadtree. If the road networks are based on different data models, they must be converted so as to share the same data model in order to allow direct comparisons of their geometry and topology.

### 4.2.2 Node Matching

During bottom-up node matching, assignments between non-bivalent nodes of the road networks are identified (see Figure 4-2 A). For this purpose, the Exact Angular Index metric described in detail in 2.5.1.4 is employed, as it provides several benefits in terms of precision compared to discrete sector-based point matching techniques such as the Spider Index. The EAI evaluates all possible projections from the edges of the reference node to the edges of the matching node and selects the projection which exhibits the lowest overall angle difference derived from aggregating the angle differences of all edge assignments, where redundant or missing edges are counted as worst-case angle differences of  $180^\circ$ .

In order to obtain a node matching solution  $P$ , a fixed-radius search in the set of non-bivalent nodes of the matching network is performed for each non-bivalent node  $p_1$  of the reference network, resulting in candidate nodes  $p_2^1 \dots p_2^n$ . Then, the EAI score is calculated for each pair  $(p_1, p_2^i)$ .

By always choosing the pair with the highest similarity score, the node matching solution comprises a functional relation, i.e. no node in the reference network is assigned to more than one node in the matching network. By repeating this process with switched roles of the networks (yielding an injective relation) and then intersecting both relation sets, a bijective node matching solution can be derived. This solution satisfies mutual optimality, i.e. for any pair  $(p_1, p_2)$  and a fixed radius  $r$ ,  $p_1$  is the best match for  $p_2$  within a circle of radius  $r$ , and  $p_2$  is also the best match for  $p_1$  within a circle of radius  $r$ .

If all nodes which are part of the solution are removed from both networks, and then the process is repeated, additional node pairs may be identified. This can be done until no additional node pairs are found in an iteration, or until a pre-defined limit for the number of passes has been reached.

Locally, the road networks to be conflated may show greater differences in their topology. Often, this can be attributed to structural differences, i.e. differences which apply to larger structures rather than elementary nodes or links. In the node matching stage, these differences surface in the form of ambiguities, so that 1:1 matchings between nodes based on local proximity achieve low scores. The IHC framework employs two strategies to identify these special situations as early as possible:

- Prior to node matching, a so-called *Structural Anomaly Detector* is applied to investigate the road networks. Special templates (filter algorithms customized to recognize certain spatial patterns) identify certain subgraphs of the induced graph of the road network representing a high-level structure, which are then excluded from the elementary and combined matching stages and dealt with over the course of the structural matching stage. One example for this is the structural anomaly detector for roundabouts, which works in two steps: First, starting from seed points, cycles are detected in the graph of a road network. Then, the geometry of the found cycles is investigated in order to determine whether they actually represent a roundabout. Therefore, an algorithm is employed which calculates a score out of the shape point geometry of a cycle in a road network expressing the degree of similarity to a “perfectly” round polygon. If a certain threshold is exceeded, the cycle in question is considered to be a roundabout. This detector is explained in greater detail in 4.4.
- For each node being evaluated over the course of the node matching, all nodes in the other road network within the search distance are clustered according to their similarity score. Then, the center of gravity is calculated for each cluster, which serves as a fusion node (so-called *super node*). Therefore, a new *virtual road network layer* is created, where all cluster members are replaced by the super node, and their incident edges are modified in their topology and geometry (the latter using affine transformations, i.e. rotation and stretching / shrinking) so that they are incident to the super node. Now, the EAI score can be calculated between the source node and the super node. If this score is better (higher) than the score of any of the cluster members, the super node is considered a better matching than any of the cluster members. If there are several clusters and thus several possible super nodes, the super node with the best score wins, except if there is any regular node with a better score. The virtual road network layer rather than the “real” road network is then employed in the further matching process. All super nodes in a road network must be based on disjoint cluster sets. This procedure yields good results in cases where 1:n associations with slight differences in topology are present in reality, as can be seen in Figure 4-3. In the IHC implementation, DBSCAN [56], a common density-based clustering algorithm, has been used for clustering.

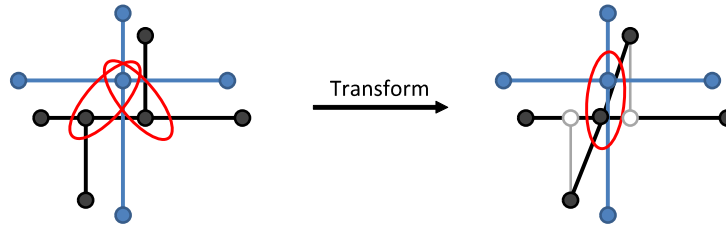


**Figure 4-3: Ambiguity resolution by clustering nodes according to their similarity scores, then replacing clusters by “supernodes” at their center of gravity and altering the structure of the road network in order to gain 1:1 associations.**

The contraction of multiple nodes into a single super node has the following consequences:

- All links interconnecting the nodes of the cluster which form the super node are removed in the virtual road network layer.
- All links which connect a node outside the cluster to more than one node within the cluster must be merged into a single link. If the geometry is given by shape points, this can be achieved by performing geometrical averaging.
- If there are several neighboring super nodes, and the nodes forming the clusters are interconnected, the super nodes must be interconnected by merging these connections into single links.

To illustrate this problem, consider Figure 4-4. There, in (A), we have two single-node pairings yielding the best score in the search radius:  $(a_1, b_1)$  and  $(a_4, b_4)$ . For the node cluster  $\{a_2, a_5\}$ , their center of gravity is roughly at the position of node  $b_2$ , and for the node cluster  $\{a_3, a_6\}$ , their center of gravity is roughly at the position of node  $b_3$ . In (B), the super nodes created at the centers of gravity have been denoted as  $a_x$  and  $a_y$ . Quite obviously,  $(a_x, b_2)$  gives a better point matching score than both  $(a_2, b_2)$  and  $(a_5, b_2)$ . In a similar fashion,  $(a_y, b_3)$  leads to a better score than both  $(a_3, b_3)$  and  $(a_6, b_3)$ .

If we now look at the local virtual network layer which is created by only clustering  $\{a_5, a_2\}$ , we get (C). It can be seen that the links  $e_1$  and  $e_2$  have been merged into the single link  $e_{12}$ . The link  $e_7$  has been removed, since it interconnects the cluster  $\{a_5, a_2\}$ . Analogously, if we look at the local virtual network layer which is created by only clustering  $\{a_3, a_6\}$ , we get (D), where links  $e_5$  and  $e_6$  have been merged into a single link  $e_{56}$ , and the interconnection link  $e_8$  has been removed.

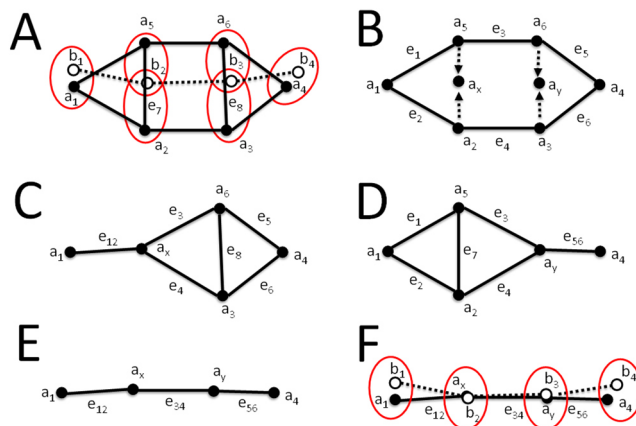


**Figure 4-4: Clustering of nodes in order to create pairings with super nodes on virtual network layers.**

However, since the two super nodes are created out of clusters which are interconnected (via links  $e_3$  and  $e_4$ ), another virtual network layer is created and evaluated, as depicted in (E). There, the links  $e_3$  and  $e_4$  have been averaged into the link  $e_{34}$ , and the other two transformations have been performed as well. Since the matching as seen in (F) yields the globally best score, the algorithm finally decides in favor of this option.

Regarding the averaging of the polyline geometries, a straightforward approach works as depicted in Figure 4-5.

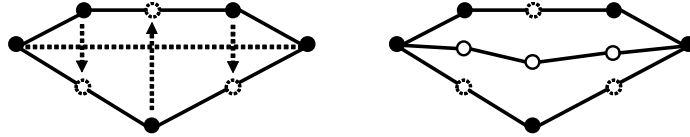


Figure 4-5: Averaging of polylines.

Given a set of polylines all sharing the same start and end point (which can be enforced prior to the averaging process by employing affine transformations), for each polyline, the intersection points of the orthogonal projection with all remaining polylines are determined. The new polyline is then constructed as the concatenation of all centers of gravity which are each calculated from averaging the respective shape point with its intersection points. The result polyline possesses as many shape points as the sum of all shape points of all polylines, minus the shared start and end point, which do not need to be averaged.

### 4.2.3 Elementary Matching

In the elementary matching stage, elementary link sequences, i.e. those consisting of only one link, are constructed starting from a given node matching solution. Two sets holding link sequences are established, one for each road network:  $T_i := \{S_i^1, \dots, S_i^{O_i}\}$ . For each node of the reference network which is part of the solution, a separate link sequence is constructed out of each incident link, and all constructed link sequences are added to the corresponding link sequence set. The same process is repeated for the nodes of the matching network contained in the solution.

For performing the actual matching, the two link sequence sets are compared. For each link sequence  $S_1^j \in T_1$ , a corresponding link sequence  $S_2^k \in T_2$  is identified if the start node of  $S_1^j$  is related to the start node of  $S_2^k$  in the node matching solution  $P$ , and also the end node of  $S_1^j$  is related to the end node of  $S_2^k$ . If a link sequence match between  $S_1^j$  and  $S_2^k$  has been found, the pair  $(S_1^j, S_2^k)$  is added to the link sequence matching relation  $L \subseteq (S_1 \times S_2)$  (see Figure 4-2 B). By employing several index structures, this process can be turned into an  $O(n + m)$  operation, where  $n = |T_1|$  and  $m = |T_2|$ . In the next step, duplicates are removed from  $L$  (i.e. those pairs which are identical apart from having swapped start and end nodes). Finally, all link sequences of  $T_1$  and  $T_2$  are removed which have links in common with link sequences of  $L$ .

### 4.2.4 Combined Matching

The combined matching stage is concerned with the identification of correspondences between composite link sequences. Therefore, new composite link sequences are created by concatenating more elementary link sequences already present in both link sequence sets. A concatenation of two link sequences in a link sequence set  $T_i$  takes place if the end node of one link sequence is the start node of the other. In this case, a new link sequence is derived from the concatenation and added to

the corresponding link sequence set. After concatenation has been performed for both link sequence sets, they are compared again in the same manner as during the elementary matching stage. As a result, new non-elementary link sequence pairs are added to the link sequence matching relation  $L$  (see Figure 4-2 C). This process may be repeated for a given number of passes, or until there is no further concatenation possible, which implies that no additional link sequences are created in an iteration.

$L$  may contain ambiguity, i.e. one link sequence of the reference network may be assigned to multiple link sequences of the matching network, or vice versa. In order to enforce bijectivity and filter improbable matches, a score is assigned to each link sequence pair of  $L$  expressing the degree of similarity of their corresponding polylines, which is projected on the interval  $[0;1]$ . This score can be calculated using any polyline distance metric or a weighted combination of these metrics. In detail, a simple distance metric yielding good results is the length ratio between the polylines. Others include the sinuosity ratio, the Hausdorff distance, the Fréchet distance or the area of the enclosed polygon [57]. Figure 4-6 shows some examples for polyline distance metrics.

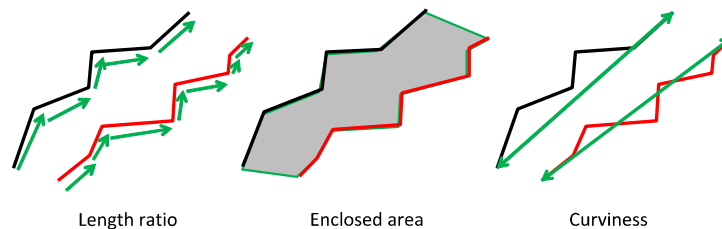


Figure 4-6: Examples for polyline distance metrics.

Once the scores of all link sequence pairs have been determined, the pairs assigned to scores below a certain threshold score are removed, as it can be assumed that they do not reflect real-world correspondences. Then,  $L$  is made bijective in the same way as it has been done with the node matching result (see Node Matching).

If there exists topological inconsistency, which may e.g. be caused by incorrect point assignment in the node matching stage, multiple link sequence pairs of  $L$  share several, but not all links. In this case, it is not possible to establish a consistent matching and thus, link sequence pairs with common links are removed from  $L$ .

A special treatment is required in order to identify *dangling link sequence pairs*, i.e. pairs of link sequences which are only associated by their start nodes, but not by their end nodes. Such situations can occur if two roads are running in parallel for a certain distance, but beyond that one road ends while the other continues until it also reaches a dead end. These may reasonably be added to  $L$  if the end nodes are not associated to other link sequences. To create a proper link sequence pair out of a dangling link sequence pair, a corresponding virtual end node must be placed near the position of the end node of the shorter link sequence on the longer link sequence, which can then be associated with the non-virtual end node of the other sequence. Then, the same procedure as for regular link sequence pairs can be applied to take care of ambiguity and inconsistency. The dangling link sequence assignment must take place subsequent to all combined matching passes, since a dangling link sequence pair might be prolonged to a regular link sequence pair after concatenation has been done. Figure 4-7 shows an example of dangling link sequence pairs and the way they are treated.

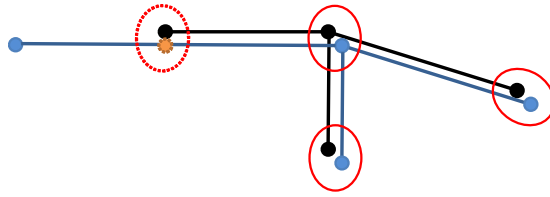


Figure 4-7: Treatment of dangling link sequence pairs. Red solid: Node associations, red dashed: association with the virtual node, orange dashed: virtual node.

#### 4.2.5 Structural Matching

In the structural matching stage, structural information detected by the structural anomaly detector (see 4.2.2) is used to create high-level associations between composite objects. Figure 4-8 shows the structural matching in the case of the mapping between a crossing and a roundabout.

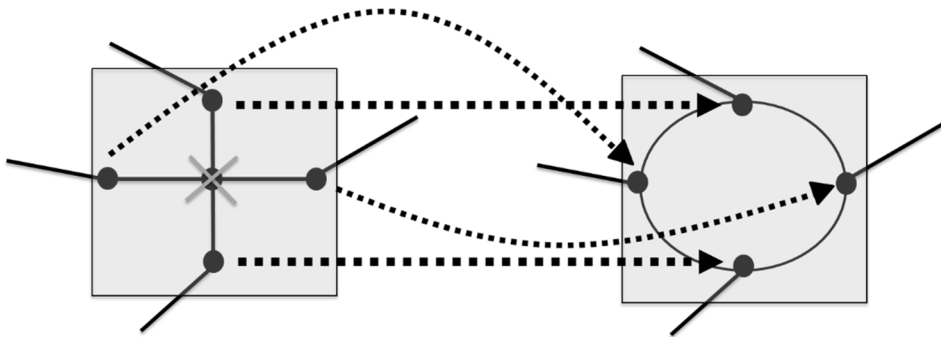


Figure 4-8: High-level association in the case of a mapping between a crossing and a roundabout

In general, any structural object represents a subgraph of a road network. Depending on the concrete type of the structural object, other information is identified by the structural anomaly detector as well. E.g., for roundabouts, the information is stored which nodes represent entry points to the roundabout. The *structural anomaly matcher* uses this information in order to create a high-level mapping. In the case of a roundabout, if no roundabout has been identified in the other road network at roughly the same position, then a crossing is looked for. If a crossing has been found, the association between this crossing and the roundabout is stored. If instead another roundabout has been found, the entry points of both roundabouts are associated in the high-level pairing. If neither of both has been found, then no high-level association can be established at all.

### 4.3 The Top-Down Phase

During the top-down phase, correlations between aggregated structures are decomposed into more elementary associations.

#### 4.3.1 Combined Matching

In the bottom-up phase, correspondences between link sequences have been identified. The implied knowledge that has been learned is the fact that the corresponding road segments refer to the same real-world entity, regardless of differences in topology and geometry. This knowledge can now be used to project nodes located on one link sequence onto a corresponding position on the other link sequence. Projection is done by multiplying the offset of a node from the start node of the link sequence by the length ratio between the two link sequences, then placing a virtual node at the resulting distance from the start node of the paired link sequence. This results in a splitting of the

affected link into two new virtual links (see Figure 4-2 D). The underlying rationale is the assumption that the link sequence of the matching network as a whole represents a reduced or stretched version of the entire corresponding link sequence of the reference network. In order to decide whether it is better to place a projected virtual node or rather associate with a nearby non-virtual node, a one-dimensional search can be performed within an interval around the projected position.

Sometimes multiple mappings are possible. Thus, we evaluate all possible projections from the nodes of the link sequence of the reference network to nodes of the associated link sequence of the matching network by aggregating and normalizing the EAI scores of the respective node pairs for every possible projection and then selecting the projection yielding the best overall score. A projection is deemed possible if there are no crossed assignments of nodes, as these cannot logically reflect real-world situations.

For a better understanding of this process, consider Figure 4-9. There, we have two link sequences which have successfully been paired, so that  $(a_1, b_1)$  and  $(a_4, b_5)$  are valid node associations. However, the assignment of the nodes in between the sequences has not yet been resolved. Several options are possible in this example. In (A), no assignment is performed at all. (B) suggests the node associations  $(a_2, b_2)$  and  $(a_3, b_3)$ , while  $b_4$  is not associated. (C) would be another valid option, with the pair  $(b_2, a_3)$ , and  $\{a_2, b_3, b_4\}$  would remain without a partner node. In (D),  $b_2$  stays unassociated while the node associations  $(a_2, b_3)$  and  $(a_3, b_5)$  are employed. (E) and (F) are actually invalid (crossed) assignments. Note that some other options are possible which are not depicted in the figure. Also note that out of the assignments shown, which would be investigated given an infinite search interval, only the ones found within the defined search interval are actually evaluated.

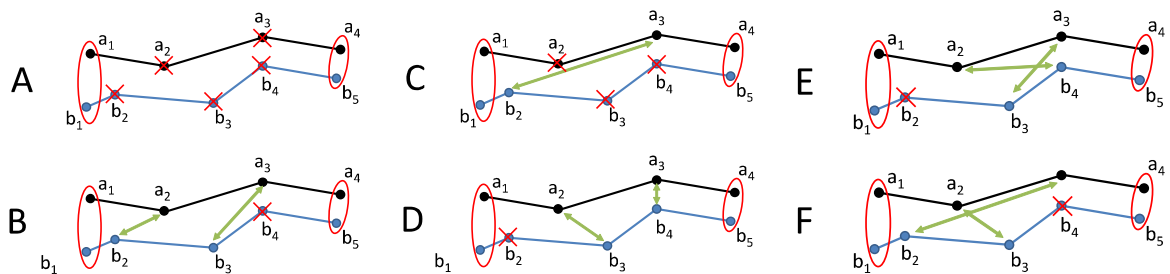


Figure 4-9: Valid (A, B, C, D) and invalid (E, F) assignments of intermediate nodes of a link sequence pair.

The algorithm first enumerates all possible options of assigning the nodes, where crossed assignments are identified and skipped. For each option (set of node assignments), the weighted (topological and geometrical) EAI distance is calculated for each node pair using the geometrical distance metric of the distance between the projected point and the actual point along the geometry of the link sequence. The option is then assigned an overall score from averaging the scores of all corresponding node pairs. After scores have been calculated for all options, the option with the highest (best) score is selected, which now determines how “real” (non-virtual) intermediate nodes are associated. For the remaining unassigned nodes, virtual nodes are created at the projected positions on the paired link sequence (see Figure 4-10).

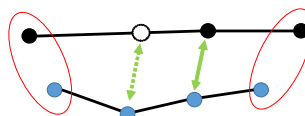


Figure 4-10: Pairing with virtual nodes created at projected positions.



Now that all cycles incorporating trivalent nodes have been identified, we may proceed to the second step, which consists of the geometrical investigation of the candidates in order to derive a score expressing the degree of similarity to a “perfect” circle. We call this score the “Circularity Index” (CI). Note that for the geometrical investigation, we look at the geometry of the cycle as given by its shape points, rather than the topological nodes. Figure 4-12 illustrates the difference.

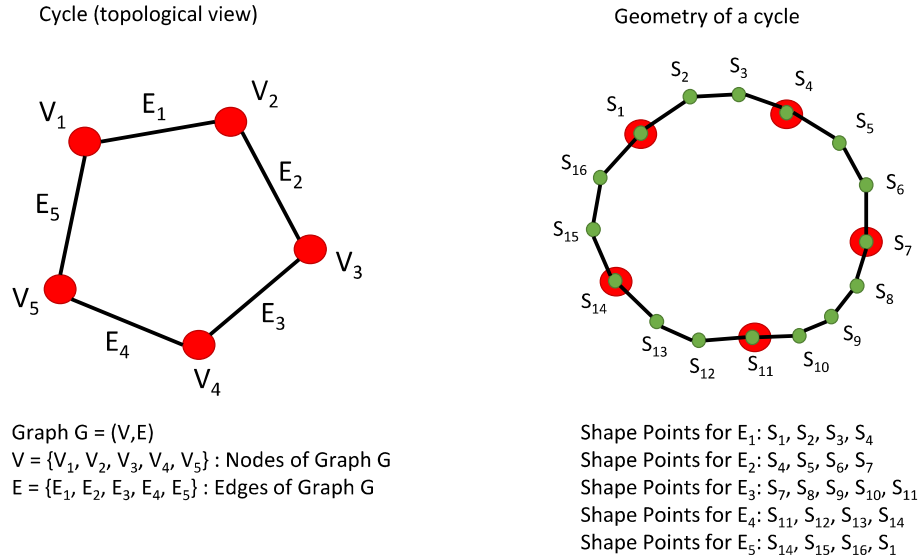


Figure 4-12: Topological and geometrical view of a cycle in a road network.

It is a well-known fact that a polygon of  $n$  vertices which approximates a circle possesses the following internal angle  $\alpha_c$  at every vertex:

$$(4.4 (1)) \quad \alpha_c = \frac{n - 2}{n} \cdot 180^\circ$$

E.g., the internal angle for a 3-sided polygon is 60 degrees (equilateral triangle), and for a 4-sided polygon it is 90 degrees (square). As the number of vertices increases, the polygon approximates an internal angle of 180 degrees without ever reaching it. Now, it can be assumed that a polygon is closer to a circle if its internal angles are closer to the internal angle of the ideal circular polygon of the same number of vertices. Here, each internal angle has to be weighted with the segment length it can be assigned to.

Let us denote every polygonal vertex with  $i$ , every angle belonging to the vertex  $i$  with  $\alpha_i$ , and every edge starting from the vertex  $i$  with  $l_i$ , starting with 1. The last edge  $l_n$  shall be equal to  $l_0$ . Also, let the total length  $l = \sum_{i=1}^n l_i$ .

The circularity index can then be calculated as follows:

$$(4.4 (2)) \quad CI = \sum_{i=1}^n \left( \frac{l_{i-1} + l_i}{2l} \cdot \left( 1 - \frac{|\alpha_i - \alpha_c|}{360^\circ - \alpha_c} \right) \right)$$

The difference between the existing and the expected (ideal) angle is, in the worst case, as large as the difference between 360 degrees and the expected angle. In this case, the quotient becomes 1, and

thus, the similarity (1-quotient) becomes zero. This similarity is weighted with the share of the according segment relative to the total length.

Two examples shall illustrate this. First, the ideal circle: If we have a polygon with 8 vertices ideally approximated to a circle, the internal angle is 135 degrees. For simplicity, let all segments be of a length of 1 meter. The similarity measure will then be 1 for each vertex, or each angle. The segments have a total length of 8 meters. The weight of each vertex is therefore  $\frac{1+1}{16}$ , thus  $\frac{1}{8}$ . So, every weighted similarity measure is  $\frac{1}{8}$ , and the sum is exactly 1.

Second, let us assume a rhomb with 8 vertices of the shape as seen in Figure 4-13.

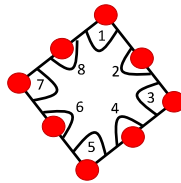


**Figure 4-13: Example rhomb for circularity index.**

It can be seen that the angles at 1, 3, 5, and 7 equal 90°, and those at 2, 4, 6, and 8 equal 180°. Regarding the 180° angles, the difference to the ideal angle of 135° is exactly 45°. For the 90° angles, the difference is also exactly 45°. This leads to a similarity of 80%:  $1 - \left(\frac{45}{360-135}\right)$ . Since the weights are the same everywhere, the total (overall) CI also equals 80%.

If we instead assign 70° to the angles 1, 3, 5, and 7, and 200° to the angles 2, 4, 6, and 8, then the result is a four-pointed star (as the angles 2, 4, 6, and 8 are contracted towards the inside). The similarity to circularity will then fall down to 71% according to the CI:  $1 - \left(\frac{65}{360-135}\right)$ , so, according to the CI, the star is a worse approximation than the rhomb. In the field, CI values of 60% have proven to be a good threshold in order to identify real roundabouts.

In addition to the circularity index, the geometry of the link shapes of the detected cycles can be investigated with regard to geometric properties such as length (circumference) or covered area. This way, cycles can be ruled out which are obviously too large, or, more rarely, too small to qualify as a roundabout. Even large roundabouts seldom possess circumferences larger than a few hundred meters, with very rare exceptions reaching more than 1 km (world record: 3,4 km, in Putrajaya, Malaysia), while very small roundabouts have lengths of usually more than 13 meters.



## 5 Implementation and Evaluation

This chapter describes the implementation as well as the evaluation of the IHC framework. It represents a further refinement and advancement of results that have been published before by Hackeloer et al. in [1].

### 5.1 Implementation

The diagram in Figure 5-1 describes the schematic high-level architecture of the IHC framework.

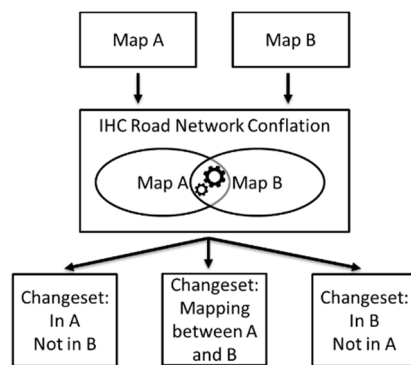


**Figure 5-1: Schematic Architecture of the IHC Framework.**

First, the maps (A and B) containing the two road networks to be conflated are loaded into the system. Then, the Matching Pipeline is employed in order to identify similarities and differences between the road networks on different levels of abstraction. The result of the conflation process can be divided into three separate change sets: One change set contains the set of elements which have only been found in A, but for which no counterpart in B has been identified. Another change set contains the set of elements which are only present in B but not associated to A. And finally, the third change set contains the elements of both road networks for which associations have been found. Thus, the first two change sets contain the differences between the two road networks, while the third one expresses the similarities.

In greater detail, the architecture of the IHC framework is depicted in Figure 5-2. All of the components in the figure are loosely coupled, which means that they only communicate via well-defined public interfaces.

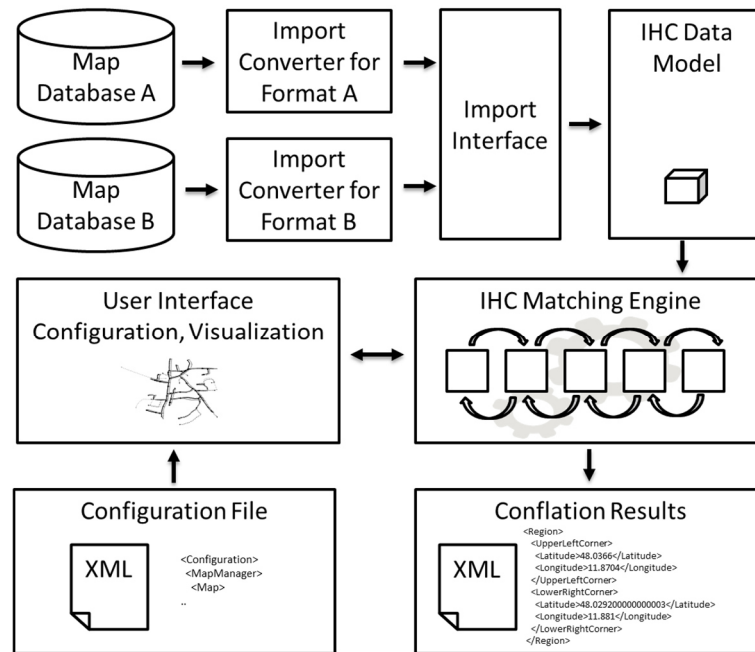


Figure 5-2: Detailed Architecture of the IHC Framework.

The flow of data starts with the upper left corner of the figure. Since map data can be stored in various formats, the IHC employs different import converters in order to import map data from heterogeneous sources. Import converters have been implemented for the following map formats:

- The **NDS** (“Navigation Data Standard”) format, which is widely used in the automotive industry in the context of on-board navigation systems. This is a binary format.
- The **GDF** (“Geographic Data Files”) format, which is used by several map vendors to provide raw vector map data to their customers. This is a plain ASCII format.
- The **NAS** (“Normbasierte Austauschchnittstelle”) format, which is defined and used by German land surveying authorities. Several official maps by German surveying authorities are provided in this format. It is based on XML.
- The **OpenStreetMap** XML format, which is used by the community behind the widespread crowd-sourced VGI (Volunteered Geographic Information) map called OpenStreetMap.
- The **ESRI Shapefile** format, which is a format for geographical data developed by the GIS software vendor ESRI (Environmental Systems Research Institute) that is widely in use in the context of professional geographic information systems such as ArcGIS.

All import converters comply with the same import interface, which ensures that the processed data are eventually converted into the IHC data model. This data model defines entities for the modelling of road networks, such as topology (nodes and links) and geometry (shapes), which are used throughout the conflation process. Along the IHC pipeline, an enhanced data model is employed which is required for the modelling of intermediate entities such as link sequences.

A graphical user interface allows the interactive control of the conflation process as well as the exploration of map features (see Figure 5-3).

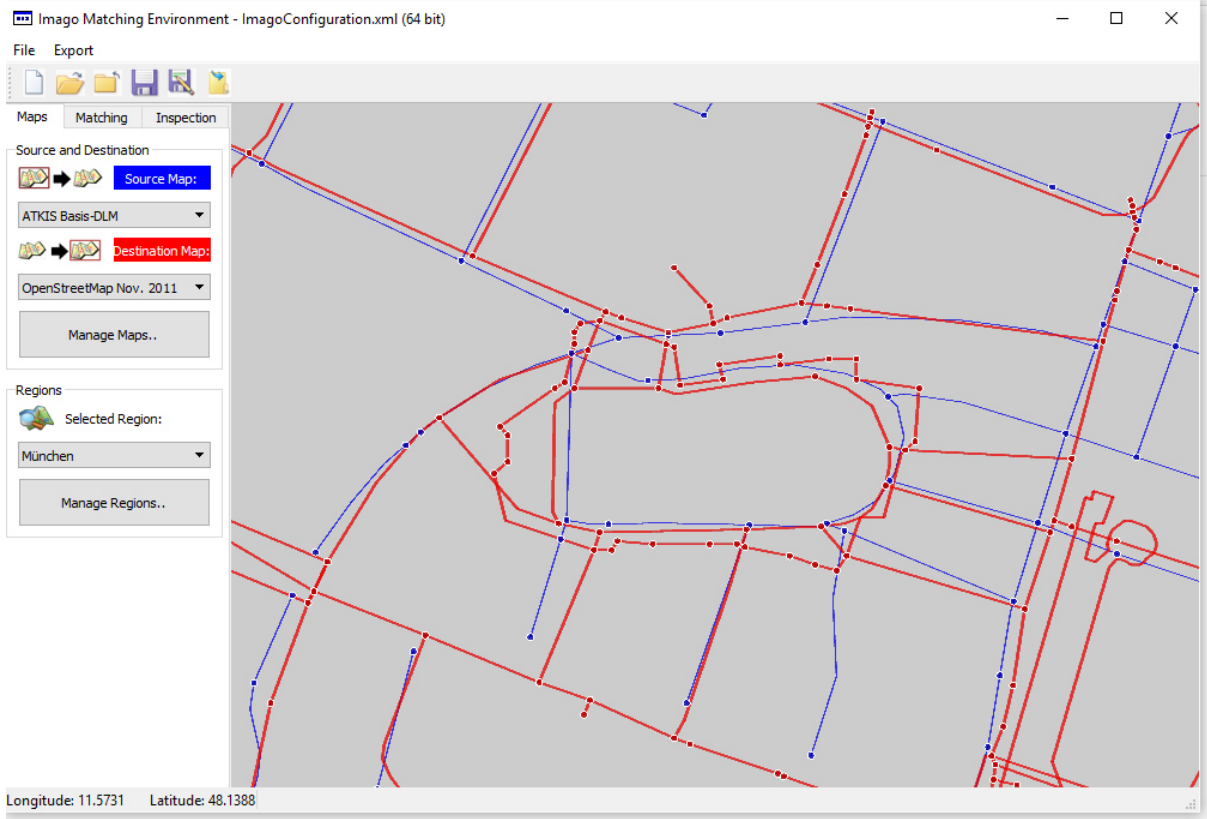


**Figure 5-3: Graphical user interface for the conflation process.**

Configurations may be loaded and saved in the form of an XML file which complies with a schema definition. A configuration consists of the following information:

- The maps to be conflated (path to files, format, title etc.).
- The region (bounding box) to be conflated, as given by WGS-84 coordinates for its corners.
- The algorithms to be used for the conflation process.
- Parameters for the algorithms to be used.

E.g., regarding the Point Matching stage, if Euclidean point matching is to be used by the conflation process, then the search radius as well as the minimum acceptable score may be passed as parameters to the algorithm. For the Exact Angular Index, there is another parameter concerning the geometrical weighting (and thus implicitly, the topological weighting as well). For the Combined Matching stage, parameters indicate which type of algorithm should be used for the geometrical comparison of link sequences, e.g. polyline length or curviness.

The conflation process may either be started via the user interface, programmatically via an API, or script-based. Status information regarding the progress of the pipeline is given to user over the course of the process. Once the conflation has finished, the result is generated in the form of an XML file which again complies with an XML schema definition. This result contains the following information:

- The maps which have been conflated (as given by the configuration).
- The region which has been conflated (as given by the configuration).
- Associations regarding the following levels of abstraction:
  - Point matching results. These also contain information about which nodes have not been matched in either map, and which virtual nodes have been created, including

- supernodes, so that the virtual road network layer can be recreated based on this information along with the geometrical affine transformations.
- Link and link sequence matching results. These also contain information about which links have not been matched in either map, and which virtual links have been created.
- Structural matching results. These contain information about what structural elements have been identified in the maps, and how they relate.

The result file can be loaded into the user interface so as to interactively explore and investigate the identified associations. Since it follows an XML schema definition, it may easily be further processed by other consumers, e.g. for the transfer of map attributes.

Technically, the graphical user interface has been built with the C++-based Qt framework. The core IHC framework is implemented in C# and runs on Microsoft's Common Language Runtime (CLR). Some components, such as the import converters, are implemented in C++/CLI, a language which enables mixing managed and unmanaged code, in order to bridge the managed and unmanaged world. It should be noted that the core IHC framework is designed as a standalone component, meaning that it is not tied to a specific user interface such as the one described here. Also, any additional map format containing enough information about the road network so as to suffice the IHC data model may be used, as long as an import converter is implemented for this format.

## 5.2 Evaluation Methodology

In order to find a solution, a conflation algorithm needs to perform a binary classification of pairs of nodes and links. Like any classifier, conflation algorithms can be assessed by means of predictive analytics. In detail, several properties derived from a table of confusion offer a starting point for the evaluation.

LEMMA 1. A solution  $R$  is optimal if it maximizes the number of true positives and true negatives in both  $P$  and  $L$ , while minimizing the number of false positives and false negatives in both  $P$  and  $L$  as defined in 3.1 (see Table 5-1).

Algorithm Decision / Reality	True	False
<b>Positive</b>	Correctly identified matching pairs	Pairs incorrectly identified as being a match
<b>Negative</b>	Pairs correctly identified as being no match	Pairs incorrectly identified as being no match

Table 5-1: Table of confusion for Road Network Conflation results.

A conflation algorithm is directed towards two rivaling goals: *correctness* and *completeness*. Correctness requires that the identified assignments reflect real-world correspondences, while completeness implies that existing real-world correspondences are actually identified as assignments. The extent to which correctness is achieved can be measured by the *precision* (sometimes called *positive predictive value*), while the degree of completeness may be expressed by the *recall* (also known as *sensitivity*). In this context, precision constitutes the percentage of correct algorithm decisions out of all algorithm decisions, and recall stands for the percentage of correct algorithm decisions out of all correspondences which are reflected by reality. Precision and recall are negatively correlated and thus cannot be optimized independently. E.g., if there are no positives at all, a perfect precision can obviously be achieved (trivially, all positives found are correct, since there are none), but

at the cost of a very poor recall, since no real-world correspondence could be found. On the other hand, if the algorithm classifies all matching pairs as positives, we have a perfect recall (all real-world correspondences are identified), but at the cost of a very poor precision (since a lot of the identified assignments are false positives).

It should be noted that the recall is not related to the actual *network coverage*, i.e. the percentage of elements which are part of the projection out of the number of all elements of a road network. If the road networks to be conflated offer few similarities, even an optimum solution with perfect precision and recall will exhibit little coverage for both networks. Since precision and recall for node and link solutions are directly correlated, it is sufficient to only evaluate either link or node solutions in order to assess a conflation algorithm.

### 5.3 Environment

All experiments have been carried out on a regular PC of the configuration as seen in Table 5-2.

<b>Operating System</b>	Microsoft Windows 7
<b>Development Environment</b>	Microsoft Visual Studio 2013
<b>Programming Languages</b>	C#, C++/CLI, C++
<b>CPU</b>	Intel Core i7-2600K, 4 cores, 3.8 GHz
<b>RAM</b>	16 GB
<b>Mainboard</b>	Asus P8P67
<b>HD</b>	2 TB

Table 5-2: Environment used for the experiments.

### 5.4 Datasets

Five sample regions were used: Two rural and three urban areas. As representatives for rural regions, Moosach, Germany ([48.0335, 11.8704], [48.0292, 11.8836]) and Sullivan, NY, USA ([43, -75.79], [42.97, -75.735]) were chosen. For the urban sample, Munich Old Town, Germany ([48.138, 11.5738], [48.1349, 11.5804]), Boston Financial District, MA, USA ([42.358, -71.062], [42.3533, -71.0553]), and finally, Eutin, Germany ([54.1472, 10.602],[54.1379, 10.62]) were employed. For the rural samples, a search radius of 40 meters and a combined matching iteration limit of 2 was used, and for the urban samples, 15 meters and a limit of 5.

Regarding the characteristics of the test sites, major differences can be seen between Germany and the USA on the one hand and between urban and rural areas on the other hand. In general, urban areas, which are densely populated, are more complex to conflate than the sparsely populated rural regions, since the former lead to more ambiguities, and the rather young cities of the USA with a geometrically simple street grid are easier to conflate than the often very old cities of Europe and Germany whose street layouts have historic roots in the Middle Ages or even Roman times. Boston is an especially interesting case: Being one of the oldest cities of the United States, its street network combines the “grid” shape commonly seen in the US with a geometrically complex layout which is predominant in the historic core. The much higher population density of Germany in contrast to the USA (about 10 times) is reflected by a denser road network even in rural regions.

For the road networks, map data from two different commercial map vendors were used who provide road maps for automotive navigation. Out of the available information, which included topological, geometrical and semantic data, only topology and geometry have been considered by the conflation algorithm, since the IHC aims to represent a generic approach independent of map-specific semantics.

Topology was represented by links and nodes, where each link has a start and an end node and each node references to its incident links. Regarding the geometry, the location of nodes was stored as WGS-84 coordinate pair, while the link geometry was approximated by a sequence of shape points, each shape point being noted as WGS-84 location. Shape points are commonly used for the representation of road centerline geometry in automotive-grade maps because unlike other approaches such as splines, they do not require computationally expansive calculations in order to derive absolute coordinates of points along a curve. Table 5-3 summarizes characteristics of the map data, also giving an indication about the shape point resolution, i.e. the geometric accuracy.

Vendor	Region	Number of nodes (excl. virtual)	Number of links (excl. virtual)	Total length of road links (km)	Average length of road links (m)	Area (m <sup>2</sup> )	Average number of shape points per link	Total number of shape points	Nodes per km <sup>2</sup>
A	Munich	110	133	5,4	40	169202	2,7	354	650
B		130	154	5,5	36		2,2	345	768
A	Boston	125	160	8,5	53	288367	2,5	392	434
B		134	156	7,7	49		2,1	335	464
A	Moosach	58	60	4,6	78	256560	4,7	280	226
B		81	85	4,8	57		2,5	212	316
A	Sullivan	31	37	28,0	755	14957527	13,2	489	2
B		49	55	25,5	464		3,2	174	3
A	Eutin	105	117	13,7	117	1215137	4,5	526	86
B		109	125	13,7	110		3	374	90

Table 5-3: Characteristics of the map data employed for the evaluation.

In order to reduce the subjectivity inevitably involved with ground truth definitions, a ground truth was employed and defined as the agreement of several people, which is disclosed in the appendix (7).

## 5.5 Results

Table 5-4 shows a summary of the evaluation results.

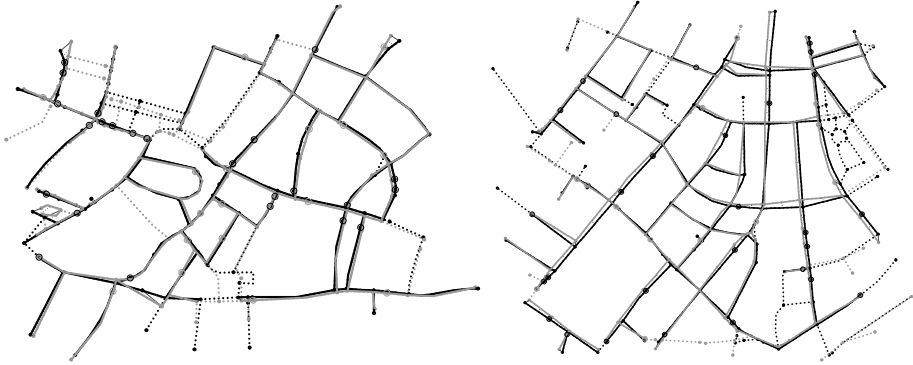
	Urban (Munich)	Urban (Boston)	Urban (Eutin)	Rural (Moosach)	Rural (Sullivan)
<b>Found associations</b>	121 / 144	121 / 140	99 / 107	100 / 100	53 / 55
<b>False negatives</b>	23	19	8	0	2
<b>False positives</b>	1	0	0	0	0
<b>True negatives</b>	10	28	30	9	4
<b>Precision</b>	99%	100%	100%	100%	100%
<b>Specificity</b>	91%	100%	100%	100%	100%
<b>Recall</b>	84%	90%	93%	100%	96%
<b>Nodes in Network A</b>	149	139	120	93	59
<b>Nodes in Network B</b>	150	157	121	98	55
<b>Network A Coverage</b>	81%	87%	83%	98%	90%
<b>Network B Coverage</b>	81%	77%	82%	93%	96%

Table 5-4: Summary of evaluation results for urban and rural regions.

### 5.5.1 Results for urban samples

The conflation result for the Munich and Boston samples can be seen in Figure 5-4. Most false negatives can be attributed to unresolved one-to-many or many-to-many correspondences between nodes and links. The modest coverage indicates that there are several major differences between the

networks, making the conflation process difficult and error-prone. It can be seen that the IHC algorithm is designed to deliver very reliable results by exploring topological relationships which are enforced for assignments, sometimes at the cost of missing some assignments which are solely related through geometry or cannot uniquely be deduced to a topological relationship.



**Figure 5-4: Conflation results for Munich Old Town (left) and Boston Financial District (right). Solid black / gray: matched links of corresponding network, dashed black / gray: unmatched links. Node and link matchings are shown as solid / thin dashed lines. Nodes are shown as black / gray dots. Virtual nodes are encircled.**

The Eutin sample shows an interesting detail in the form of a crossing which has been replaced with a roundabout in the other map. Figure 5-5 shows an overlay of the two maps along with the matching result. A virtual network layer which merges the roundabout is created in such a way that it can be associated with the crossing.

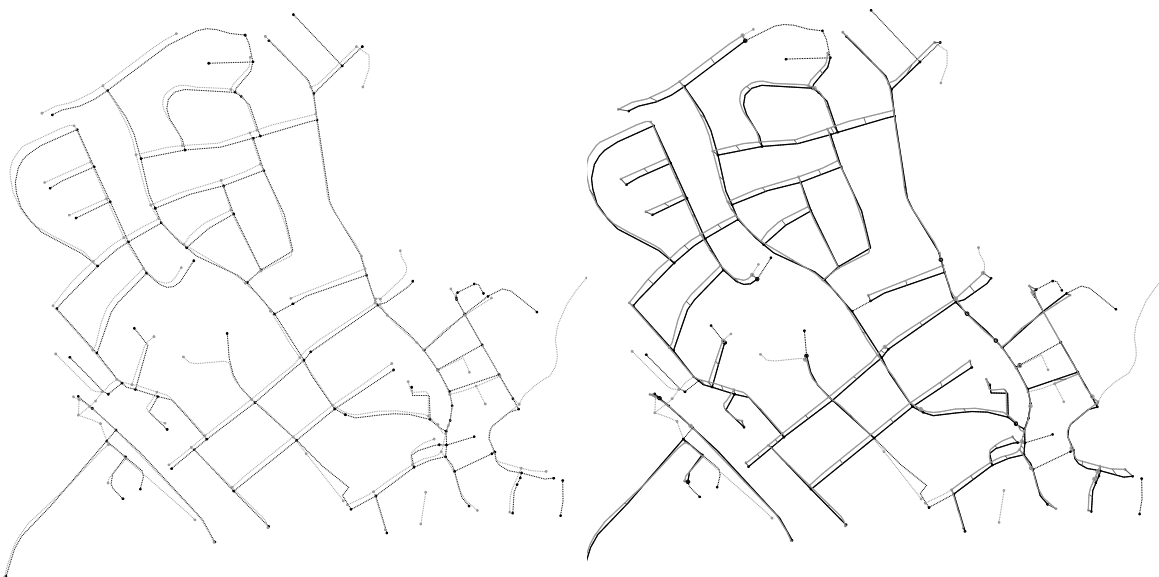


**Figure 5-5: Original map overlay of Eutin sample (left), conflation result for Eutin sample (right).**

A closer look at the area where a crossing has been replaced with a roundabout in the more recent map can be seen in Figure 5-6: To the left, the original overlay of the two maps is shown, and to the right, the structural matching has collapsed the entry points of the roundabout into one single node at the center, so that a 1:1 type matching to the crossing in the other map can be found on the virtual network level.

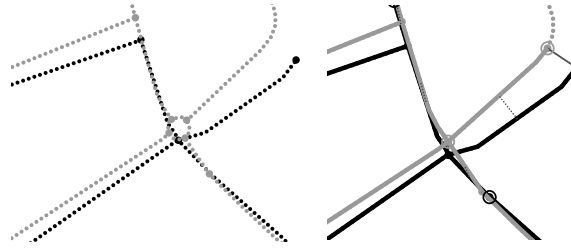


Figure 5-6: Crossing vs. roundabout in the original maps (left), virtual crossing after structural matching (right).

### 5.5.2 Results for rural samples

Figure 5-7 shows a visualization of the conflation results for the rural samples.

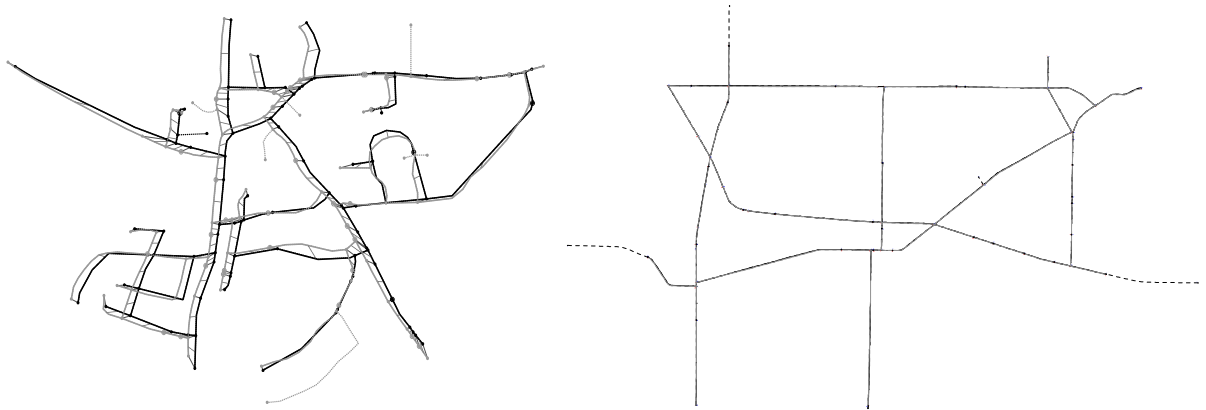


Figure 5-7: Conflation results for rural samples (left: Moosach, right: Sullivan). Note that results are shown on virtual network layers.

For Moosach, the coverage suggests that the networks are fairly similar. The ground truth solution perfectly matches the algorithmic solution on the virtual network level where topological ambiguities have been resolved. Figure 5-8 shows a close-up of a topological ambiguity to the southwest of the Moosach sample and compares it to the suggested matching solution which employs a virtual network.

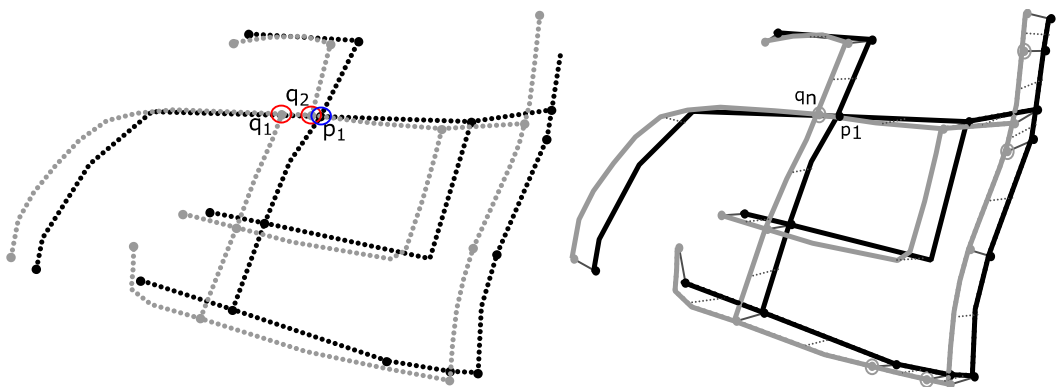


Figure 5-8: Close-up of a topological ambiguity (left), matching solution employing a virtual network (right).

In this case, the matching pairs  $(p_1, q_1)$  and  $(p_1, q_2)$  both lead to a lower matching score than the matching pair  $(p_1, q_n)$ , where  $q_n$  is a super node created from contracting  $q_1$  and  $q_2$  along with their incident edges. Thus, both T-crossings are merged into one regular 4-directional crossing, which mimics the way the crossing is modeled in the other map, leading to a 1:1 mapping on the virtual

network level. Implicitly, the result describes a 1:n type mapping between the node  $p_1$  of map A and the two nodes  $q_1$  and  $q_2$ .

The simple, but very large-scale Sullivan sample also exhibits a very good recall and perfect precision. No topological ambiguity must be resolved in this sample, which is consistent with the fact that the topological information density is very low (2-3 nodes per  $\text{km}^2$ ). The two networks do exhibit a shift, however it is nearly invisible due to the scale of the image.



## 6 Conclusions and Outlook

This chapter summarizes the achievements from the thesis by drawing conclusions and providing an outlook of the ongoing and further developments in the field.

### 6.1 Conclusions

This thesis represents a further step towards the development of novel approaches for referencing, conflation, analysis, and comparison of road networks of digital maps. Therefore, at first, the relevance of the thesis work to the industry as well as to the scientific community is explained. It is followed by a review of the state of the art, starting with an overview of the georeferencing domain. Delving down from a general definition of georeferencing and associated concepts, the characteristics of various research tasks and methods in the field are identified. Three different perspectives are presented to classify the domain of georeferencing: First, methods are distinguished by the type of reference, i.e. vector and raster based. Second, the identification category used for establishing a spatial reference (topological, geometrical, and semantical) is employed as a basis for a classification approach. Finally, a classification by application scenario which includes map-focused applications as well as geographic referencing in media is made.

On this basis, the issue of Road Network Conflation is further explored in detail, which is first described from a holistic point of view, followed by a comparative study of the conflation methods, which can be divided into point-based and line-based approaches, both of which are discussed thoroughly. The description of the point-based methods also includes a novel point-matching algorithm called Exact Angular Index, which is a part of the IHC framework.

A dedicated investigation of Road Network Conflation by the author then takes place. A mathematical foundation is proposed, followed by a discussion of the problem of ambiguity, which almost always arises in non-trivial real world scenarios.

The core of this thesis is formed by the IHC framework for the Road Network Conflation. It comprises a comprehensive multi-stage and two-phase model in a pipeline building upon a combination of Multi-Stage Matching and Buffer Growing in order to iteratively find correlations between geographical structures on different levels of aggregation. Thereby, each step during the progress through the pipeline is detailed. The result of the IHC process describes associations starting from elementary node assignments via elementary and composite associations between road segments to high-level associations between structures representing arbitrary subgraphs of the induced graph of the road network. The problem of ambiguity is dealt with by employing virtual road network layers which contain virtual as well as clustered nodes and segments. While the concept of virtual nodes serves as a means of dealing with partial correspondences, clustering of nodes and topological and geographical modification of the road network in virtual network layers is employed to handle the ambiguity problem.

Finally, the implementation and evaluation of the IHC framework is described, including a detailed explanation of the software architecture of the framework. The IHC framework was implemented on regular PC hardware using common industry toolsets and conforms to software engineering and design standards. Regarding the evaluation, first the methodology used to evaluate the IHC framework is described, which includes measures commonly used by predictive analytics in order to assess properties such as correctness and completeness. Five datasets were taken to evaluate the IHC framework: Three urban datasets (Boston Financial District, USA, as well as Munich Old Town and

Eutin, Germany) and two rural datasets (Sullivan, NY, USA, and Moosach, Germany). The evaluation is based on a ground truth definition which represents the consensus of several independent reviewers and is fully disclosed in the appendix. The results of the IHC framework are compared against the ground truth definition in order to assess performance indicators such as precision and recall. The comparison shows that the IHC framework works very well in terms of both correctness and completeness in the rural sample regions and provides a very high correctness while maintaining considerable, but not perfect completeness in the urban sample regions.

Regarding the research questions mentioned in the motivation, the IHC framework deals with several aspects. It avoids a large number of heuristics and only requires very few parameters, such as the search radius, in order to deliver acceptable results. The algorithms introduced in the IHC have been shown to perform at high speeds (all sample regions can be conflated on a single machine within less than one second), which enables on-the-fly matching in automotive applications. Identified similarities on the level of complex structures as well as link sequences are propagated down to the level of elementary links and nodes. Ambiguities are systematically resolved using topological alteration in virtual network layers. Finally, the IHC only requires very basic map information limited to elementary topology along with link and node geometry, so that it can be used for the conflation of very heterogeneous data sources, even if their semantic model differs extensively.

In a nutshell, this thesis basically contributes to the field in three ways. First, the task of Road Network Conflation as well as solutions to this task and a methodology to evaluate algorithms are modelled in terms of mathematical definitions, which will improve further discussion with regard to terminology and mathematical understanding, especially regarding the aspect of ambiguity. Second, the IHC framework introduced by this thesis provides a means of dealing with complex Road Network Conflation problems which include several special aspects such as m:n as well as high-level associations, while, at the same time, offering correspondence information on multiple levels of aggregation. The mechanism provided for structural matching can be extended to incorporate any kind of complex structure which can be modelled as a subgraph of the road network. Thus, the IHC approach offers a way of iteratively refining the quality and reliability of the algorithm by gradually incorporating templates for situations where standard approaches fail. In order to prevent the algorithm from being drifted too far towards heuristic solutions, the IHC only relies on a very small set of parameters and encourages the re-use of templates. Third, the IHC has been designed with the special requirements of the automotive industry in mind, such as real-time processing, and was tested with automotive-grade digital maps, so that the employed algorithms work reliably with heterogeneous map schemata including diverging semantic models and provide high performance in computationally limited environments.

## 6.2 Outlook

The domain of Road Network Conflation has gained increasing attention in recent times, especially propelled by new demands of the map-making and automotive industry, which is still searching for efficient and reliable solutions to the conflation problem that would enable several important use cases, such as incremental map updating using the smallest possible increment or the integration of volunteered geographical information. Further impulses to the research in the domain will come from the requirements of the growing geographical information services.

Further development of the IHC framework may focus on finding and defining situations which motivate additional structural templates to tackle very specific problems such as custom modelling

principles which are specific to a certain map vendor. In particular, modelling philosophies may differ considerably between the vendors in urban crossing situations and highway interchanges. The definition of structural templates which are able to identify and deal with such vendor-specific modelling decisions may further contribute to improving the correctness and completeness of the approach.

The approach introduced in this thesis has been evaluated with sample regions of roughly the size of city centers. While a large-scale evaluation of densely populated areas could not be performed due to practical reasons, the evaluation of the large-scale rural Sullivan sample demonstrates that there are no technical constraints which would prevent the algorithm from conflating very large regions, given that enough memory is available to hold the road networks. For the efficient conflation of entire states or countries, it would be beneficial to segment the area to be conflated into several tiles with each being conflated separately in parallel. Further development of the IHC conflation approach may target the ideal granularity of such a segmentation as well as the problems related to the horizontal conflation of neighboring tiles, which must take place after the vertical conflation of the tiles has been performed. In addition, the algorithm itself may be investigated with regard to parallelization efforts, so that even within a single tile pair to be conflated, execution may run in parallel in different sub-regions. Especially in the automotive context, such optimizations would leverage the industrialization and automation of the conflation, which could then run efficiently on cloud-based clusters.

In order to further improve the matching accuracy, semantic information may be included into the matching process, given that the maps to be conflated rely on similar semantic models. While the conflation approach introduced in this thesis deliberately avoids semantic matching to lower the requirements imposed on the maps and facilitate generality, the algorithm could be extended by incorporating semantic distance metrics such as the Levenshtein distance into score projections. This would furthermore reduce ambiguities, for example when comparing links or link sequences, at the cost of requiring schema similarity. However, the inclusion of semantic matching into the algorithm would also introduce a new potential source for errors; for example, there may be different streets of the same name within a region and, more frequently, different names for the same street, and there may be differences between the maps regarding the spatial validity of street names.



## 7 References

- [1] A. Hackeloer, K. Klasing, J. M. Krisp and L. Meng, "Road Network Conflation: An Iterative Hierarchical Approach," in *Progress in Location-Based Services 2014*, vol. Part III, G. Gartner and H. Huang, Eds., Springer International Publishing, pp. 137-151, 2015.
- [2] J. A. Harrell and V. M. Brown, "The world's oldest surviving geological map - the 1150 BC Turin papyrus from Egypt," *Journal of Geology*, vol. 100, no. 1, pp. 3-18, 1992.
- [3] B. Englisch, "Erhard Etzlaub's projection and methods of mapping," *Imago Mundi: The International Journal for the History of Cartography*, vol. 48, no. 1, pp. 103-123, 1996.
- [4] E. W. Dijkstra, "A note on two problems in connexion with graphs," *Numerische Mathematik*, vol. 1, no. 1, pp. 269-271, 1959.
- [5] C. Boucher and Z. Altamimi, "ITRS, PZ-90 and WGS 84: current realizations and the related transformation parameters," *Journal of Geodesy*, vol. 75, pp. 613-619, 2001.
- [6] A. Saalfeld, "Conflation: Automated Map Compilation," *International Journal for Geographical Information Systems*, vol. 2, pp. 217-228, 1988.
- [7] A. Hackeloer, K. Klasing, J. M. Krisp and L. Meng, "Georeferencing: a review of methods and applications," *Annals of GIS*, vol. 20, no. 1, pp. 61-69, 2014.
- [8] L. L. Hill, *Georeferencing: the geographic associations of information*, Cambridge: MIT Press, p.2, 2006.
- [9] S. Sommer and T. Wade, *A to Z GIS: An Illustrated Dictionary of Geographic Information Systems*, 2nd ed., Redlands: Esri Press, p. 89, 2006.
- [10] Y. Zheng, Z. Zha and T. Chua, "Research and applications on georeferenced multimedia: a survey," *Multimedia Tools and Applications*, vol. 51, no. 1, pp. 77-98, 2011.
- [11] National Imagery and Mapping Agency, "Department of Defense World Geodetic System 1984 TR 8350.2 3rd edition," 2000.
- [12] P. A. Longley, M. F. Goodchild, D. J. Maguire and D. W. Rhind, *Geographic Information Systems and Science*, Hoboken, NJ, USA: John Wiley & Sons, 2005.
- [13] S. Yuan and C. Tao, "Development of Conflation Components," in *International Symposium of Geoinformatics and Socioinformatics and Geoinformatics*, Ann Arbor, Michigan, 1999.
- [14] M. Zhang, "Methods and implementations of road-network matching," München, 2009.
- [15] T. Lindeberg, "Edge detection," in *Encyclopedia of Mathematics*, Springer, 2001.

- [16] R. Adams and L. Bischof, "Seeded Region Growing," *IEEE Transactions on Pattern Analysis and Machine Intelligence*, vol. 16, no. 6, pp. 641-647, June 1994.
- [17] D. H. Douglas and T. K. Peucker, "Algorithms for the reduction of the number of points required to represent a digitized line or its caricature," *Cartographica: The International Journal for Geographic Information and Geovisualization*, vol. 2, no. 10, pp. 112-122, December 1973.
- [18] I. Guyon and A. Elisseeff, "An Introduction to Variable and Feature Selection," *Journal of Machine Learning Research*, vol. 3, pp. 1157-1182, 2003.
- [19] A. J. De Leeuw, L. M. M. Veugen and H. T. C. Van Stokkom, "Geometric correction of remotely-sensed imagery using ground control points and orthogonal polynomials," *International Journal of Remote Sensing*, vol. 9, no. 10-11, pp. 1751-1759, 1988.
- [20] U.S. Army Corps of Engineers, "Chapter 6 - Ground Control Requirements for Photogrammetric Mapping," in *Engineering and Design - Photogrammetric Mapping, No. 1110-1-1000*, Department of the Army, pp. 6-1, 2002.
- [21] C. Schneebauer and M. Wartenberg, "On-The-Fly Location Referencing Methods for Establishing Traffic Information Services," *IEEE Aerospace and Electronic Systems Magazine*, vol. 22, no. 2, pp. 14-21, February 2007.
- [22] ISO 14819-1, *Traffic and Traveller Information (TTI)*, 2003.
- [23] S. Yamada, "The strategy and deployment plan for VICS," *IEEE Communications Magazine*, vol. 34, no. 10, pp. 94-97, October 1996.
- [24] K. Wevers and T. Hendriks, "AGORA-C On-the-Fly Location Referencing," in *12th World Congress on Intelligent Transport Systems*, San Francisco, CA, 2005.
- [25] D. Xi, L. Weifeng and Z. Tongyu, "Improved Dynamic Location Reference Method Agora-C Based on Rule Optimization," in *Int. Conference on Computer Science and Software Engineering*, Wuhan, China, 2008.
- [26] TomTom International B.V., "OpenLR Whitepaper," 2012. [Online]. Available: [http://www.openlr.org/data/docs/OpenLR-Whitepaper\\_v1.5.pdf](http://www.openlr.org/data/docs/OpenLR-Whitepaper_v1.5.pdf). [Accessed 07 11 2012].
- [27] CEN ISO/TS, *18234-6*, 2006.
- [28] M. Wartenberg, *Mathematical Methods for Location Referencing*, Aachen: Shaker Verlag, 2008.
- [29] Fraunhofer FIRST, "Universal Location Referencing: A New Approach for Dynamic Location Referencing in TPEG," 13 January 2012. [Online]. Available: <http://publica.fraunhofer.de/eprints/urn:nbn:de:0011-n-1925605.pdf>. [Accessed 13 November 2012].

- [30] Y. Diez, M. A. Lopez and J. A. Sellarès, "Noisy Road Network Matching," in *Geographic Information Science*, vol. 5266, T. J. Cova, H. J. Miller, K. Beard, A. U. Frank and M. F. Goodchild, Eds., Berlin, Springer, 2008, pp. 38-54.
- [31] H. Qian, Z. Qiang and G. Min, "Stroke Oriented Road Network Macrostructure Matching Algorithm," *Physical and Numerical Simulation of Geotechnical Engineering*, vol. 3, pp. 18-21, June 2011.
- [32] S. N. Soffer and A. Vásquez, "Network clustering coefficient without degree-correlation biases," *Physical Review E*, vol. 71, no. 5, p. 057101, 2005.
- [33] H. Alt and L. J. Guibas, "Discrete Geometric Shapes: Matching, Interpolation and Approximation," in *Handbook of Computational Geometry*, J. Sack, Ed., Amsterdam, Elsevier Science B.V., pp. 121-153, 1999.
- [34] H. Foley and F. E. Petry, "Fuzzy Knowledge-Based System for Performing Conflation in Geographical Information Systems," in *Lecture Notes in Computer Science*, vol. 1821, R. Loganathanaraj, Ed., Heidelberg, Springer, pp. 260-269, 2000.
- [35] S. Rahimi, M. Cobb, D. Ali, M. Paprzycki and F. E. Petry, "A Knowledge-Based Multi-Agent System for Geospatial Data Conflation," *Journal of Geographic Information and Decision Analysis*, vol. 6, no. 2, pp. 67-81, 2002.
- [36] V. Walter and D. Fritsch, "Matching spatial data sets : a statistical approach," *International Journal of Geographical Information Science*, vol. 13, no. July 1999, pp. 445-473(29), 1999.
- [37] D. Xiong, "A three-stage computational approach to network matching," *Transportation Research Part C*, vol. 8, pp. 71-89, 2000.
- [38] J. J. Ruiz, F. J. Ariza, M. A. Urena and E. B. Blàzquez, "Digital map conflation: a review of the process and a proposal for classification," *International Journal of Geographical Information Science*, vol. 25, no. 9, pp. 1439-1466, 2011.
- [39] E. Basiaensen, "ActMAP: real-time map updates for advanced in-vehicle applications," in *Proceedings of the 10th World Congress on ITS*, Madrid, 2003.
- [40] M. Scheu, W. Effenberg and I. Williamson, "Incremental update and upgrade of Spatial Data," *Zeitschrift für Vermessungswesen*, vol. 125, no. 4, pp. 115-120.
- [41] M. Kurihara, H. Nonaka and T. Yoshikawa, "Use of highly accurate GPS in network-based barrier-free street map creation system," *Proc. of the 2004 IEEE International Conference on Systems, Man and Cybernetics*, pp. 1169-1173, 2004.
- [42] H. Pundt and K. Brinkkötter-Runde, "Visualization of spatial data for field based GIS," *Computers & Geosciences*, vol. 26, pp. 51-56, 2000.

- [43] Q. Zhang and I. Couloigner, "Spatio-Temporal Modeling in Road Network Change Detection and Updating," in *Proc. of the International Symposium on Spatio-temporal Modeling, Spatial Reasoning, Analysis, Data Mining and Data Fusion*, Peking University, China, 2005.
- [44] D. Xiong and J. Sperling, "Semiautomated matching for network database integration," *ISPRS Journal of Photogrammetry and Remote Sensing*, no. 59, pp. 35-46, 2004.
- [45] N. Snavely, S. Seitz and R. Szeliski, "Photo tourism: Exploring photo collections in 3D," *ACM Transactions on Graphics*, vol. 25, no. 3, pp. 137-154, 2006.
- [46] I. Mani, C. Doran, D. Harris, J. Hitzeman, R. Quimby, J. Richer, B. Wellner, S. Mardis and S. Clancy, "SpatialML: annotation scheme, resources, and evaluation," *Lang Resources & Evaluation*, vol. 44, pp. 263-280, 2010.
- [47] B. Rosen and A. Saalfeld, "Match criteria for automatic alignment," *Proc. Auto-Carto*, vol. 7, 1985.
- [48] R. Sinnott, "Virtues of the Haversine," *Sky and Telescope*, vol. 68, no. 2, p. 159, 1984.
- [49] A. Hackeloeer, K. Klasing, J. M. Krisp and L. Meng, "Comparison of Point Matching Techniques for Road Network Matching," *Int. Archives of the Photogrammetry, Remote Sensing and Spatial Information Sciences*, Vols. XL-2/W1, pp. 87-92, 13 May 2013.
- [50] V. Walter, „Zuordnung von raumbezogenen Daten - am Beispiel der Datenmodelle ATKIS und GDF,“ Bayerische Akademie der Wissenschaften, München, 1997.
- [51] D. Mantel and U. Lipeck, "Matching Cartographic Objects in Spatial Databases," in *ISPRS Vol. 35, ISPRS Congress, Commission 4*, Istanbul, Turkey, 2004.
- [52] M. Zhang and L. Meng, "An iterative road-matching approach for the integration of postal data," *Computers, Environment and Urban Systems*, no. 31/5, pp. 598-616, 2007.
- [53] S. Volz, "An iterative approach for matching multiple representations of street data," in *ISPRS Vol. 36, ISPRS Workshop - Multiple representation and interoperability of spatial data*, Hanover, Germany, 2006.
- [54] M. Zhang and L. Meng, "Delimited Stroke Oriented Algorithm Working Principle and Implementation for the Matching of Road Networks," *Journal of Geographic Information Sciences*, vol. 14, no. 1, pp. 44-53, June 2008.
- [55] M. Zhang and L. Meng, "An iterative road-matching approach for the integration of postal data," *Computers, Environment and Urban Systems*, vol. 31, no. 5, pp. 597-615, 2007.
- [56] M. Ester, H.-P. Kriegel, J. Sander and X. Xu, "A density-based algorithm for discovering clusters in large spatial databases with noise," *Proceedings of the Second International Conference on Knowledge Discovery and Data Mining (KDD-96)*, pp. 226-231, 1996.

- [57] S. Yuan and C. Tao, "Development of Conflation Components," in *Proc. of the International Symposium of Geoinformatics and Socioinformatics*, Ann Arbor, MI, USA, 1999.
- [58] EBU\_B/TPEG, *TPEG Specifications, Part 6: Location Referencing for Applications, TPEG-Loc\_3.0/001*, 2002.
- [59] S. Rusinkiewicz and M. Levoy, "Efficient variants of the ICP algorithm," in *Proceedings Third International Conference on 3-D Digital Imaging and Modeling*, Quebec, Canada, 2001.
- [60] G. Gösseln and M. Sester, "Integration of geoscientific data sets and the German digital map using a matching approach," in *XXth ISPRS Congress*, Istanbul, Turkey, 2004.
- [61] G. Gösseln, "A matching approach for the integration, change detection and adaptation of heterogeneous vector data sets," in *XXII International Cartography Conference*, A Coruna, Spain, 2005.
- [62] Y. Zhang, B. Yang and L. Xuechen, "Automated Matching Crowdsourcing Road Networks Using Probabilistic Relaxation," *ISPRS Annals of the Photogrammetry, Remote Sensing and Spatial Information Sciences*, no. I-4, pp. 281-286, 2012.
- [63] Q. Xuan, L. Yu, F. Du and T.-J. Wu, "A review on node-matching between networks," in *New Frontiers in Graph Theory*, Rijeka, 2012.
- [64] K. Lakakis, P. Savvaidis, I. Ifadis and I. D. Doukas, "FIG Working Week," in *Quality of Map-Matching Procedures based on DGPS and Stand-Alone GPS Positioning in an Urban Area*, Athens, Greece, 2004.
- [65] B. Kovalerchuk, P. Doucette, G. Seedahmed, R. Brigantic, M. Kovalerchuk and B. Graff, "Automated vector-to-raster image registration," *Proceedings of SPIE*, vol. 6966, pp. 69660W-1-69660W-12, 2008.
- [66] D. G. O'Donohue, "Matching of image features and vector objects to automatically correct spatial misalignment between image and vector data sets," 2010.
- [67] R. Péteri, J. Celle and T. Ranchin, "Detection and extraction of road networks from high resolution satellite images," in *International Conference on Image Processing*, 2003.
- [68] D. Tien, Y. Xiao and Q.-h. Qin, "A novel up-to-down algorithm for road extraction," *International Journal of Tomography & Statistics*, vol. 9, no. S08, pp. 1-11, 2008.
- [69] M. Mokhtarzade and V. Zoj, "Road detection from high-resolution satellite images using artificial neural networks," *International Journal of Applied Earth Observation and Geoinformation*, vol. 9, pp. 32-40, 2007.
- [70] A. Gruen and H. Li, "Road extraction from aerial and satellite images by dynamic programming," *ISPRS Journal of Photogrammetry and Remote Sensing*, vol. 50, no. 4, pp. 11-21, 1995.

- [71] B. Zitová and J. Flusser, "Image registration methods: a survey," *Image and Vision Computing*, vol. 21, pp. 977-1000, 2003.
- [72] L. Brown, "A survey of image registration techniques," *ACM Computing Surveys*, vol. 24, pp. 326-376, 1992.
- [73] M. A. Quddus, W. Y. Ochieng and R. B. Noland, "Integrity of map-matching algorithms," *Transportation Research Part C*, no. 14, pp. 283-302, 2006.
- [74] M. Quddus, W. Y. Ochieng and R. B. Noland, "Current map-matching algorithms for transport applications: State-of-the art and future research directions," *Transportation Research Part C* 15, pp. 312-328, 2007.
- [75] M. A. Quddus, W. Y. Ochieng, L. Zhao and R. B. Noland, "A general map matching algorithm for transport telematics applications," *GPS Solutions*, vol. 7, no. 3, pp. 157-167, 12 2003.
- [76] C. Poullis and S. You, "Delineation and geometric modeling of road networks," *ISPRS Journal of Photogrammetry and Remote Sensing*, vol. 65, no. 2, pp. 165-181, 2010.
- [77] S. Filin and Y. Doytsher, "The Detection of Corresponding Objects in a Linear-Based Map Conflation," *Surveying and Land Information Systems*, vol. 60, no. 2, pp. 117-128, 2000.
- [78] P. Besl and N. McKay, "A method for registration of 3-d shapes," *IEEE Transactions on Pattern Analysis and Machine Intelligence*, no. 14 (2), pp. 239-256, 1992.
- [79] W. Christmas, J. Kittler and M. Petrou, "Matching of road segments using probabilistic relaxation: a hierarchical approach," in *Neural and Stochastic Methods in Image and Signal Processing III*, vol. SPIE 2220, San Diego, CA, USA, Chen, S.-S., 1994, pp. 166-174.
- [80] C.-F. Zhu, S.-X. Li, H.-X. Chang and J.-X. Zhang, "Matching Road Networks Extracted from Aerial Images to GIS Data," in *Asia-Pacific Conference on Information Processing*, Shenzhen, China, 2009.
- [81] R. C. Veltkamp and M. Hagedoorn, "State-of-the-Art in Shape Matching," in *Principles of Visual Information Retrieval*, M. Lew, Ed., Berlin, Springer, pp. 87-119, 2001.
- [82] G. Vosselman, *Lecture Notes on Computer Science*, Vol. 628: Relational Matching, Springer, 1992.
- [83] Q. Hao, R. Cai, C. Wang, R. Xiao, J.-M. Yang, Y. Pang and L. Zhang, "Equip tourists with knowledge mined from travelogues," in *WWW '10: Proceedings of the 19th international conference on World wide web*, New York, NY, USA, 2010.
- [84] S. S. Maras, H. H. Maras, B. Aktug, E. E. Maras and F. Yildiz, "Topological error correction of GIS vector data," *International Journal of the Physical Sciences*, vol. 5, no. 5, pp. 476-483, 2010.

- [85] B. Rao and L. Minakakis, "Mobile commerce opportunities and challenges: Evolution of mobile location-based services," *Communications of the ACM*, vol. 46, no. 12, pp. 61-65, 12 2003.
- [86] W. Ochieng, M. Quddus and R. Noland, "Map-Matching in complex urban road networks," *Revista Brasileira de Cartografia*, no. 55/2, pp. 1-18, 2003.



## 8 Appendix: Ground Truth Definitions for Evaluation

### 8.1 Boston Sample

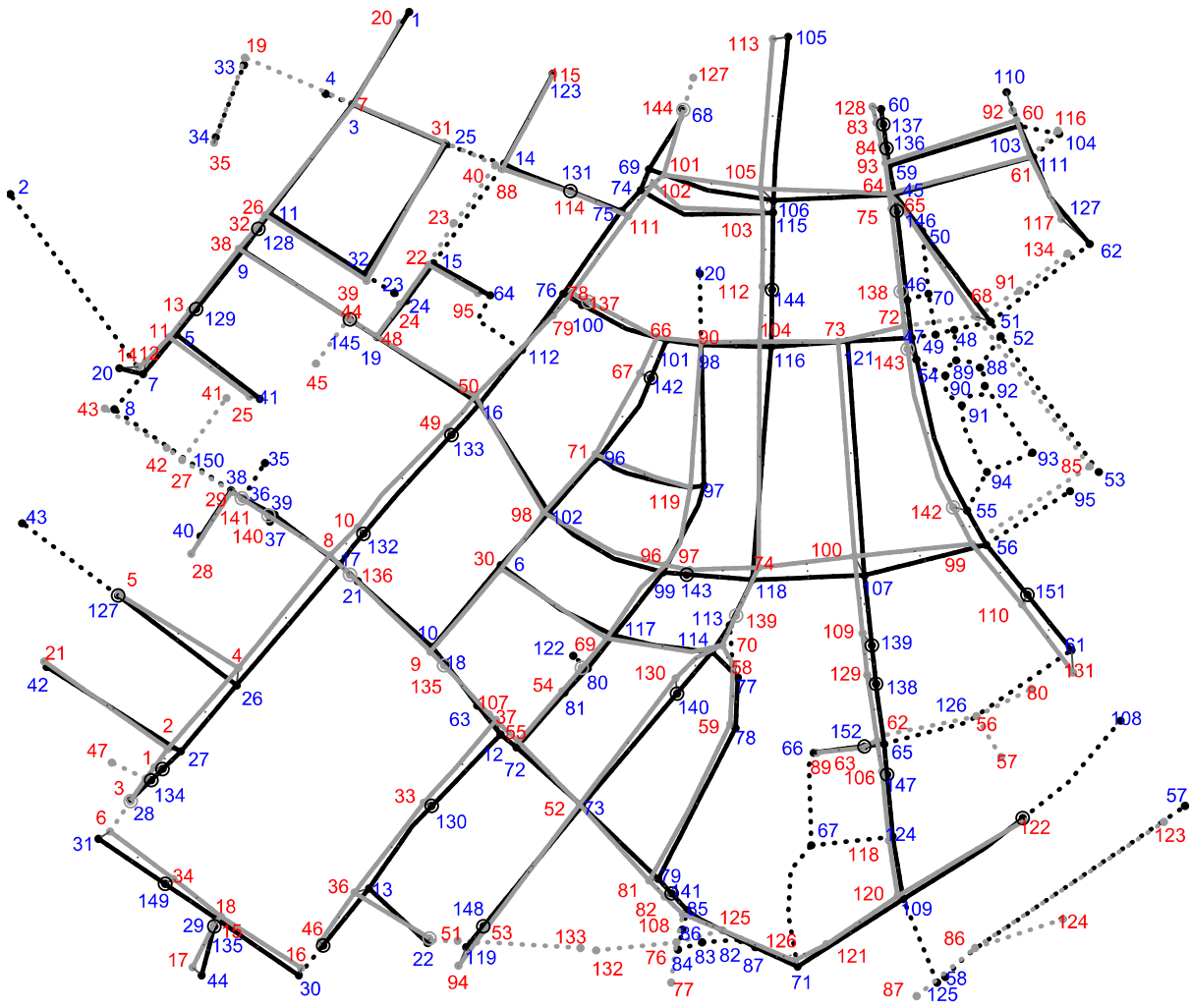


Figure 8-1: Labeling for Ground Truth Definition for Boston Downtown Sample. Blue: Map A, Red: Map B.

Map A	Map B	Comments	TP	FP	TN	FN
1	20			1		
2	x					1
3	7			1		
4	x	Missing virtual node				1
5	11			1		
6	30			1		
7	12			1		
8	43	Missing match: 43				1
9	38			1		
10	9			1		
11	26			1		
12	37			1		
13	36			1		
14	88			1		

15	22		1			
16	50		1			
17	8		1			
18	135	Map B virtual node	1			
19	48		1			
20	14		1			
21	136	Map B virtual node	1			
22	51		1			
23	x				1	
24	24		1			
25	31		1			
26	4		1			
27	2		1			
28	3		1			
29	18		1			
30	16		1			
31	6		1			
32	39		1			
33	x	Missing match: 19				1
34	35		1			
35	x				1	
36	141	Map B virtual node	1			
37	x				1	
38	29		1			
39	140	Map B virtual node	1			
40	28		1			
41	25		1			
42	21		1			
43	x				1	
44	17		1			
45	64		1			
46	138	Map B virtual node	1			
47	72		1			
48	x	Missing virtual node				1
49	x	Missing virtual node				1
50	65		1			
51	68		1			
52	x	Missing virtual node				1
53	x	Missing match: 85				1
54	143		1			
55	142		1			
56	99		1			
57	123	Missing match: 123				1

58	x				1	
59		93		1		
60		128		1		
61		131		1		
62		117		1		
63		107		1		
64		95		1		
65		62		1		
66		89		1		
67	x				1	
68		144		1		
69		101		1		
70	x				1	
71		121		1		
72		55		1		
73		52		1		
74		102		1		
75		111		1		
76		78		1		
77		58		1		
78		59		1		
79		81		1		
80		145		1		
81		54		1		
82		125		1		
83	x		Missing virtual node			1
84	x		Missing match: 76			1
85		108		1		
86	x		Missing virtual node			1
87		126		1		
88	x				1	
89	x				1	
90	x				1	
91	x				1	
92	x				1	
93	x				1	
94	x				1	
95	x		Missing virtual node			1
96		71		1		
97		119		1		
98		90		1		
99		96		1		
100		137	Map B virtual node	1		

101	66		1		
102	98		1		
103	60		1		
104	x	Missing match: 116			1
105	113		1		
106	105		1		
107	100		1		
108	x			1	
109	120		1		
110	92		1		
111	61		1		
112	79		1		
113	139		1		
114	70		1		
115	103		1		
116	104		1		
117	69		1		
118	74		1		
119	94		1		
120	x			1	
121	73		1		
122	x			1	
123	115		1		
124	118		1		
125	x			1	
126	x	Missing virtual node			1
127	5		1		
128	32	Map A virtual node	1		
129	13	Map A virtual node	1		
130	33	Map A virtual node	1		
131	114	Map A virtual node	1		
132	10	Map A virtual node	1		
133	49	Map A virtual node	1		
134	1	Map A virtual node	1		
135	15	Map A virtual node	1		
136	84	Map A virtual node	1		
137	83	Map A virtual node	1		
138	129	Map A virtual node	1		
139	109	Map A virtual node	1		
140	130	Map A virtual node	1		
141	82	Map A virtual node	1		
142	67	Map A virtual node	1		
143	97	Map A virtual node	1		
144	112	Map A virtual node	1		

145	44	Map A virtual node	1			
146	75	Map A virtual node	1			
147	106	Map A virtual node	1			
148	53	Map A virtual node	1			
149	34	Map A virtual node	1			
150	42	Map A virtual node	1			
151	110	Map A virtual node	1			
152	63	Map A virtual node	1			
x	27	Missing virtual node				1
x	40	1:n assoc. to 14				1
x	41				1	
x	45				1	
154	46		1			
x	47				1	
x	57				1	
x	77				1	
x	80	Missing virtual node				1
x	91	Missing virtual node				1
153	122		1			
x	124				1	
x	127				1	
x	132				1	
x	133				1	
x	134	Missing virtual node				1
		<b>Total</b>	<b>121</b>	<b>0</b>	<b>28</b>	<b>19</b>
		<b>Precision</b>	<b>100,00%</b>			
		<b>Recall</b>	<b>86,43%</b>			
		Sensitivity	86,43%			
		Specificity	100,00%			
		Precision (PPV)	100,00%			
		NPV	59,57%			
		False Positive Rate	0,00%			
		False Disc. Rate	0,00%			
		Accuracy	88,69%			

Table 8-1: Ground Truth Definition for Boston Downtown Sample.

### 8.2 Munich Sample

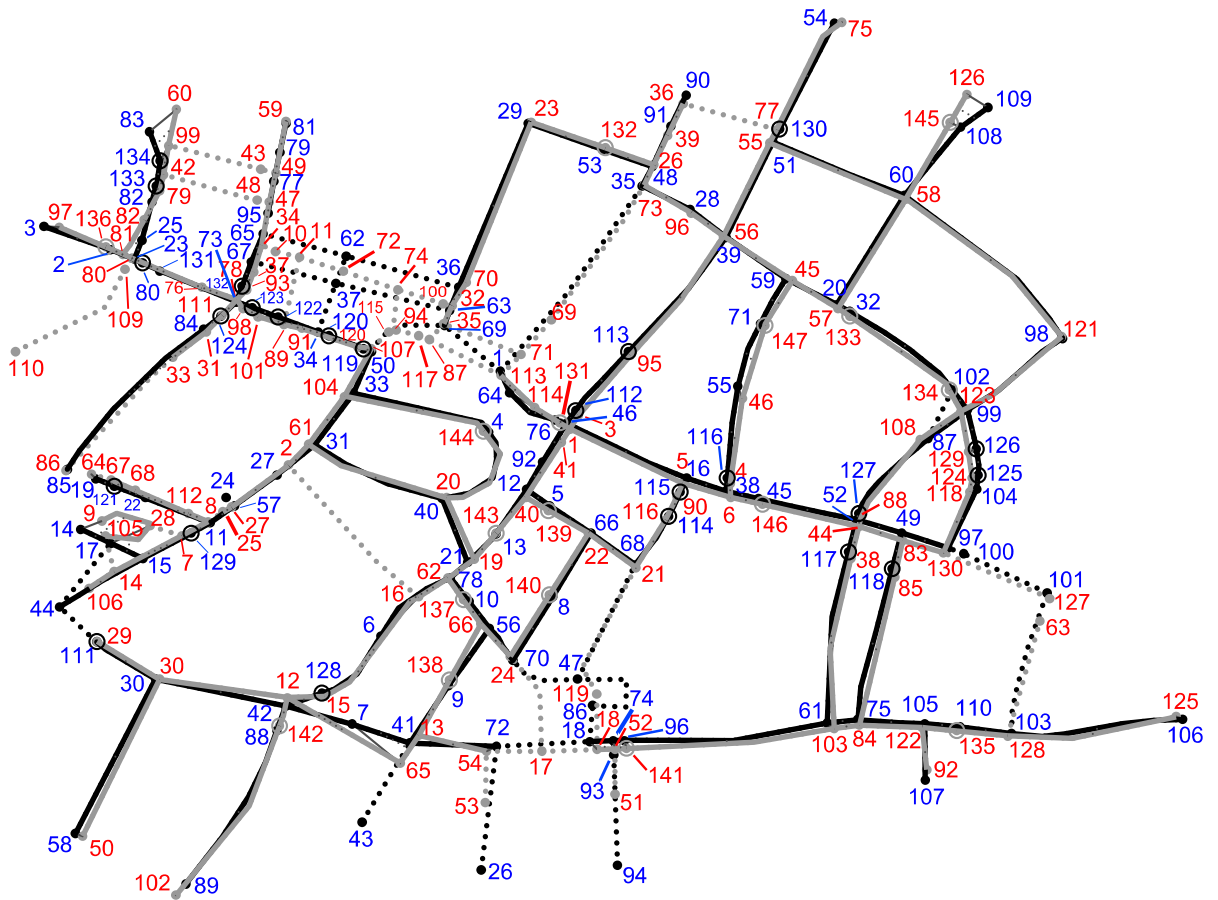


Figure 8-2: Labeling for Ground Truth Definition for Munich Sample. Blue: Map A, Red: Map B.

Map A	Map B	Errors	TP	FP	TN	FN
1	113			1		
2	136			1		
3	97			1		
4	144			1		
5	139			1		
6	16			1		
7	65			1		
8	140			1		
9	138			1		
10	137			1		
11	8			1		
12	40			1		
13	143			1		
14	9			1		
15	14			1		
16	5			1		
17	28			1		
18	18			1		
19	64			1		

20	57		1		
21	19		1		
22	68		1		
23	81		1		
24	x			1	
25	82		1		
26	x			1	
27	27		1		
28	96		1		
29	23		1		
30	30		1		
31	61		1		
32	133		1		
33	104		1		
34	89		1		
35	73		1		
36	70		1		
37	72	Missed n:1 match			1
38	6		1		
39	56		1		
40	20		1		
41	13		1		
42	12		1		
43	x			1	
44	106		1		
45	146		1		
46	1		1		
47	119	Missed 1:n match			1
48	26		1		
49	83		1		
50	107		1		
51	55		1		
52	44		1		
53	132		1		
54	75		1		
55	46		1		
56	66		1		
57	25		1		
58	50		1		
59	45		1		
60	58		1		
61	103		1		
62	72	Missed n:1 match			1
63	32		1		
64	114		1		

65	34		1			
66	22		1			
67	37	Missed n:1 match (34)		1		
68	21		1			
69	35		1			
70	24		1			
71	147		1			
72	54		1			
73	78		1			
74	52		1			
75	84		1			
76	131		1			
77	47		1			
78	62		1			
79	49		1			
80	80		1			
81	59		1			
82	79		1			
83	60		1			
84	31		1			
85	86		1			
86	119	Missed n:1 match				1
87	108		1			
88	142		1			
89	102		1			
90	36		1			
91	39		1			
92	41		1			
93	x	Missed virtual node				1
94	x			1		
95	x	Missed virtual node				1
96	141		1			
97	130		1			
98	121		1			
99	123		1			
100	x	Missed virtual node				1
101	127	Missed match				1
102	134		1			
103	128		1			
104	118		1			
105	122		1			
106	125		1			
107	92		1			
108	145		1			

109	126		1			
110	135		1			
111	29		1			
112	3		1			
113	95		1			
114	116		1			
115	90		1			
116	4		1			
117	38		1			
118	85		1			
119	120		1			
120	91		1			
121	67		1			
122	101		1			
123	98		1			
124	111		1			
125	124		1			
126	129		1			
127	88		1			
128	15		1			
129	7		1			
130	77		1			
131	76		1			
132	93		1			
133	42		1			
134	99		1			
x	2	Missed virtual node				1
x	10	Missed virtual node				1
x	11	Missed virtual node				1
x	17	Missed virtual node				1
x	43				1	
x	48				1	
x	51	Missed virtual node				1
x	53	Missed virtual node				1
x	63	Missed virtual node				1
x	69	Missed virtual node				1
x	71	Missed virtual node				1
x	74	Missed virtual node				1
x	87				1	
x	94	Missed virtual node				1
x	100	Missed virtual node				1
x	105				1	
x	109				1	
x	110				1	
x	112	Missed virtual node				1

x	115	Missed virtual node				1
x	117	Missed virtual node				1
		Total	121	1	10	23
		Precision	99,18%			
		Recall	84,03%			
		Sensitivity	84,03%			
		Specificity	90,91%			
		Precision (PPV)	99,18%			
		NPV	30,30%			
		False Positive Rate	9,09%			
		False Disc. Rate	0,82%			
		Accuracy	84,52%			

Table 8-2: Ground Truth Definition for Munich Sample.

### 8.3 Eutin Sample

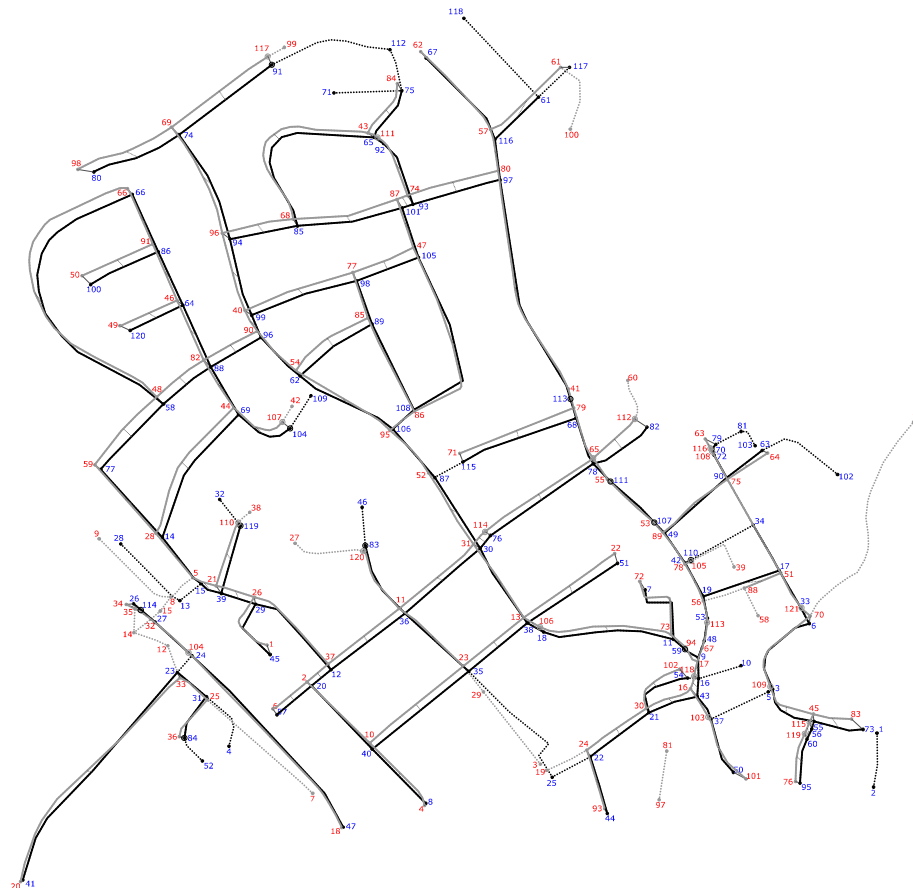


Figure 8-3: Labeling for Ground Truth Definition for Eutin Sample. Blue: Map A, Red: Map B.

Map A	Map B	Comments	TP	FP	TN	FN
1	x				1	
2	x				1	

3		109	Virtual node map B	1		
4	x					1
5	x					1
6		70		1		
7		72		1		
8		4		1		
9		17		1		
10	x					1
11		73		1		
12		37		1		
13		8				1
14		28		1		
15		5		1		
16		118	Virtual node map B	1		
17		51		1		
18		106	Virtual node map B	1		
19		56		1		
20		2		1		
21		30		1		
22		24		1		
23		33		1		
24		104	Virtual node map B	1		
25		19				1
26		34		1		
27		32		1		
28	x					1
29		26		1		
30		31		1		
31		25		1		
32	x					1
33		121	Virtual node map B	1		
34	(v)		Missing virtual node			1
35		23		1		
36		11		1		
37		103	Virtual node map B	1		
38		13		1		
39		21		1		
40		10		1		
41		20		1		
42		78		1		
43		16		1		
44		93		1		
45		1		1		
46	x					1
47		18		1		
48		67		1		
49		89		1		

50	101		1		
51	22		1		
52	x				1
53	113	Virtual node map B	1		
54	102		1		
55	45				
56	115	Virtual node map B	1		
57	6		1		
58	48		1		
59	94	Virtual node map A	1		
60	119	Virtual node map B	1		
61	(v)	Missing virtual node			1
62	54		1		
63	64		1		
64	46		1		
65	43		1		
66	66		1		
67	62		1		
68	79		1		
69	44		1		
70	116	Virtual node map B	1		
71	x				1
72	108	Virtual node map B	1		
73	83		1		
74	69		1		
75	84		1		
76	114	Virtual node map B	1		
77	59		1		
78	65	Fusioned roundabout	1		
79	63		1		
80	98		1		
81	x				1
82	112	Virtual node map B	1		
83	120	Virtual node map A+B	1		
84	36	Virtual node map A	1		
85	68		1		
86	91		1		
87	52		1		
88	82		1		
89	85		1		
90	75		1		
91	117	Virtual node map A+B	1		
92	111	Virtual node map B	1		
93	74		1		
94	96		1		
95	76		1		
96	90		1		

97	80		1			
98	77		1			
99	40		1			
100	50		1			
101	87		1			
102	x				1	
103	x				1	
104	107	Virtual node map A+B	1			
105	47		1			
106	95		1			
107	53	Virtual node map A	1			
108	86		1			
109	x				1	
110	105	Virtual node map B	1			
111	55	Virtual node map A	1			
112	x				1	
113	41	Virtual node map A	1			
114	35	Virtual node map A	1			
115	71		1			
116	57		1			
117	61		1			
118	x				1	
119	110	Virtual node map B	1			
120	49		1			
(v)	3	Missing virtual node				1
x	7				1	
x	9				1	
x	12				1	
x	14				1	
x	15				1	
x	27				1	
(v)	29	Missing virtual node				1
x	38				1	
x	39				1	
(v)	42	Missing virtual node				1
x	58				1	
x	60				1	
x	81				1	
x	92				1	
x	97				1	
(v)	99	Missing virtual node				1
x	100				1	
		Total	99	0	30	8
		Precision	100,00%			
		Recall	92,52%			

		Sensitivity	92,52%		
		Specificity	100,00%		
		Precision (PPV)	100,00%		
		NPV	78,95%		
		False Positive Rate	0,00%		
		False Disc. Rate	0,00%		
		Accuracy	94,16%		

Table 8-3: Ground Truth Definition for Eutin Sample.

### 8.4 Sullivan Sample

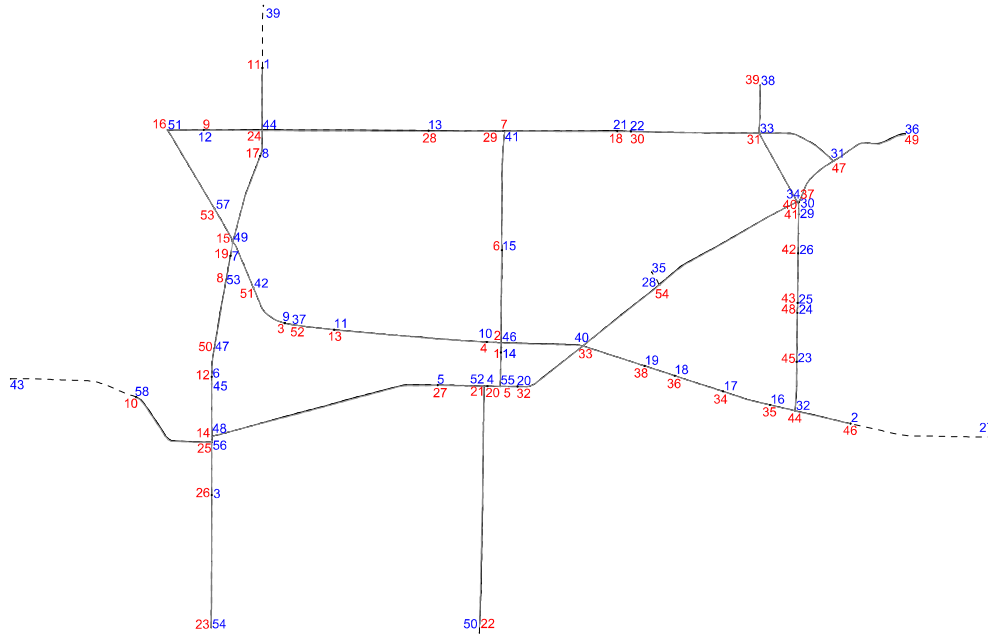


Figure 8-4: Labeling for Ground Truth Definition for Sullivan Sample. Blue: Map A, Red: Map B.

Map A	Map B	Errors	TP	FP	TN	FN
1	11		1			
2	46		1			
3	26		1			
4	20		1			
5	27		1			
6	12		1			
7	19		1			
8	17		1			
9	3		1			
10	4		1			
11	13		1			
12	9		1			
13	28		1			
14	1		1			
15	6		1			
16	35		1			
17	34		1			

18	36		1			
19	38		1			
20	32		1			
21	18		1			
22	30		1			
23	45		1			
24	48		1			
25	43		1			
26	42		1			
27	x				1	
28	54		1			
29	41		1			
30	40		1			
31	47		1			
32	44		1			
33	31		1			
34	37		1			
35	x				1	
36	49		1			
37	52		1			
38	39		1			
39	x				1	
40	33		1			
41	7		1			
42	51		1			
43	x				1	
44	24		1			
45	x	Missing virtual node				1
46	2		1			
47	50		1			
48	14		1			
49	15		1			
50	22		1			
51	16		1			
52	21		1			
53	8		1			
54	23		1			
55	5		1			
56	25		1			
57	53		1			
58	10		1			
x	29	Missing virtual node				1
		Total	<b>53</b>	<b>0</b>	<b>4</b>	<b>2</b>

		<b>Precision</b>	<b>100,00%</b>		
		<b>Recall</b>	<b>96,36%</b>		
		Sensitivity	96,36%		
		Specificity	100,00%		
		Precision (PPV)	100,00%		
		NPV	66,67%		
		False Positive Rate	0,00%		
		False Disc. Rate	0,00%		
		Accuracy	96,61%		

Table 8-4: Ground Truth Definition for Sullivan Sample.

### 8.5 Moosach Sample

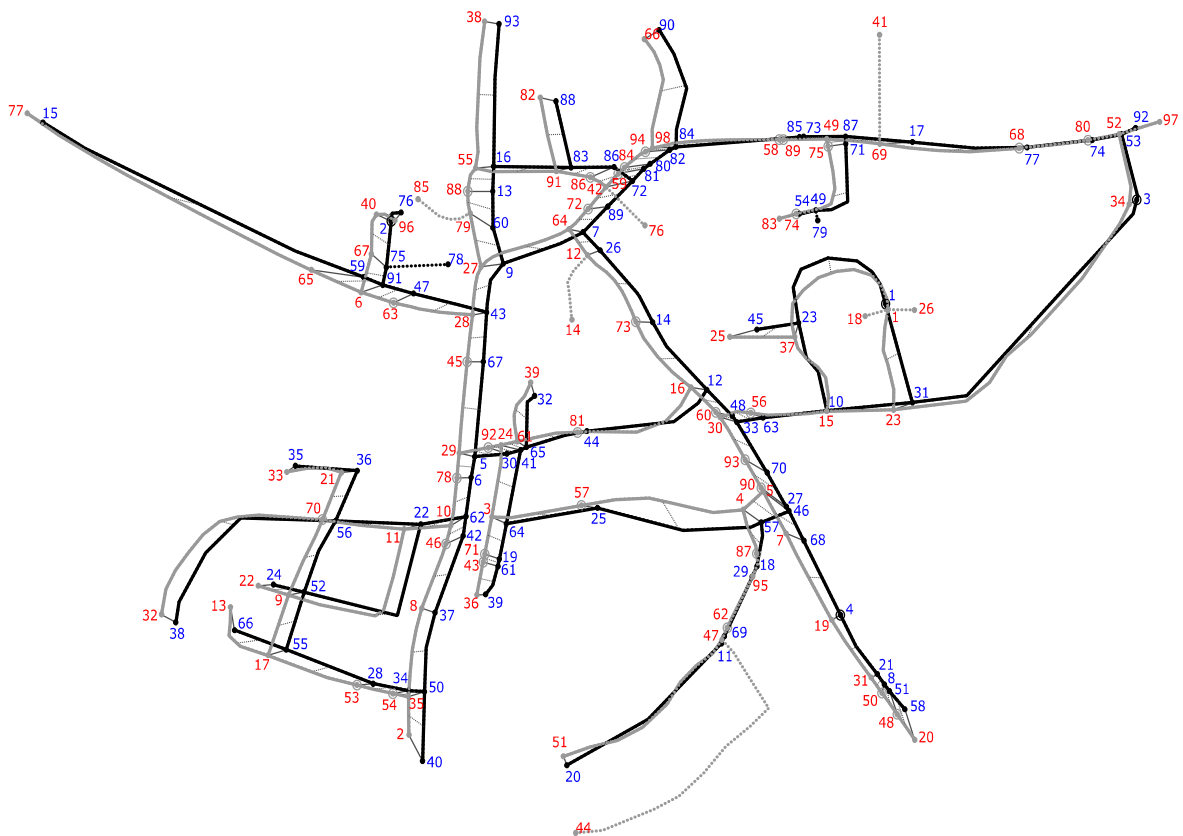


Figure 8-5: Labeling for Ground Truth Definition for Moosach Sample. Blue: Map A, Red: Map B.

Map A	Map B	Comments	TP	FP	TN	FN
1	1	Map A virtual node	1			
2	40	Map A virtual node	1			
3	34	Map A virtual node	1			
4	19	Map A virtual node	1			
5	29		1			
6	78	Map B virtual node	1			
7	64		1			
8	50	Map B virtual node	1			

9	27		1			
10	15		1			
11	47		1			
12	16		1			
13	88	Map B virtual node	1			
14	73	Map B virtual node	1			
15	77		1			
16	55		1			
17	69		1			
18	87	Map B virtual node	1			
19	71	Map B virtual node	1			
20	51		1			
21	31		1			
22	11		1			
23	37		1			
24	22		1			
25	57	Map B virtual node	1			
26	12		1			
27	90	Map B virtual node	1			
28	53	Map B virtual node	1			
29	95		1			
30	92	Map B virtual node	1			
31	23		1			
32	39		1			
33	30		1			
34	54	Map B virtual node	1			
35	33		1			
36	21		1			
37	8		1			
38	32		1			
39	36		1			
40	2		1			
41	24		1			
42	46	Map B virtual node	1			
43	28		1			
44	81	Map B virtual node	1			
45	25		1			
46	5		1			
47	63	Map B virtual node	1			
48	60	Map B virtual node	1			
49	74	Map B virtual node	1			
50	35		1			
51	48	Map B virtual node	1			
52	9		1			
53	52		1			
54	83		1			
55	17		1			



		<b>Precision</b>	<b>100,00%</b>			
		<b>Recall</b>	<b>100,00%</b>			
		Sensitivity	100,00%			
		Specificity	100,00%			
		Precision (PPV)	100,00%			
		NPV	100,00%			
		False Positive Rate	0,00%			
		False Disc. Rate	0,00%			
		Accuracy	100,00%			

**Table 8-5: Ground Truth Definition for Moosach Sample.**